3337

Ordered returned 2/1/83

Numbers should be 12591 (see next page)

756

AD A124100

R and D CENTER LABORATORY TECHNICAL REPORT

NO. 12644 12591 used

U.S. ARMY TACOM

DYNAMIC ANALYSIS OF

THREE DIMENSIONAL CONSTRAINED MECHANICAL SYSTEMS

USING EULER PARAMETERS

Contract Number DAAK 30-80-C-0042

OCTOBER 1981

In-Soo Chung, Chia-Ou Chang,
Edward J. Haug, and Roger A. Wehage
College of Engineering
The University of Iowa
Iowa City, IA 52242
University of Iowa Report No. 81-11

by Ronald R. Beck, Project Engineer, TACOM

US Army Tank-Automotive Command
ATTN: DRSTA-ZSA
Warren, MI 48090

Approved for public release; distribution unlimited.

20031211056

U.S. ARMY TANK-AUTOMOTIVE COMMAND
RESEARCH AND DEVELOPMENT CENTER
Warren, Michigan 48090

NOTICES

The findings in this report are not to be construed as an official Department of the Army position.

Mention of any trade names or manufacturers in this report shall not be construed as advertising nor as an official endorsement of approval of such products or companies by the U.S. Government.

Destroy this report when it is no longer needed. Do not return it to originator.

UNCLASSIFIED

SECURITY CLASSIFICATION OF THIS PAGE *(When Data Entered)*

REPORT DOCUMENTATION PAGE

READ INSTRUCTIONS BEFORE COMPLETING FORM

1. REPORT NUMBER: 12591

2. GOVT ACCESSION NO.:

3. RECIPIENT'S CATALOG NUMBER:

4. TITLE *(and Subtitle)*: Dynamic Analysis of Three Dimensional Constrained Mechanical Systems Using Euler Parameters

5. TYPE OF REPORT & PERIOD COVERED: Interim to October 1981

6. PERFORMING ORG. REPORT NUMBER: 84

7. AUTHOR(s):
In-Soo Chung, Chia-Ou Chang, Edward J. Haug, and Roger A. Wehage, The University of Iowa
Ronald R. Beck, TACOM

8. CONTRACT OR GRANT NUMBER(s): DAAK30-80-C-0042

9. PERFORMING ORGANIZATION NAME AND ADDRESS:
The University of Iowa
College of Engineering
Iowa City, IA 52242

10. PROGRAM ELEMENT, PROJECT, TASK AREA & WORK UNIT NUMBERS:

11. CONTROLLING OFFICE NAME AND ADDRESS:
U.S. Army Tank-Automotive Command, R&D Center
Tank-Automotive Concepts Lab, DRSTA-ZSA
Warren, MI 48090

12. REPORT DATE: October 1981

13. NUMBER OF PAGES: 149

14. MONITORING AGENCY NAME & ADDRESS *(if different from Controlling Office)*:

15. SECURITY CLASS. *(of this report)*: Unclassified

15a. DECLASSIFICATION/DOWNGRADING SCHEDULE:

16. DISTRIBUTION STATEMENT *(of this Report)*:
Approved for public release; distribution unlimited.

17. DISTRIBUTION STATEMENT *(of the abstract entered in Block 20, if different from Report)*:

18. SUPPLEMENTARY NOTES:

19. KEY WORDS *(Continue on reverse side if necessary and identify by block number)*:
Euler angles, Dynamics, Bodies, Response, Interaction, Stability, Lagrangian functions

20. ABSTRACT *(Continue on reverse side if necessary and identify by block number)*:

This report presents a computer-based method for formulation and efficient solution of nonlinear, constrained differential equations of motion for spatial dynamic analysis of mechanical systems. Nonlinear holonomic constraint equations and differential equations of motion are written in terms of maximal set of Cartesian generalized coordinates, three translational and four rotational coordinates for each rigid body in the system, where the rotational coordinates are the Euler parameters. Euler parameters, in

DD FORM 1 JAN 73 1473 EDITION OF 1 NOV 65 IS OBSOLETE

UNCLASSIFIED

SECURITY CLASSIFICATION OF THIS PAGE *(When Data Entered)*

contrast to Euler angles or any other set of three-rotational generalized coordinates, have no critical singular cases. The maximal set of generalized coordinates facilitates the general formulation of constraints and forcing functions. A Gaussian elimination algorithm with full pivoting decomposes the constraint Jacobian matrix, identifies dependent variables, and constructs an influence coefficient matrix relating variations in dependent and independent variables. This information is employed to numerically construct a reduced system of differential equations of motion whose solution yields the total system dynamic response. A numerical integration algorithm with positive-error control, employing a predictor-corrector algorithm with variable order and step size, integrates for only the independent variables, yet effectively determines dependent variables. A three-dimensional model of a tracked vehicle has been modeled and the response of the simulations are presented.

TABLE OF CONTENTS

1. Introduction 1

2. Generalized Coordinate Partitioning 3

3. Generalized Coordinates for the Angular Orientation of A Rigid Body 6

   3.1 Transformation Matrix 6

4. Constraint Equations 7

5. Rigid Body Dynamics 10

6. Forces 12

   6.1 Friction 15

7. DADS-3-D Computer Program 16

8. Three-Dimensional Model of Tracked Vehicles 17

   8.1 Platform Stability Analysis 18

   8.2 Elevation and Azimuth Stabilization 20

   REFERENCES 21

Appendix A Response Plots
Appendix B Response Plots
Appendix C Response Plots
Appendix D Response Plots
Appendix E Response Plots
Appendix F DADS-3-D User Manual

1. INTRODUCTION

An effective method of formulating and solving differential equations of motion for general mechanical systems subject to holonomic constraints has recently been presented [1,2,3]. For planar systems, a three vector of Cartesian generalized coordinates is defined for each rigid body of the system. Standard and user-supplied constraints are formulated, yielding algebraic relations involving generalized coordinates of the bodies connected by each joint. A Lagrange multiplier technique allows coupling of the algebraic constraint equations and differential equations, yielding a large system of differential and algebraic equations which are solved iteratively using implicit numerical integration methods [1,2,3]. Because of weak constraint equation coupling, the Jacobian matrix associated with the implicit numerical integration method is sparse, and sparse matrix algorithms are effectively employed to gain computational efficiency [4]. However, implicit numerical integration methods applied to mixed systems of differential and algebraic equations lead to numerical difficulties associated with badly conditioned matrices and artificially stiff problems [5].

Numerical difficulties associated with stiffness of equations have to some extent been circumvented in other methods of equation formulation by replacing the Cartesian coordinates with a smaller set of Lagrangian coordinates, equal in number to the constrained system degrees of freedom [6,7,8]. Loop closure or related methods are used to formulate constraint relations, yielding a smaller number of highly coupled differential equations. This is desirable from a numerical integration standpoint and leads to effective computer programs. However, depending upon the set of Lagrangian coordinates selected and the method of constraint formulation, it is difficult to incorporate nonstandard user-supplied constraints. Provision for user-supplied

constraints thus leads to increased complexity in general-purpose computer programs. It is apparent that there is a trade-off between program generality in the first approach and program efficiency in the second.

A generalized coordinate partitioning method presented in reference 9 retains desirable features of both of the above methods: (1) the simple constraint formulation of the first in terms of Cartesian coordinates, and (2) the minimal system of differential equations of motion of the second, equal in number to the constrained system degrees of freedom. Excess coordinates are eliminated numerically, rather than analytically in the second method above. Gaussian elimination with full pivoting and subsequent L-U factorization [10] is applied to the Jacobian matrix of the constraint equations to determine: (1) the number of system degrees of freedom [11,12], (2) partitioning of generalized coordinates into independent and dependent sets, and (3) construction of an influence coefficient matrix expressing dependent velocities in terms of independent velocities [6, 13, 14]. This method incorporates the desirable numerical stability properties of Gaussian elimination with full pivoting; that is associated with the resulting L and U matrices [15]. The numerical advantages of this approach have been demonstrated from a kinematic point of view in references 16 and 17. The generalized coordinate partitioning method was employed to develop a computer code for the solution of dynamic response of planar mechanical systems. Numerical results have demonstrated improved computational efficiency and superiority of the method over the previously developed codes.

In this report, the generalized coordinate partitioning method is applied to determine the dynamic response of three-dimensional mechanical systems. Cartesian generalized coordinates define the translational degrees of freedom of each rigid body.

In a preliminary formulation and code development of three-dimensional rigid-body mechanics, Euler angles were employed to define rotational degrees of freedom. The computer code was used to determine the dynamic response of a variety of three-dimensional mechanisms. A significant reduction in computer execution time was demonstrated in all of the simulations, using the generalized coordinate partitioning method. However, the use of Euler angles often causes numerical difficulties when one or more of the rigid bodies experience large rotations. In particular, when the second Euler rotation angle is equal to $k\pi$ ($k = 0,1,2,\ldots$), the axes of the first and third rotation angles coincide, so these two angles cannot be uniquely determined. Therefore, some constraint equations become dependent at that instant and a unique solution does not exist. A method to circumvent this problem is to monitor the row rank of the constraint Jacobian matrix. The matrix loses rank when the second Euler rotation angles approach $k\pi$. Before this occurs, the computation can be interrupted and the body fixed coordinate systems rotated to new positions. This technique can be performed automatically by the algorithm. However, it is time-consuming and in general cannot be done easily. The above feature is an inherent problem of Euler angle representation and cannot be eliminated completely. Euler parameters, in contrast to Euler angles or any other set of three-rotational generalized coordinates, have no critical singular cases [17], thus they are attractive for formulating system constraint and differential equations of motion in this respect.

2. GENERALIZED COORDINATE PARTITIONING

Denote the vector of generalized coordinate of body i by $\underline{q}_i$; $\underline{q}_i \equiv [x, y, z, e_0, e_1, e_2, e_3]_i^T$, and the composite vector of all system generalized

coordinate by $\underline{q} = [\underline{q}_1^T, \underline{q}_2^T, \ldots, \underline{q}_n^T]^T$, where n is the number of rigid bodies and T denotes vector or matrix transpose. In this notation, holonomic constraint equations can be written in vector function form as

$$\underline{\Phi}(\underline{q};t) = 0 \tag{2.1}$$

where $\underline{\Phi}(\underline{q};t) = [\Phi_1(\underline{q};t), \Phi_2(\underline{q};t), \ldots, \Phi_m(\underline{q};t)]^T$ are assumed to be independent. The Jacobian matrix for Eq. (2.1) is defined as

$$\underline{\Phi}_{\underline{q}} = \frac{\partial \underline{\Phi}}{\partial \underline{q}} \equiv \frac{\partial \Phi_i}{\partial q_j} \tag{2.2}$$

and has full row rank. Differentiation of Eq. (2.1) with respect to time gives the kinematic velocity equation

$$\underline{\Phi}_{\underline{q}} \dot{\underline{q}} + \underline{\Phi}_t = 0 \tag{2.3}$$

Gauss-Jordan reduction of the matrix $\underline{\Phi}_{\underline{q}}$ with full pivoting obtains a partitioning of $\underline{\Phi}_{\underline{q}} = [\underline{\Phi}_{\underline{u}}, \underline{\Phi}_{\underline{v}}]$ and $\underline{q} = [\underline{u}^T, \underline{v}^T]^T$, where $\underline{u}$ and $\underline{v}$ are the vectors of dependent and independent coordinates respectively, such that $\underline{\Phi}_{\underline{u}}$ is the nonsingular submatrix of $\underline{\Phi}_{\underline{q}}$ whose columns correspond to elements $\underline{u}$ of $\underline{q}$ and $\underline{\Phi}_{\underline{v}}$ is the submatrix of $\underline{\Phi}_{\underline{q}}$ whose columns correspond to elements $\underline{v}$ of $\underline{q}$ [9]. Eq. (2.3) can be written in partitioned form as

$$\underline{\Phi}_{\underline{u}} \dot{\underline{u}} + \underline{\Phi}_{\underline{v}} \dot{\underline{v}} = -\underline{\Phi}_t$$

Since $\underline{\Phi}_{\underline{u}}$ is nonsingular,

$$\dot{\underline{u}} = -\underline{\Phi}_{\underline{u}}^{-1} \underline{\Phi}_{\underline{v}} \dot{\underline{v}} - \underline{\Phi}_{\underline{u}}^{-1} \underline{\Phi}_t = \underline{H}\dot{\underline{v}} - \underline{\Phi}_{\underline{u}}^{-1} \underline{\Phi}_t \tag{2.4}$$

The system equations of motion can be expressed as [9]

$$\underline{M}(\underline{q})\ddot{\underline{q}} = \underline{g}(\underline{q},\dot{\underline{q}};t) - \underline{\Phi}_{\underline{q}}^T(\underline{q};t)\underline{\lambda} \tag{2.5}$$

where $\underline{M}(\underline{q})$ is the system mass matrix, $\underline{g}(\underline{q},\dot{\underline{q}};t)$ is the vector of modified generalized forces (refer to Eqs. (5.6) through (5.10)), and $\underline{\lambda}$ is a vector of

Lagrange multipliers. Partitioning Eq. (2.5) according to $\underline{u}$ and $\underline{v}$ yields

$$M^{uu}\ddot{\underline{u}} + M^{uv}\ddot{\underline{v}} = \underline{g}^{u} - \underline{\Phi}_{u}^{T}\underline{\lambda} \tag{2.6}$$

$$M^{vu}\ddot{\underline{u}} + M^{vv}\ddot{\underline{v}} = \underline{g}^{v} - \underline{\Phi}_{v}^{T}\underline{\lambda} \tag{2.7}$$

By eliminating $\underline{\lambda}$ from Eqs. (2.6) and (2.7), since $\underline{\Phi}_{u}^{T}$ is nonsingular, it can be found that

$$\left(M^{vv} + H^{T}M^{uv}\right)\ddot{\underline{v}} + \left(M^{vu} + H^{T}M^{uu}\right)\ddot{\underline{u}} = \underline{g}^{v} + H^{T}\underline{g}^{u} \tag{2.8}$$

Differentiation and partitioning of Eq. (2.3) yields

$$\ddot{\underline{u}} = H\ddot{\underline{v}} - \underline{\Phi}_{u}^{-1}\left[\left(\underline{\Phi}_{q}\dot{\underline{q}}\right)\dot{\underline{q}} + 2\underline{\Phi}_{tq}\dot{\underline{q}} + \underline{\Phi}_{tt}\right] \tag{2.9}$$

Equation (2.5) can thus be reduced to a system of second-order differential equations explicitly in terms of the independent generalized coordinates $\underline{v}$. In order to express Eq. (2.9) in first order form, define the vector $\underline{s}$ of independent velocities as

$$\dot{\underline{v}} = \underline{s} \tag{2.10}$$

The velocities $\dot{\underline{q}}$, in terms of $\underline{s}$, using Eq. (2.4), can be written as

$$\underline{w}(\underline{s}) = \dot{\underline{q}}(\underline{s}) = \begin{Bmatrix} \dot{\underline{u}} \\ \dot{\underline{v}} \end{Bmatrix} = \begin{Bmatrix} H\underline{s} - \underline{\Phi}_{u}^{-1}\underline{\Phi}_{t} \\ \underline{s} \end{Bmatrix} \tag{2.11}$$

With this notation and Eq. (2.9), Eq. (2.8) becomes

$$\left[\left(M^{vv} + H^{T}M^{uv}\right) + \left(M^{vu} + H^{T}M^{uu}\right)H\right]\dot{\underline{s}} = \underline{g}^{v} + H^{T}\underline{g}^{u} +$$

$$\left(M^{vu} + H^{T}M^{uu}\right)\underline{\Phi}_{u}^{-1}\left[\left(\underline{\Phi}_{q}\underline{w}\right)\underline{w} + 2\underline{\Phi}_{tq}\underline{w} + \underline{\Phi}_{tt}\right] \tag{2.12}$$

Equations (2.10) and (2.12) form a set of the first-order differential equations for the independent generalized coordinates $\underline{v}$ and velocities $\underline{s}$. All terms in Eq. (2.3) are determined as functions of $\underline{v}$ and $\underline{s}$ through the constraint equations

of Eq. (2.1) and Eq. (2.11). Solution of this system yields the complete system state, including Lagrange multipliers if constraint reaction forces are desired.

3. GENERALIZED COORDINATES FOR THE ANGULAR ORIENTATION OF A RIGID BODY

In order to specify the angular orientation of a rigid body in an inertial (global) coordinate system xyz, it is sufficient to specify the angular orientation of a coordinate system $\xi\eta\zeta$ that is rigidly attached to the body. In this paper, coordinate rotations defined by Euler parameters are discussed and employed in the following formulation.

3.1 Transformation Matrix

Let the coordinate system $\xi_i \eta_i \zeta_i$ be attached to body i as shown in Fig. 3.1, where the origin O_i is located at its center of mass (CM). A point P_i on body i is located in the inertial coordinate system xyz by

$$\underset{-i}{r}^P = \underset{-i}{r} + A_i \underset{-i}{s'}^P \tag{3.1}$$

where $\underset{-i}{s'}^P \equiv [\xi^P, \eta^P, \zeta^P]_i^T$ are the coordinates of P_i in the $\xi_i \eta_i \zeta_i$ coordinate system, $\underset{-i}{r} \equiv [x, y, z]_i^T$ are the coordinates of O_i in the xyz coordinate system, and A_i is the rotational transformation matrix of body i. Matrix A_i, expressed in terms of Euler parameters e_0, e_1, e_2, e_3, is

$$A_i = 2\begin{bmatrix} e_0^2 + e_1^2 - 1/2 & e_1 e_2 - e_0 e_3 & e_1 e_3 + e_0 e_2 \\ e_1 e_2 + e_0 e_3 & e_0^2 + e_2^2 - 1/2 & e_2 e_3 - e_0 e_1 \\ e_1 e_3 - e_0 e_2 & e_2 e_3 + e_0 e_1 & e_0^2 + e_3^2 - 1/2 \end{bmatrix}_i \tag{3.2}$$

where subscript i indicates transformation matrix for body i [17]. The four Euler parameters are required to satisfy the equation

$$e_0^2 + \underline{e}^T \underline{e} \equiv e_0^2 + e_1^2 + e_2^2 + e_3^2 = 1 \tag{3.3}$$

The parameters $\underline{e} \equiv [e_1, e_2, e_3]^T$ are the x, y, z or ξ, η, ζ projections of a vector $\vec{e}$ lying on the axis of instantaneous rotation, as shown in Fig. 3.2, and $\vec{e}$ is defined by

$$\vec{e} = \vec{u} \sin \frac{\chi}{2} \tag{3.4}$$

where $\vec{u}$ is a unit vector on the axis of rotation and χ is the angle of rotation. The fourth parameter e_0 is given by

$$e_0 = \cos \frac{\chi}{2}$$

It should be noted that the constraint equations (2.1) include Eqs. (3.3) for all of the n rigid bodies.

4. CONSTRAINT EQUATIONS

Standard constraints between rigid bodies are taken as friction free (workless) joints. Formulations for five types of constraints are presented here as follows:

Spherical Joint: Figure 4.1 shows two adjacent bodies i and j connected by a spherical joint (ball joint). A vector loop equation can be written as

$$\vec{r}_i + \vec{s}_i - \vec{s}_j - \vec{r}_j = \vec{0} \tag{4.1}$$

The scalar equations for this joint, determined by the use of Eq. (3.1), are

$$\underline{r}_i + A_i \underline{s}_i'^P - \underline{r}_j - A_j \underline{s}_j'^P = \underline{0} \tag{4.2}$$

Revolute Joint: Figure 4.2 depicts a revolute joint between bodies i and j. Point P is common to both bodies and points Q_i and Q_j are located on bodies i and j, respectively defining the axis of rotation of the joint. Scalar Eq. (4.2) holds for this joint, since point P simply acts as a sperical joint. Additional constraints are obtained by requiring the cross product of vectors $\vec{g}_i$ and $\vec{g}_j$ to be zero, which forces the points P, Q_i, and Q_j to be on a common line. Vectors $\vec{g}_i$ and $\vec{g}_j$ can be expressed in component form as

$\underline{g}_i \equiv [u,v,w]_i^T$ and $\underline{g}_j \equiv [u,v,w]_j^T$ respectively where

$$\underline{g}_k \equiv A_k(\underline{s}'^Q_k - \underline{s}'^P_k) \quad ; \qquad k = i, j \tag{4.3}$$

Then, the cross product of $\underline{g}_i$ and $\underline{g}_j$, set equal to zero, yields three scalar equations

$$\tilde{\underline{g}}_i \underline{g}_j = \underline{0} \tag{4.4}$$

where $\tilde{\underline{g}}_i$ is a skew-symmetric matrix containing the components of $\underline{g}_i$, defined as

$$\tilde{\underline{g}}_i \equiv \begin{bmatrix} o & -w & v \\ w & o & -u \\ -v & u & o \end{bmatrix}_i$$

From the three equations of Eq. (4.4), only two are independent. The best two should be selected, with Eq. (4.2), to form five constraint equations for the revolute joint. To avoid numerical difficulties, proper selection of equations from Eq. (4.4) is important, particularly when the joint axis is parallel to one of the global axes. For example, when the joint axis is

parallel to the z axis, the first equation of (4.4) yields zero entries in the corresponding row of the Jacobian matrix, reducing its rank. The second and third equations would be selected in this case. A technique for selection of the proper equations is:

> compare the absolute values of u_i, v_i, and w_i (or u_j, v_j, and w_j) and select the two equations having the largest terms.

Universal Joint: A universal joint between bodies i and j is shown in Fig. 4.3. Since point P is common to both bodies, constraint Eqs. (4.2) again apply to this joint. The remaining constraint is that the two vectors $\vec{g}_i$ and $\vec{g}_j$ remain perpendicular, thus their dot product is set to zero, i.e.

$$\underline{g}_i^T \underline{g}_j = 0 \tag{4.5}$$

Cylindrical Joint: A cylindrical joint forces two bodies i and j to move along a common axis. Four points, P_i, Q_i on body i and P_j, Q_j on body j, are to lie on the same axis as shown in Fig. 4.4. The vectors $\vec{g}_i$ and $\vec{g}_j$ of constant magnitudes and $\vec{g}_{ij}$ of variable magnitude are required to remain collinear. Therefore, the constraint equations defining a cylindrical joint can be found from two cross products

$$\tilde{\underline{g}}_i \underline{g}_j = 0 \tag{4.6}$$

$$\tilde{\underline{g}}_i \underline{g}_{ij} = 0 \tag{4.7}$$

where two equations from Eqs. (4.6) and two from Eqs. (4.7) should be selected based on the technique described for the revolute joint.

Translational (Prismatic) Joint: A translational joint is similar to a cylindrical joint, with the exception that the two bodies cannot rotate relative to each other. Therefore, the cylindrical joint equations must hold and one additional equation is required. Two vectors, $\vec{h}_i$ and $\vec{h}_j$ on bodies i and j as shown in Fig. 4.5, are to be perpendicular, so

$$\underset{-i}{h}^T \underset{-j}{h} = 0 \tag{4.8}$$

5. RIGID BODY DYNAMICS

For body i, let $\underset{-i}{\omega'} = [\omega_\xi, \omega_\eta, \omega_\zeta]_i^T$ be the projection of the angular velocity vector on the local coordinates axes, $\underset{-i}{r} = [x, y, z]_i^T$ be the global location of the center of mass, m_i be the mass and $I_{\xi\xi}$, $I_{\eta\eta}$, $I_{\zeta\zeta}$, $I_{\xi\eta}$, $I_{\eta\zeta}$, $I_{\zeta\xi}$ be the moments and products of inertia about the ξ_i, η_i, ζ_i axes. The kinetic energy of the ith body can be written as

$$T_i = \frac{1}{2} \dot{\underset{-i}{r}}^T J_{i-i} \dot{\underset{-i}{r}} + \frac{1}{2} \underset{-i}{\omega'}^T I_{i-i} \underset{-i}{\omega'} \tag{5.1}$$

where

$$J_i = \begin{bmatrix} m & 0 & 0 \\ 0 & m & 0 \\ 0 & 0 & m \end{bmatrix}_i , \qquad I_i = \begin{bmatrix} I_{\xi\xi} & I_{\xi\eta} & I_{\xi\zeta} \\ I_{\eta\xi} & I_{\eta\eta} & I_{\eta\zeta} \\ I_{\zeta\xi} & I_{\zeta\eta} & I_{\zeta\zeta} \end{bmatrix}_i$$

Angular velocity $\underset{-i}{\omega'}$ in terms of Euler parameters can be expressed as [17]

$$\underset{-i}{\omega'} = 2B_{i-i} \dot{\underset{-i}{p}} \tag{5.2}$$

where $\underset{-}{p}_i \equiv [e_0, e_1, e_2, e_3]_i^T$, $\dot{\underset{-}{p}}_i \equiv [\dot{e}_0, \dot{e}_1, \dot{e}_2, \dot{e}_3]_i^T$ and

$$B_i = \begin{bmatrix} -e_1 & e_0 & e_3 & -e_2 \\ -e_2 & -e_3 & e_0 & e_1 \\ -e_3 & e_2 & -e_1 & e_0 \end{bmatrix}_i \tag{5.3}$$

Seven equations of motion for the ith body are written as [19]

$$\frac{d}{dt}\left(T_{\underline{r}_i}\right)^T + \Phi_{\underline{r}_i}^T \underline{\lambda} - \underset{-}{f}_i = 0 \qquad \text{(3 eqs)} \tag{5.4}$$

$$\frac{d}{dt}\left(T_{\underline{p}_i}\right)^T - T_{\underline{p}_i}^T + \Phi_{\underline{p}_i}^T \lambda - \underset{-}{h}_i = 0 \qquad \text{(4 eqs)} \tag{5.5}$$

where $\underline{f}_i$ and $\underline{h}_i$ are the vectors of generalized forces and torques corresponding to generalized coordinates $\underset{-}{r}_i$ and $\underset{-}{p}_i$ respectively. Substitution of Eq. (5.1) into Eqs. (5.4) and (5.5) yields

$$J_i \ddot{\underset{-}{r}}_i + \Phi_{\underline{r}_i}^T \lambda = \underset{-}{f}_i \tag{5.6}$$

$$4B_i^T I_i B_i \ddot{\underset{-}{p}}_i + \Phi_{\underline{p}_i}^T \lambda = \underset{-}{h}_i - 8\dot{\underset{-}{P}}_i^T I_i B_i \dot{\underset{-}{p}}_i \tag{5.7}$$

Defining $\underset{-}{g}_i = [\underline{f}^T, (\underline{h} - 8\dot{\underline{p}}^T IB\dot{\underline{p}})^T]_i^T$ and

$$M_i = \begin{bmatrix} \begin{bmatrix} m & 0 & 0 \\ 0 & m & 0 \\ 0 & 0 & m \end{bmatrix}_i & \phi \\ \phi & [4B^T IB]_i \end{bmatrix} \quad (7\times 7 \text{ matrix}) \tag{5.8}$$

Eqs. (5.6) and (5.7) can be written as

$$M_i \ddot{\underline{q}}_i = \underline{g}_i - \Phi_{\underline{q}_i}^T \lambda \tag{5.9}$$

where $\underline{q}_i = [\underline{r}^T, \underline{p}^T]_i^T \equiv [x, y, z, e_0, e_1, e_2, e_3]_i^T$. The total system equations of motion for n rigid bodies is then

$$M\ddot{\underline{q}} = \underline{g} - \Phi_{\underline{q}}^T \lambda \tag{5.10}$$

where $M \equiv \text{diag.}\ [M_1, M_2, \ldots, M_n]$, $\underline{g} \equiv [\underline{g}_1^T, \underline{g}_2^T, \ldots, \underline{g}_n^T]^T$ and $\underline{q} \equiv [\underline{q}_1^T, \underline{q}_2^T, \ldots, \underline{q}_n^T]^T$. It should be noted that Eq. (5.10) defines the equations of motion of Eq. (2.5).

6. FORCES

Internal forces acting between bodies may be obtained by a process similar to the constraint equation development. For example, since springs, dampers, and actuators generally appear together, as shown in Fig. 6.1, they are incorporated into a single set of equations [1]. Let the global coordinates of the attachment points be $\underline{r}_k \equiv [u,v,w]_k^T$, $k = i,j$. The length of the spring-damper-actuator is thus

$$\ell = [(u_j - u_i)^2 + (v_j - v_i)^2 + (w_j - w_i)^2]^{1/2} \tag{6.1}$$

and the time rate of change in spring length is

$$\dot{\ell} = [(u_j - u_i)(\dot{u}_j - \dot{u}_i) + (v_j - v_i)(\dot{v}_j - \dot{v}_i) + (w_j - w_i)(\dot{w}_j - \dot{w}_i)]/\ell \tag{6.2}$$

The magnitude of the spring-damper-actuator force is then written as

$$f = k(\ell - \ell^{o}) + c\dot{\ell} + a \tag{6.3}$$

where ℓ^{o} is the undeformed length of the spring and k, c, and a are the spring constant, damping coefficient, and actuator force, respectively. The components of spring-damper-actuator force in the global coordinate system can be determined from

$$\underset{-k}{f} = f(\underset{-k}{r} - \underset{-m}{r})/\ell \quad ; \quad k,m = i,j \text{ and } k \neq m \tag{6.4}$$

When the spring-damper-actuator force does not act through the center of mass of the attached bodies, torque components for each body can be calculated from

$$\underset{-k}{h'} = \underset{-k}{\tilde{r}'} \underset{k}{A}^{T} \underset{-k}{f} \quad ; \quad k = i,j \tag{6.5}$$

where $\underset{-k}{h'}$ is the vector of components of torque about ξ_k, η_k, ζ_k axes. Transformation of the components of the torque $\underset{-i}{h'} \equiv [h_\xi, h_\eta, h_\zeta]_i^T$ to $\underset{-i}{h'} \equiv [h_{e_0}, h_{e1}, h_{e2}, h_{e3}]_i^T$ can be obtained by multiplying both sides of Eq. (5.2) by $\underset{-i}{h'}^{T}$ to get

$$\underset{-i}{h'}^{T} \underset{-i}{\omega'} = 2\, \underset{-i}{h'}^{T} \underset{-i}{B}\, \underset{-i}{\dot{p}} \tag{6.6}$$

The instantaneous power $\underset{-i}{h'}^{T} \underset{-i}{\omega'}$ is independent of coordinate system representation, so $\underset{-i}{h'}^{T} \underset{-i}{\omega'} = \underset{-i}{h}^{T} \underset{-i}{\dot{p}}$ and Eq. (6.6) becomes

$$\underset{-i}{h} = 2\underset{i}{B}^{T} \underset{-i}{h'} \tag{6.7}$$

Substitution of Eq. (6.5) into Eq. (6.7) yields

$$\underline{h}_k = 2B_k^T \underline{r}'^{\sim}_k A_k^T \underline{f}_k \quad ; \; k = i,j \tag{6.8}$$

Similar to the translational spring-damper-actuator, torsional spring-damper-actuator elements may be defined between adjacent bodies i and j that are connected by a revolute joint, as shown in Fig. 6.2. Two vectors, $\vec{s}_i$ and $\vec{s}_j$, embedded in bodies i and j respectively, define a plane perpendicular to the revolute joint axes. In addition, the two vectors define the torsional spring attachment points on the two bodies. The angle between $\vec{s}_i$ and $\vec{s}_j$ is denoted by θ and is initially assumed to be $0 \leq \theta \leq \pi$. Angle θ can be calculated from the equation

$$\theta = \cos^{-1} \frac{\underline{s}_i^T \underline{s}_j}{|\vec{s}_i| \cdot |\vec{s}_j|} , \qquad 0 \leq \theta \leq \pi \tag{6.9}$$

To determine all possible values of θ, a point K is initially defined on the revolute joint axis such that the direction of vector $\vec{s}$ is determined by the right hand screw law rotating from $\vec{s}_i$ to $\vec{s}_j$ and sweeping angle θ (initially $0 \leq \theta \leq \pi$). During the dynamic analysis, the cross product of $\vec{s}_i$ and $\vec{s}_j$ yields a vector parallel to $\vec{s}$, having the same direction if $0 \leq \theta \leq \pi$, and opposite direction if $\pi \leq \theta \leq 2\pi$, i.e.;

$$\underline{s}^T \underline{s}_i^{\sim} \underline{s}_j \begin{cases} > 0 \; ; & 0 \leq \theta \leq \pi \\ < 0 \; ; & \pi \leq \theta \leq 2\pi \end{cases} \tag{6.10}$$

The torque of a torsional spring-damper-actuator element can be calculated from

$$h = k\,(\theta - \theta^{o}) + c\dot{\theta} + a_t \tag{6.11}$$

where k, c, a_t, and θ^{o} are the torsional spring stiffness, damping coefficient, actuator torque, and undeformed angle of the element, respectively. If the components of a unit vector $\vec{u}$ located on the revolute joint axis are $\underline{u}'_i$ and $\underline{u}'_j$, expressed in body i and body j coordinate systems, respectively, the components of torque expressed in these coordinate systems is

$$\underline{h}'_k = h\underline{u}'_k \quad ; \qquad k = i,j \tag{6.12}$$

Thus the generalized torques corresponding to the Euler parameters coordinates can be determined by employing Eq. (6.7).

6.1 Friction [20]

The characteristics of sliding or Coulomb friction obtained from a simple experiment shown in Fig. 6.3 are illustrated in Fig. 6.4. In Fig. 6.4, μ_s and μ_k represent the static and kinetic coefficients of friction respective. If the absolute value of the applied force $\vec{P}$ on the body is less than $\mu_s N$, where N is the normal force, the friction force may vary from zero to $\mu_s N$. In this case the magnitude of friction force should be determined from an equation of static equilibrium. When the absolute value of P is greater than $\mu_s N$, the friction force is $\mu_k N$ which is relatively constant until a high velocity is reached.

The friction force expressed in terms of relative displacement is a step function as shown in Fig. 6.5. In the case of no relative displacement between the two bodies, friction force may vary from $-\mu N$ to μN. To find the magnitude of friction force in this case, assume a shear deformation without relative

displacement. If the proportional constant between shear deformation and shear force is given, the shear force may be obtained from the shear deformation. By taking the smaller of shear force or friction force, the magnitude of friction force can be determined.

To find the direction of friction force, the relative velocity, $\vec{v}_r$, between the two bodies at the point of contact is determined. The friction force can be obtained from:

$$\vec{F}_f = \min(F_f, F_s) \frac{\vec{V}_r}{|V_r|}$$

where $F_f = \mu N$ and F_s is the shear force. Since the friction force acts along the body surfaces and its line of action does not generally pass through the conter of mass of the body, the moment components due to this force must also be considered. For this purpose an equation similar to Eq. 6.8 can be applied.

7. DADS-3-D COMPUTER PROGRAM

A general-purpose computer program, Dynamic Analysis and Design System for analysis of three-dimensional mechanisms (DADS-3-D), has been developed, using the algebraic equations of constraint and differential equations of motion described in the preceding sections. All of the algebraic and differential equations are automatically assembled by the program from the input data describing the system. Additional nonstandard constraints and differential equations can be provided through user-supplied subroutines. Since interpretation of Euler parameters is difficult, input data can be expressed in terms of Euler angles or direction cosines.

The use of the Cartesian and Euler parameter generalized coordinates yields a maximal set of loosely coupled nonlinear holonomic constraints and differential equations of motion. A Gaussian elimination algorithm with full

pivoting [10] decomposes the constraint Jacobian matrix and identifies dependent and independent generalized coordinates. The constraint Jacobian matrix in general is sparse, thus the algorithm provides the necessary information to establish a modified sparse matrix relating variations in dependent and independent variables. This process eliminates the need for carrying out products of sparse matrices. This information is then employed to identify a minimal system of the second-order differential equations of motion equal in number to system degrees of freedom. The second-order differential equations of motion are reduced to the first-order form by a change of variable and solved by the predictor/corrector numerical integration algorithm DE/STEP/INTRP [18]. The algorithm numerically integrates the differential equations for independent generalized coordinates and extrapolates the remaining equations for the dependent generalized coordinates. At each step, integration error is evaluated and time step and integration order are adjusted accordingly [18].

The generalized coordinate partitioning technique and the predictor/ corrector numerical integration method have demonstrated improved efficiency over a previously developed computer code. However, the major contribution of this investigation is application of Euler parameters to circumvent singularity problems and enhance program efficiency. The user manual for DADS-3-D code is provided in Appendix F.

8. THREE-DIMENSIONAL MODEL OF TRACKED VEHICLES

The DADS-3-D code is employed to simulate a highly nonlinear multiple degree-of-freedom vehicular system. Figure 8.1 depicts a computer-generated three-dimensional model of a 26 degree-of-freedom tracked vehicle with five roadwheels per side. The transient response of the vehicle to a large weapon firing impulse is desired. Figure 8.2 illustrates the side view of the model in detail. The model consists of 17 rigid bodies. Bodies 1 to 10 represent

roadwheels. Bodies 11 and 12 are the chassis and turret respectively. These two bodies are connected by a vertical revolute joint. Body 13 models the recoiling and nonrecoiling parts of the gun. A second revolute joint between bodies 12 and 13 models the trunion centerline. Bodies 14 to 17 represent road arms connecting the front and rear roadwheels to the chassis with revolute joints. These bodies are introduced for the convenience of connecting shock absorbers between road arms and chassis. The remaining six roadwheels are attached to the chassis using massless links with revolute joints at the ends.

The vehicle has a torsion bar suspension system. Translational spring-damper-actuators 1 to 10 are employed to incorporate the nonlinear suspension characteristics, including jounce stops. Figure 8.3 illustrates typical force-displacement suspension characteristics. This force displacement relation as well as other nonlinear functions are incorporated into the model from discrete data points. Actuators 11 to 14 implement the damping characteristics of Fig. 8.4. Springs 15 to 26 simulate two pretentioned tracks connecting the drive sprockets and roadwheels. These nonlinear springs do not support compression.

Additional generalized forces are introduced to represent roadwheel-ground interaction. These nonlinear functions allow the wheels to leave the ground and include damping. Frictional forces proportional to the normal component of the wheel-ground reaction oppose tangential displacement at the point of contact.

8.1 Platform Stability Analysis

The vehicle is allowed to achieve an equilibrium configuration prior to initiating transient analysis. Prior to firing, two additional constraints are applied to lock the relative rotational degrees-of-freedom between the

turret-chassis and the gun-turret. A force with an impulse of 3851 lbs.s (139300 lbs. lasting 0.02765 s), that simulates recoil due to firing the main weapon, is applied to the model along the gun barrel centerline.

First simulation is performed for forward-firing of the gun. The gun is initially horizontal. Friction model includes only the coulomb friction. Appendix A presents the response plots for this simulation. A peak longitudinal acceleration of 3.25 g's is reached. Maximum longitudinal displacement of the chassis is 3 in., where approximately 1.5 in. is due to sliding. The chassis pitches about 4°, while the maximum lift of the front wheels is 7 in.

The gun is rotated 45° horizontally for the second simulation. The response plots are given in Appendix B. The longitudinal and lateral peak accelerations are 2.33 g's and 2.22 g's respectively. The maximum pitch, roll, and yaw angles are 3.2°, 3.0°, and 1.7° respectively. The plot of the yaw angle versus time reveals the yaw rotation does not recover, i.e., the vehicle comes to rest with 1.7° rotation about the vertical axis from its original orientation. Longitudinal and lateral displacement curves of the chassis show that the c.g. of the chassis has moved 3 in. longitudinally and 2.8 in. laterally.

Response plots of a side fire simulation are given in Appendix C. A peak lateral acceleration of 3.25 g's has been achieved for the chassis. The lateral displacement curve of the chassis indicates 5.5 in. of sliding. The maximum roll angle is 4° and a non-recoverable yaw of 1.5° can be observed. The yaw rotation is the result of the impulse line of action not crossing the vertical line which passes through the combined c.g. of the vehicle.

Two additional simulations for the 45° impulse and side fire have been made. The response plots are presented in Appendices D and E. The major difference between these two models and previous models is the inclusion of ground-track shear deformation in the friction model. These simulations show that the shear deformation model introduces high-frequency components in the system (stiff system), therefore the CPU time increases drastically. The responses shown in Appendices D and E should not be compared with the plots of Appendices B and C, because some of the inertial characteristics of the models are different.

8.2 Elevation and Azimuth Stabilization

In order to test the nonstandard element capability (user-supplied equations) of the DADS-3-D code, an additional set of differential equations is formulated and solved along with the mechanical system differential equations. This set of additional differential equations models two stabilization systems for elevation and azimuth controls. The basic structure of the elevation and azimuth control systems is identical, and Fig. 8.5 shows the schematics of one of the two control systems [21]. The input to the control system is the gunner's command on the desired angle, with the additional feedback input from the gun angular position and velocity. Each control system, containing an electro-hydraulic servocontrol device, generates a torque output which is applied to change the angular position of the gun in elevation or azimuth. Figure 8.6 shows the responses of a simulation of the vehicle with two-axis controller to the gunner's command to readjust the elevation angle of the gun from its initial position. Readjustment of the azimuth angle to the gunner's command is illustrated in Fig. 8.7. Figure 8.8 shows the response of simultaneous change in elevation and azimuth angles with the two-axis controller.

REFERENCES

1. Orlandea, N., Chase, M.A., and Calahan, D.A., "A Sparsity-Oriented Approach to the Dynamic Analysis and Design of Mechanical Systems, Parts I and II", ASME, Journal of Engineering for Industry, Vol. 99, Series B, August 1977, pp. 773-784.

2. Orlandea, N. and Calahan, D.A., "Description of a Program for the Analysis and Optimal Design of Mechanical Systems", Report No. AFOSRTR-73-2026, University of Michigan, Nov. 15, 1973.

3. Haug, E.J., Wehage, R.A. and Barman, N.C., "Dynamic Analysis and Design of Constrained Mechanical Systems", ASME Journal of Mechanical Design, Vol. 103, No. 3, 1981, pp. 560-570.

4. Duff, I.S., "MA29-A Set of FORTRAN Subroutines for Sparse Unsymmetric Linear Equations", Report No. AERE-R.8730, Computer Science and System Division, AERE Harwell, Oxfordshire, July 1977.

5. Gear, C.W., "Simultaneous Numerical Solution of Differential Algebraic Equations", IEEE Transactions on Circuit Theory, Vol. CT-18, Jan. 1971, pp. 89-95.

6. Paul, B., "Analytical Dynamics of Mechanisms-A Computer Oriented Overview", Mechanism and Machine Theory, 1975, Vol. 10, pp. 481-507.

7. Chace, M.A., and Sheth, P.M., "Adaptation of Computer Techniques to the Design of Mechanical Dynamic Machinery", ASME Paper 73-DET-58, 1973.

8. Paul, B., "Dynamic Analysis of Machinery Via Program DYMAC", SAE Paper 770049, 1977.

9. Wehage, R.A. and Haug, E.J., "Generalized Coordinate Partitioning for Dimension Reduction in Analysis of Constrained Dynamic Systems", ASME Paper 80-DET-106, 1980.

10. System/360 Scientific Subroutine Package (360A-CM-03X), Programmer's Manual (H20-0205-4), 1970.

11. Paul, B., "A Unified Criterion for the Degree of Constraint of Plane Kinematic Chains", ASME, Journal of Applied Mechanics, Vol. 27, Series E., Vol. 82, 1960, pp. 196-200.

12. Freudenstein, F., "On the Variety of Motions Generated by Mechanisms", ASME, Journal of Engineering for Industry, Vol. 84, Ser. B, 1962, pp. 156-160.

13. Paul, B., and Krajcinovic, D., "Computer Analysis of Machines with Planar Motion, Part 1-Kinematics, Part 2-Dynamics", ASME, Journal of Applied Mechanics, Vol. 37, No. 3, Trans. ASME, Vol. 92, Series E, Sept. 1970, pp. 697-712.

14. Forsythe, G.E., and Moler, C.B., Computer Solution of Linear Algebraic Systems, Prentice-Hall, Englewood Cliffs, N.J., 1967.

15. Sheth, P.N., "Improved Iterative Techniques for the (4 x 4) Matrix Method of Kinematic Analysis", M.S. Thesis, Mechanical Engineering, University of Wisconsin, 1968.

16. Sheth, P.N., "A Digital Computer Based Simulation Procedure for Multiple Degree of Freedom Mechanical Systems with Geometrical Constraints", Ph.D. Thesis, Mechanical Engineering, University of Wisconsin, 1972.

17. Wittenberg, J., Dynamics of Systems of Rigid Bodies, G.G. Teubner Stuttgart, 1977.

18. Shampine, L.F., and Gordon, M.K., Computer Solution of Ordinary Differential Equations: The Initial Value Problem, W.J. Freeman, San Francisco, CA, 1975.

19. Greenwood, D. T., Principles of Dynamics, Prentice-Hall, 1965.

20. Agrowal, O.P., Haug, E.J., and Wehage, R.A., "Some Friction Models for Dynamic Analysis of Mechanical Systems", Technical Report No. 81-10, CCAD, University of Iowa, October 1981.

21. Lance, G.M., "Control of Systems with Mass Unbalance", Technical Report No. 81-8, CCAD, University of Iowa, September 1981.

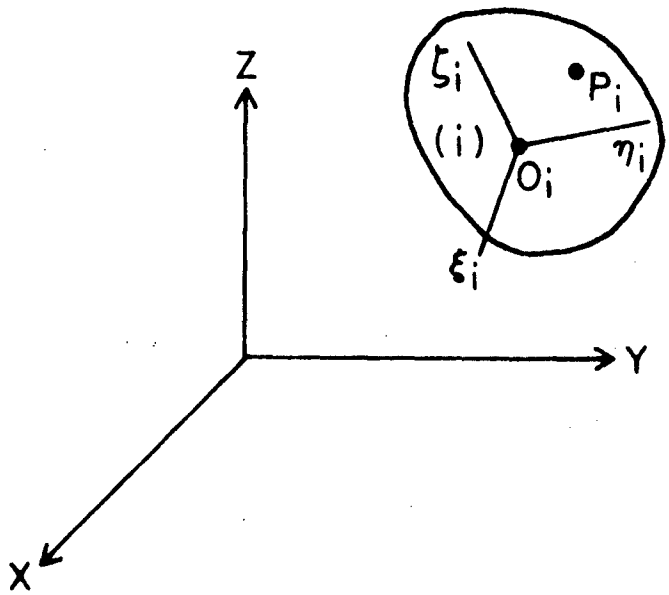

Figure 3.1 Body Fixed $\xi_i\eta_i\zeta_i$ and Global xyz Coordinate Systems

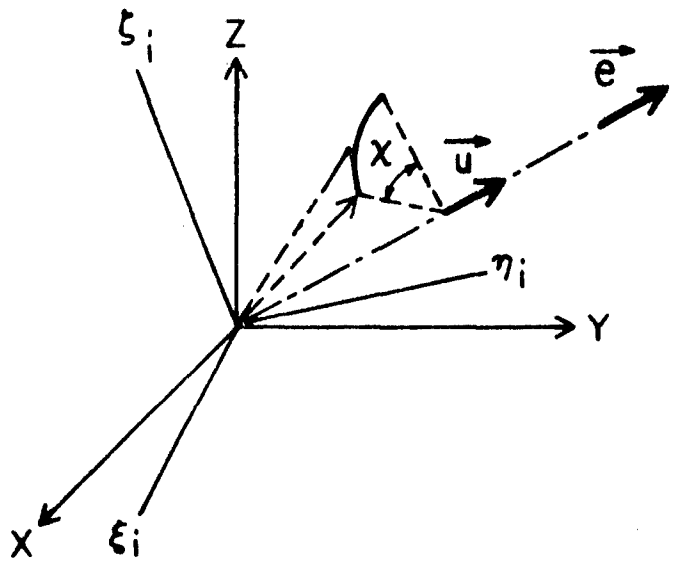

Figure 3.2 Angular Rotation of $\xi_i \eta_i \zeta_i$ Coordinate System About $\vec{u}$ Axis

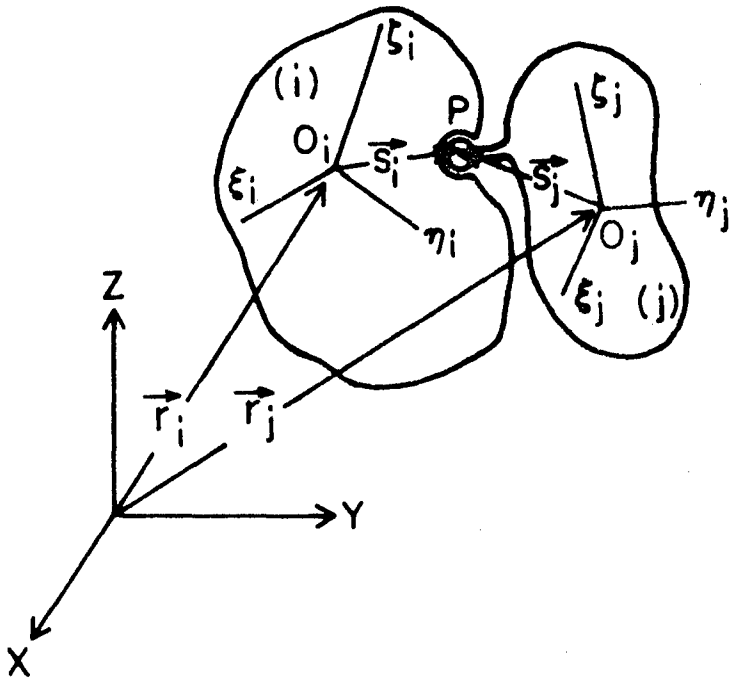

Figure 4.1 Spherical Joint Between Two Rigid Bodies

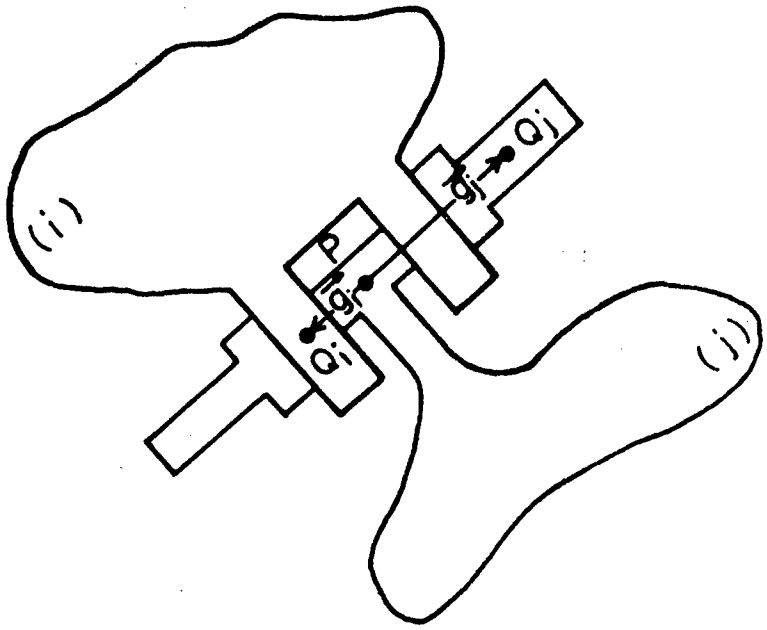

Figure 4.2 Revolute Joint

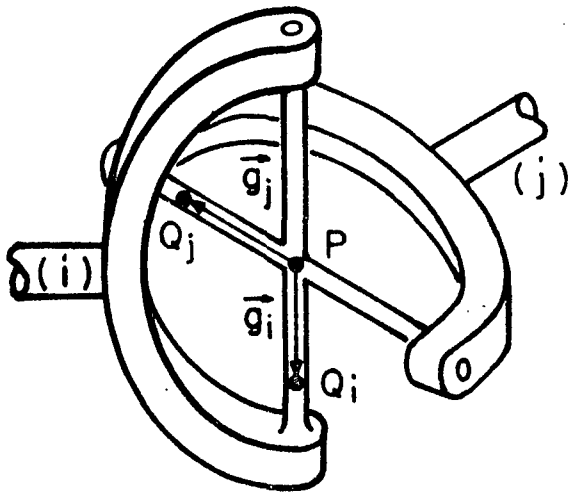

Figure 4.3 Universal Joint

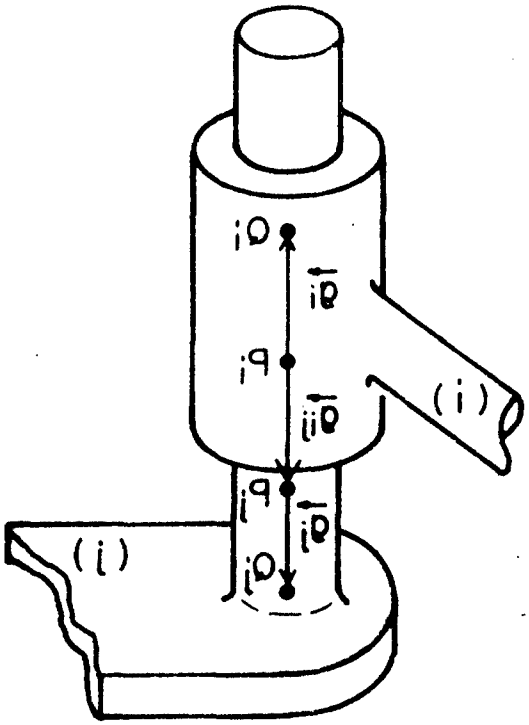

Figure 4.4 Cylindrical Joint

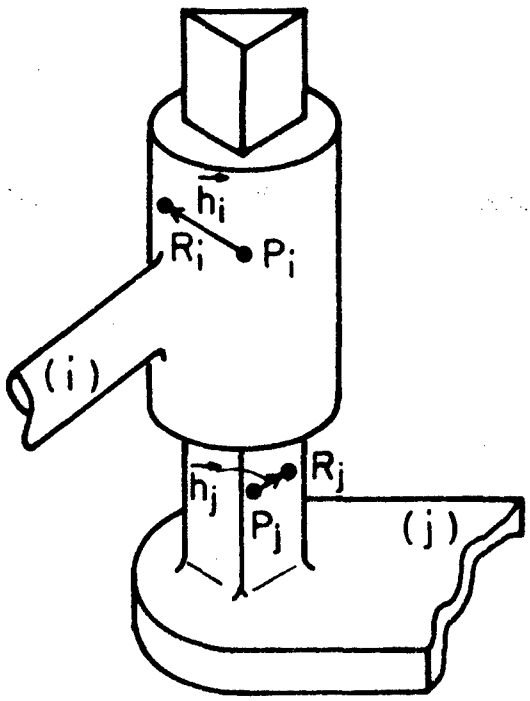

Figure 4.5 Translational Joint

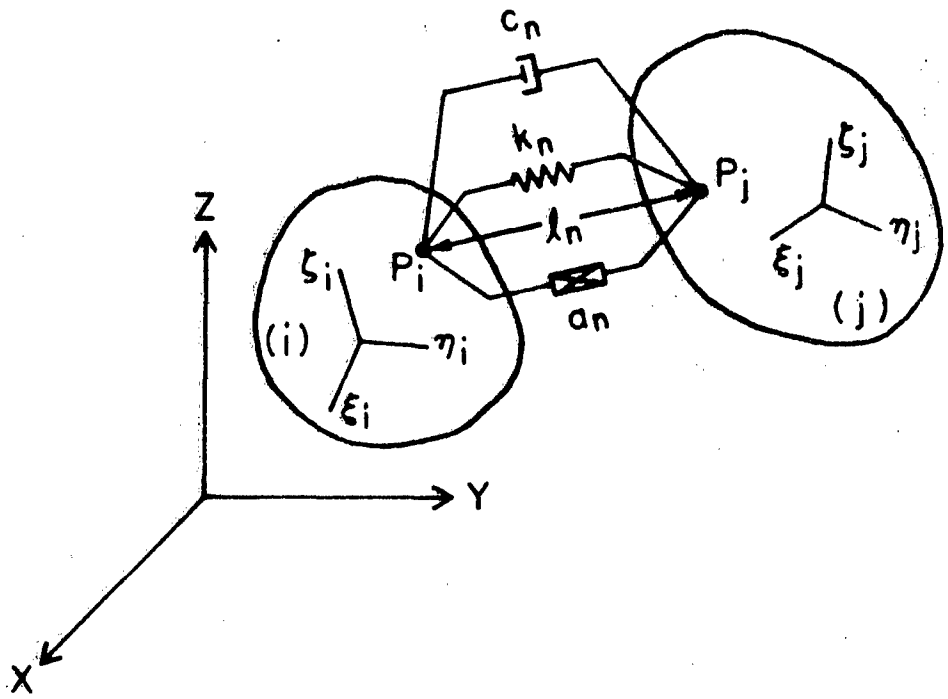

Figure 6.1 Translational Spring-Damper-Actuator Element

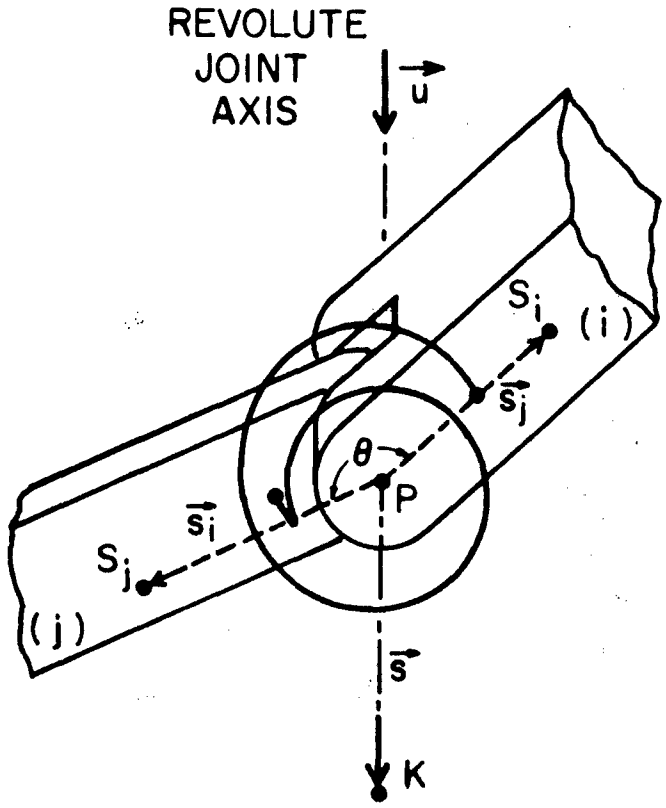

Figure 6.2 Torsional Spring-Damper-Actuator Element

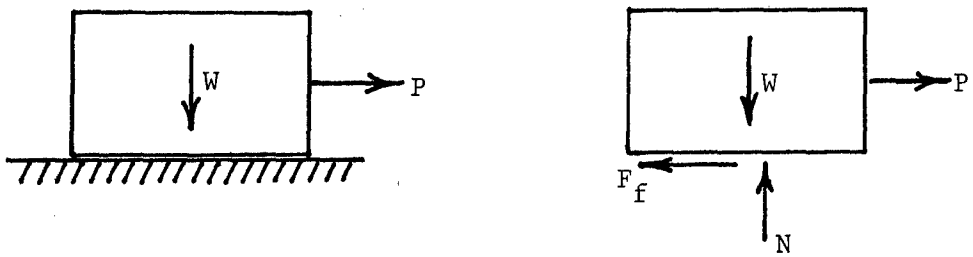

Figure 6.3 Coulomb friction in a simple experiment

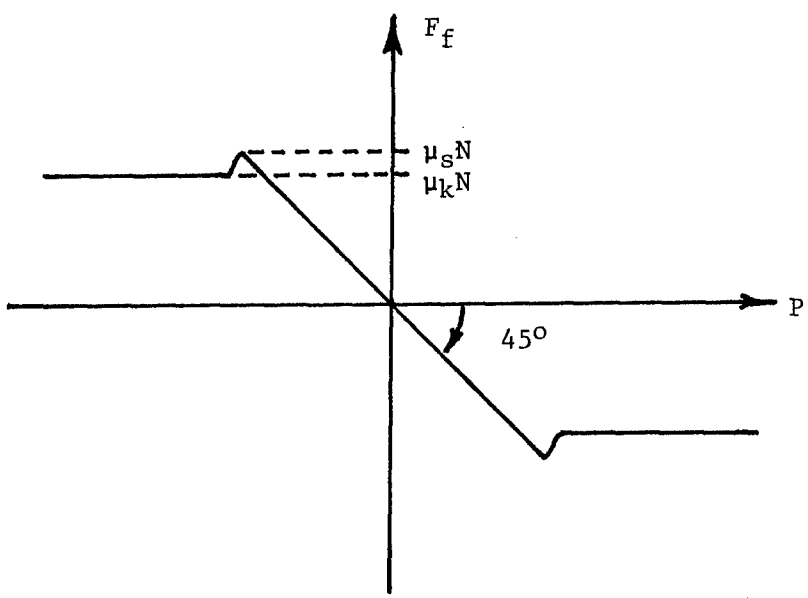

Figure 6.4 Static and kinetic coefficient of friction

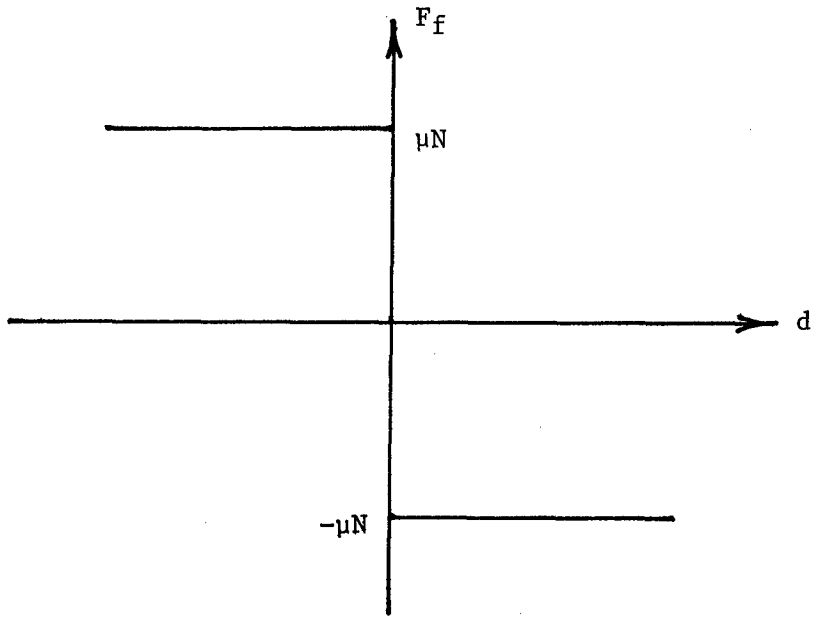

Figure 6.5 Friction force in terms of relative displacement

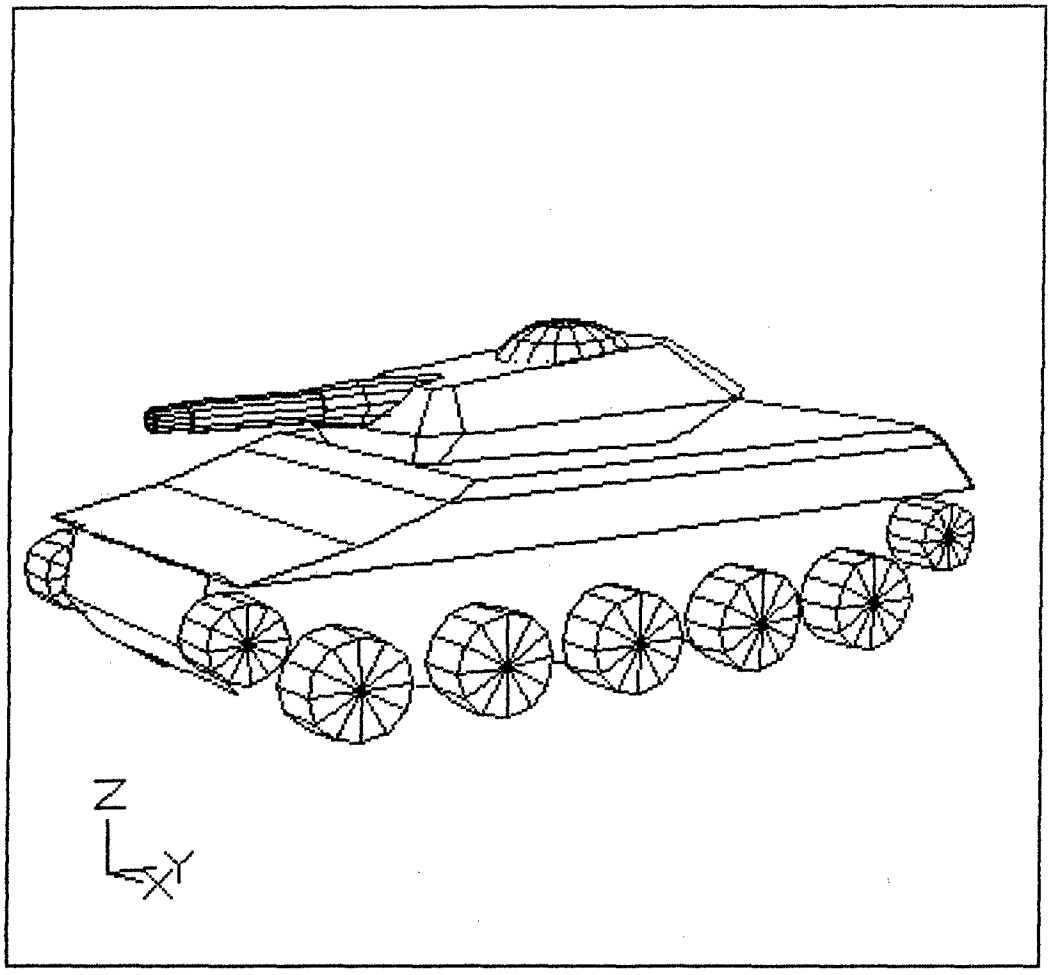

Figure 8.1 A computer generated three-dimensional model of a 26 degrees-of-freedom tracked vehicle

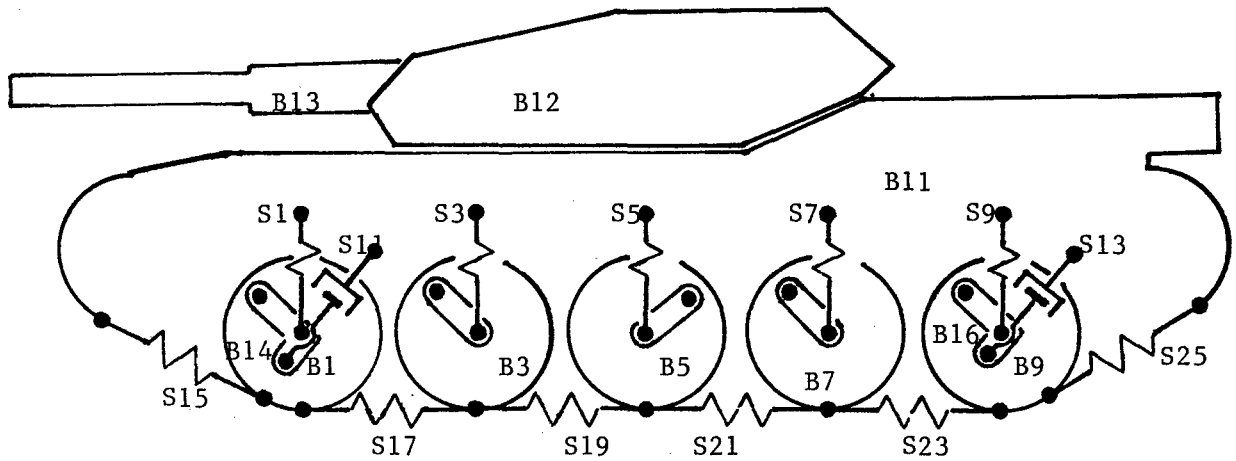

Figure 8.2 Side view of a computer model of the M551

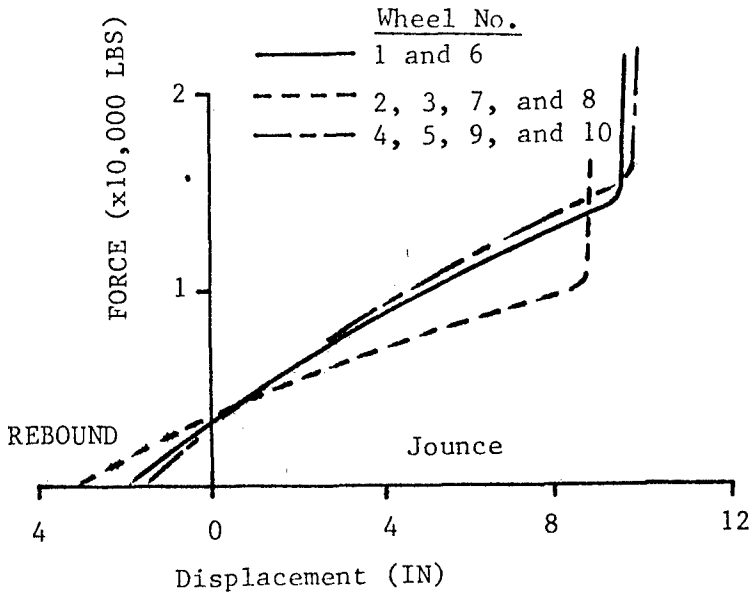

Figure 8.3 Suspension spring characteristics for the M551

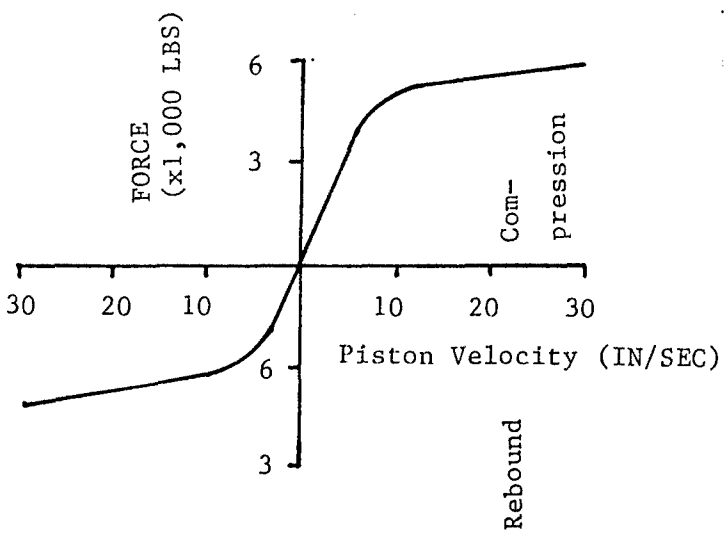

Figure 8.4 Suspension damping characteristic for the M551

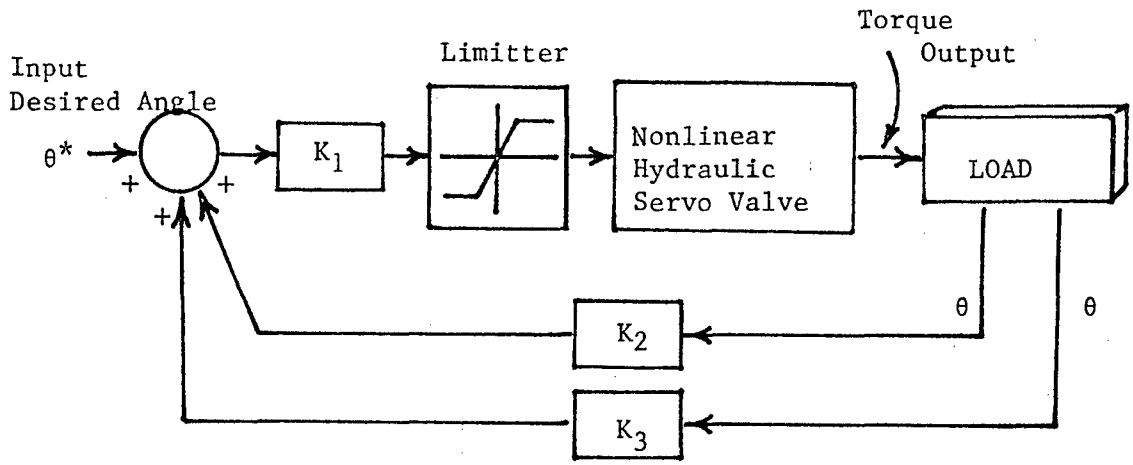

Figure 8.5 Control system diagram for gun elevation or azimuth stabilization

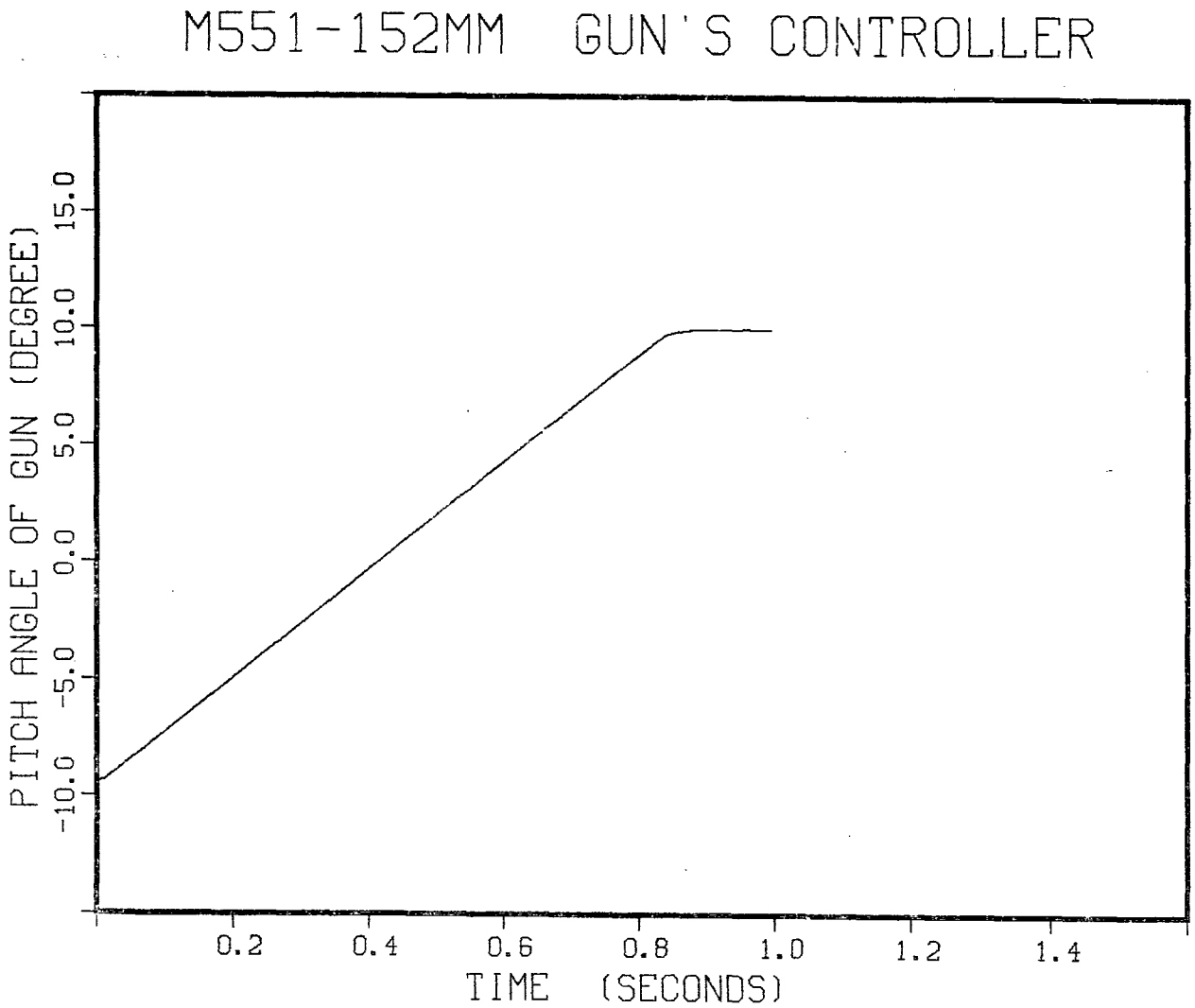

ELEVATION OF GUN
(GUNNER'S COMMAND : 10 DEGREE)

Figure 8.6

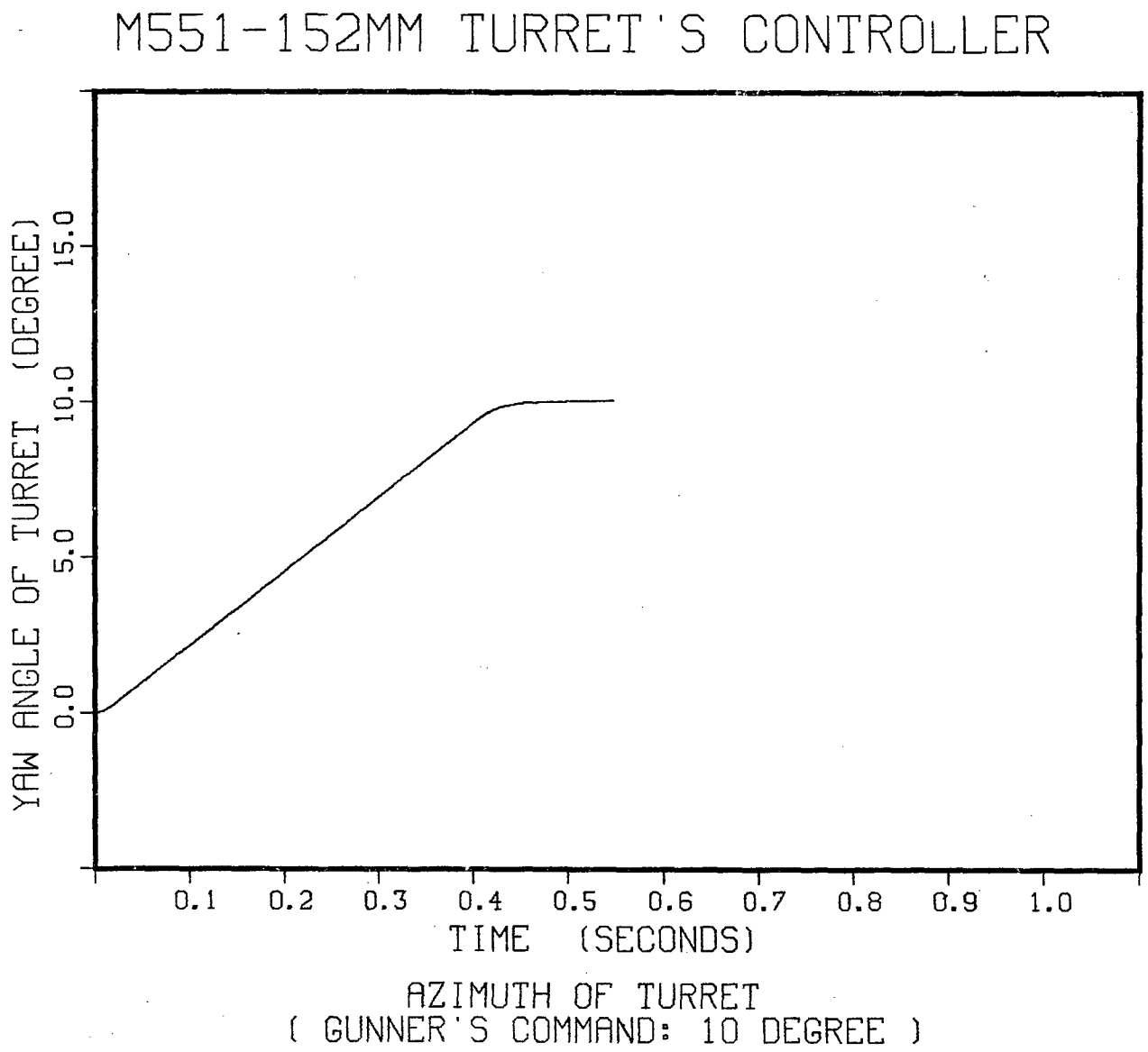
M551-152MM TURRET'S CONTROLLER
YAW ANGLE OF TURRET (DEGREE)
0.0
5.0
10.0
15.0
0.1
0.2
0.3
0.4
0.5
0.6
0.7
0.8
0.9
1.0
TIME (SECONDS)
AZIMUTH OF TURRET
(GUNNER'S COMMAND: 10 DEGREE)

Figure 8.7

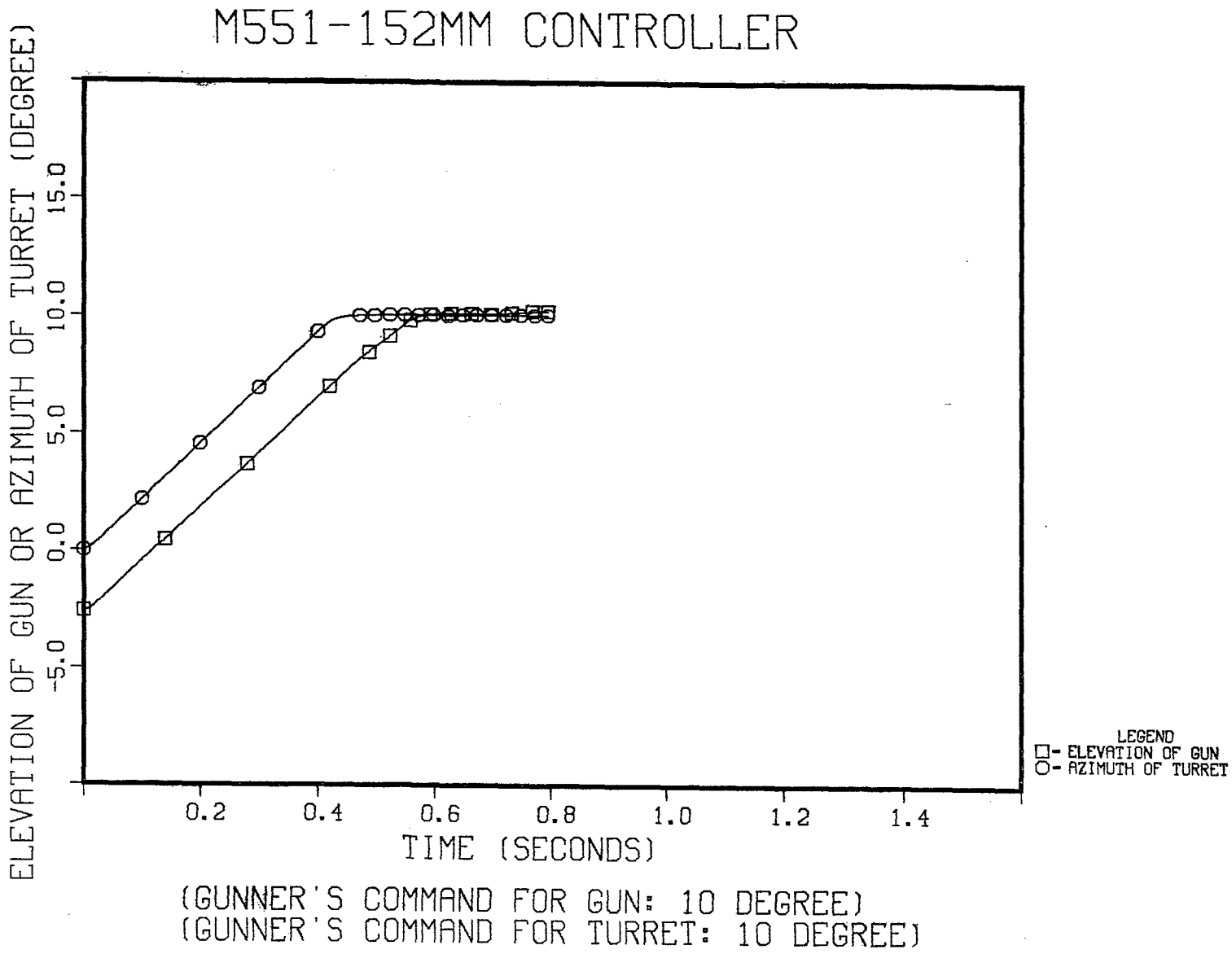
M551-152MM CONTROLLER
ELEVATION OF GUN OR AZIMUTH OF TURRET (DEGREE)
15.0
10.0
5.0
0.0
-5.0
0.2
0.4
0.6
0.8
1.0
1.2
1.4
TIME (SECONDS)
LEGEND
□- ELEVATION OF GUN
○- AZIMUTH OF TURRET
(GUNNER'S COMMAND FOR GUN: 10 DEGREE)
(GUNNER'S COMMAND FOR TURRET: 10 DEGREE)

Figure 8.8

Appendix A

Response Plots for Platform Stability Analysis

Forward-Fire Simulation

* Coulomb friction
* coefficient of friction = 0.5
* 1.0 second simulation
* CPU time on PRIME - 750 ≈ 7000 sec.

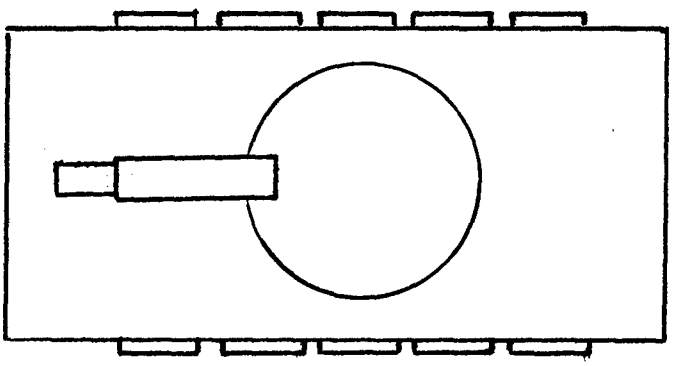

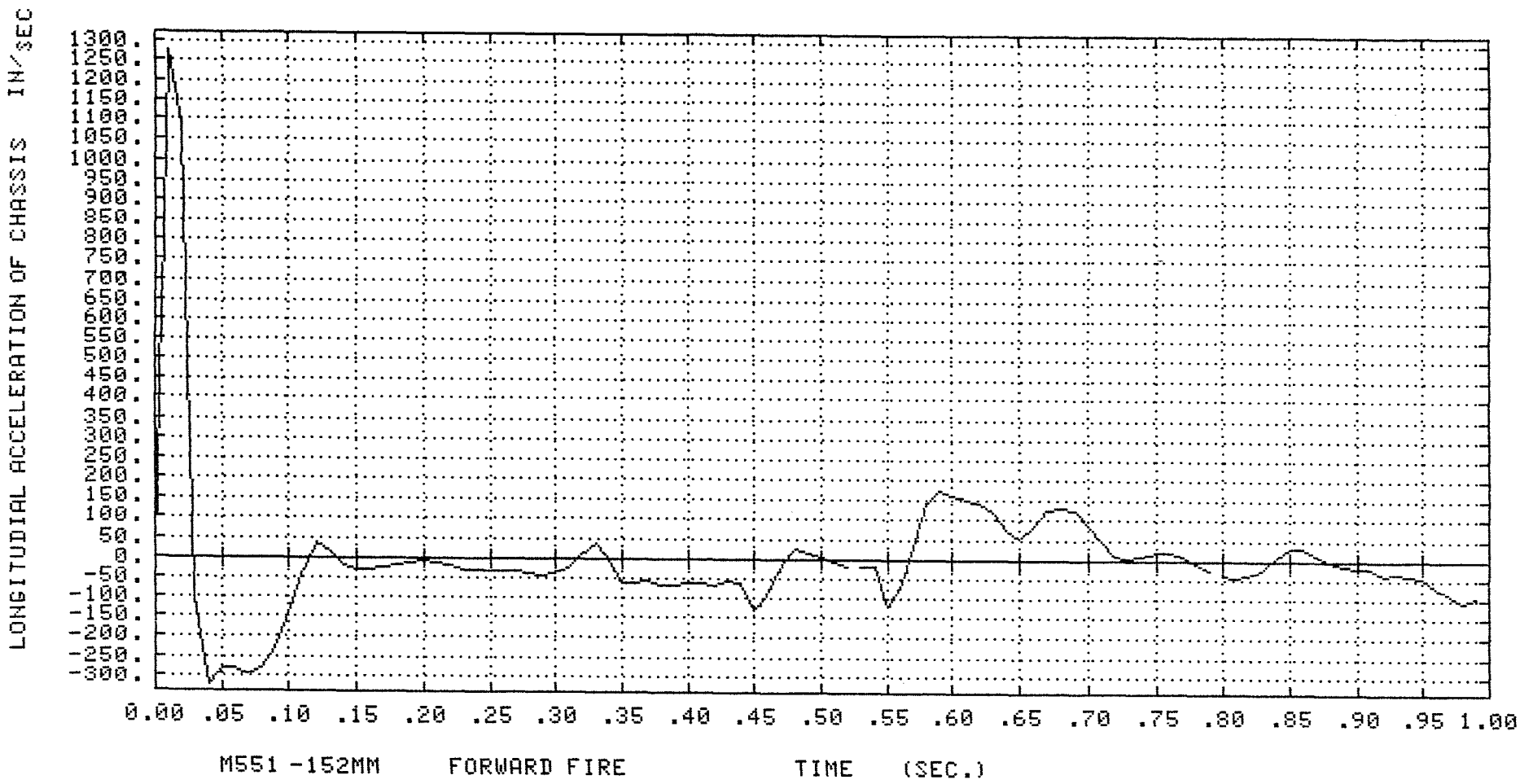
LONGITUDIAL ACCELERATION OF CHASSIS IN/SEC
1300.
1250.
1200.
1150.
1100.
1050.
1000.
950.
900.
850.
800.
750.
700.
650.
600.
550.
500.
450.
400.
350.
300.
250.
200.
150.
100.
50.
0.
-50.
-100.
-150.
-200.
-250.
-300.
0.00 .05 .10 .15 .20 .25 .30 .35 .40 .45 .50 .55 .60 .65 .70 .75 .80 .85 .90 .95 1.00
M551 -152MM FORWARD FIRE
TIME (SEC.)

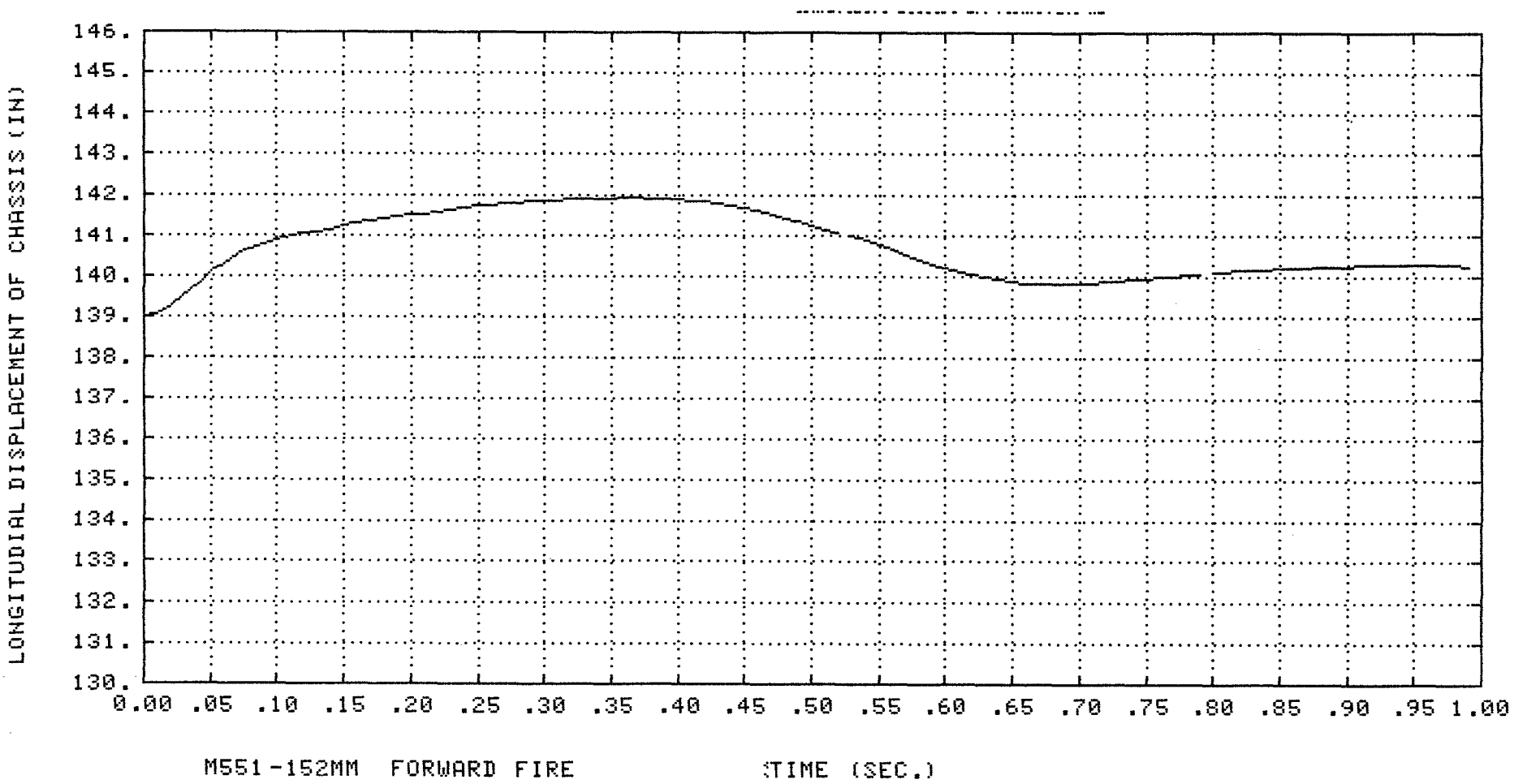
LONGITUDIAL DISPLACEMENT OF CHASSIS (IN)
146.
145.
144.
143.
142.
141.
140.
139.
138.
137.
136.
135.
134.
133.
132.
131.
130.
0.00 .05 .10 .15 .20 .25 .30 .35 .40 .45 .50 .55 .60 .65 .70 .75 .80 .85 .90 .95 1.00
M551-152MM FORWARD FIRE
TIME (SEC.)

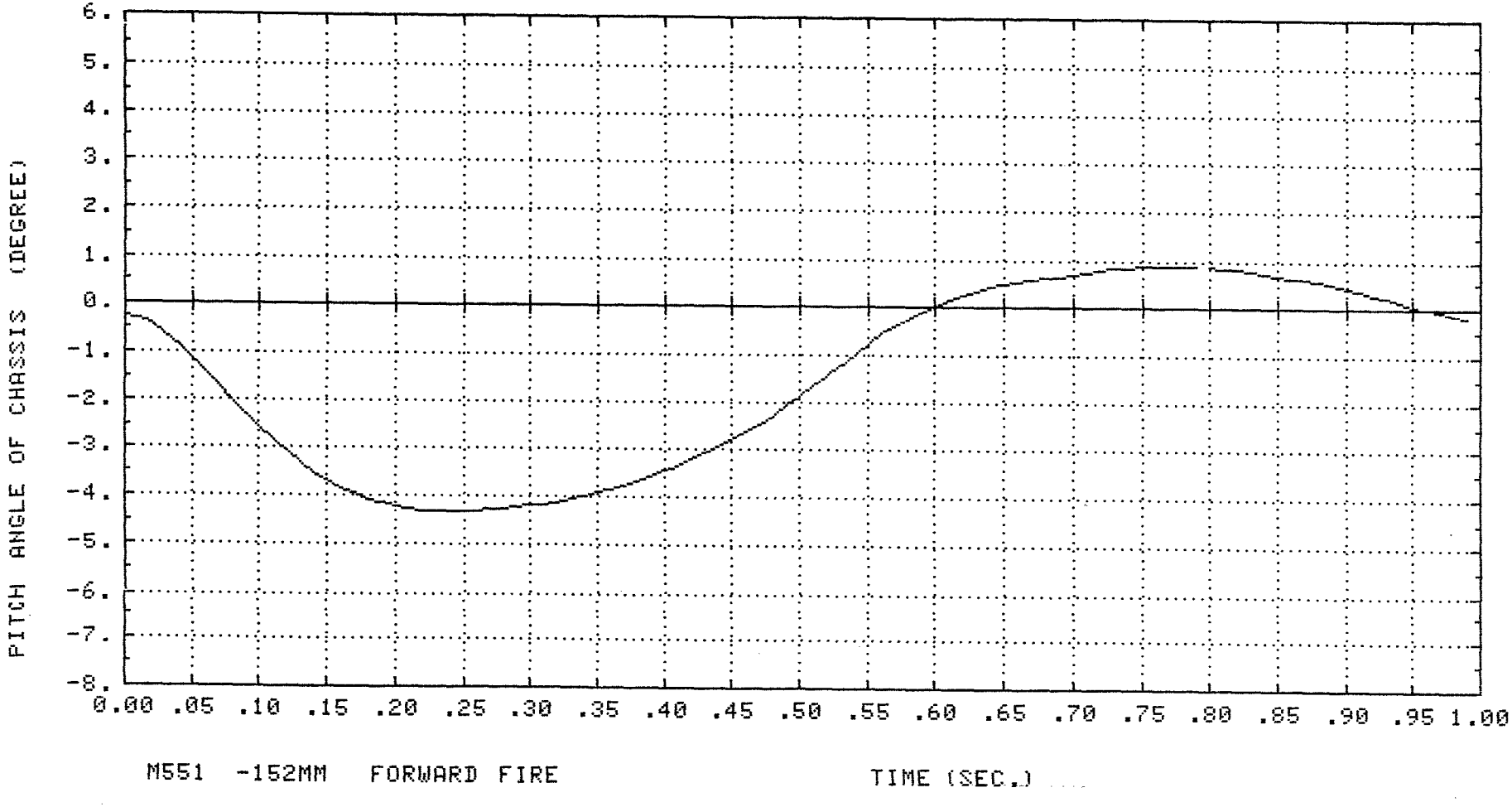

M551 -152MM FORWARD FIRE

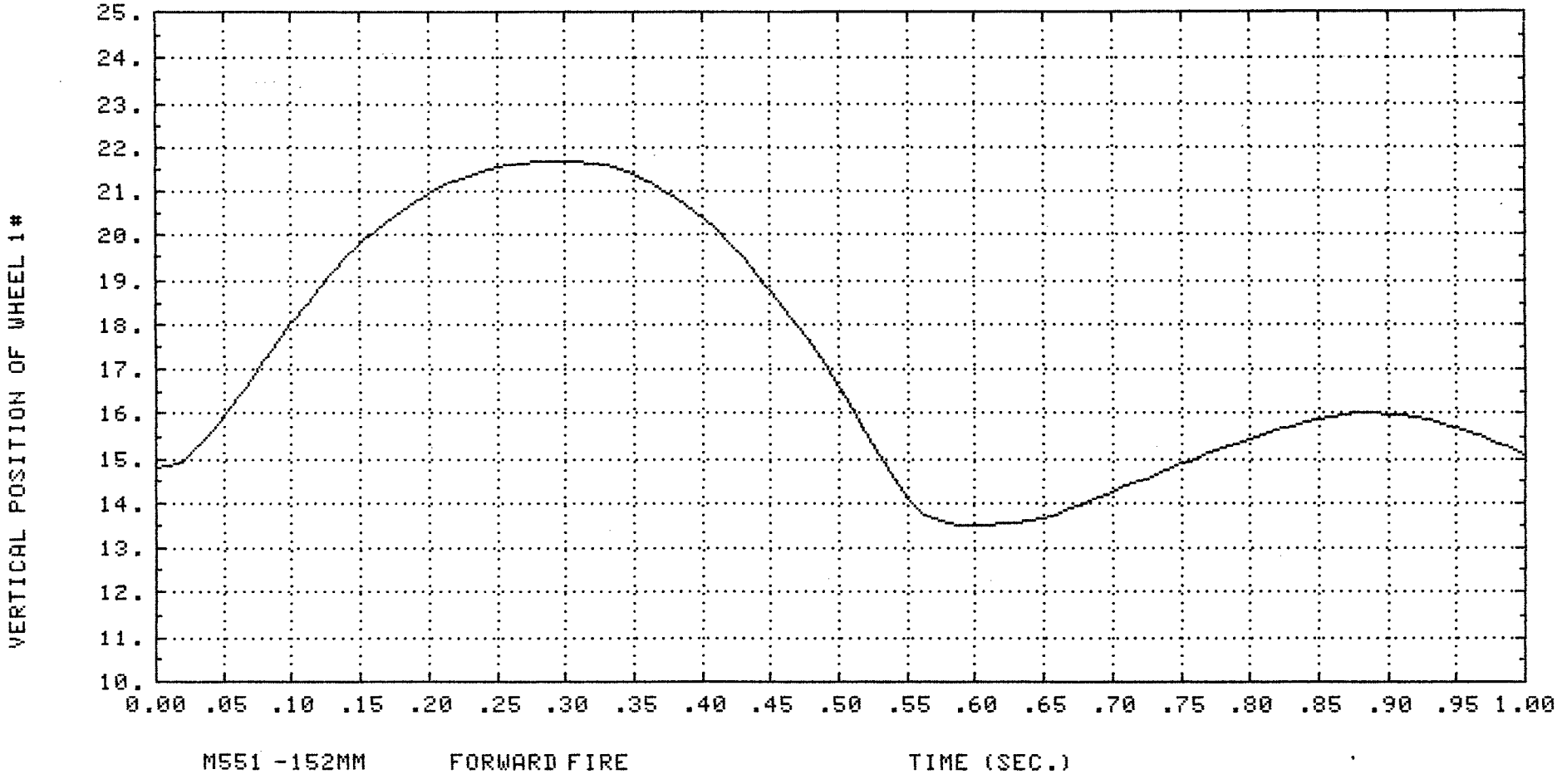
VERTICAL POSITION OF WHEEL 1#
25.
24.
23.
22.
21.
20.
19.
18.
17.
16.
15.
14.
13.
12.
11.
10.
0.00 .05 .10 .15 .20 .25 .30 .35 .40 .45 .50 .55 .60 .65 .70 .75 .80 .85 .90 .95 1.00
M551 -152MM FORWARD FIRE
TIME (SEC.)

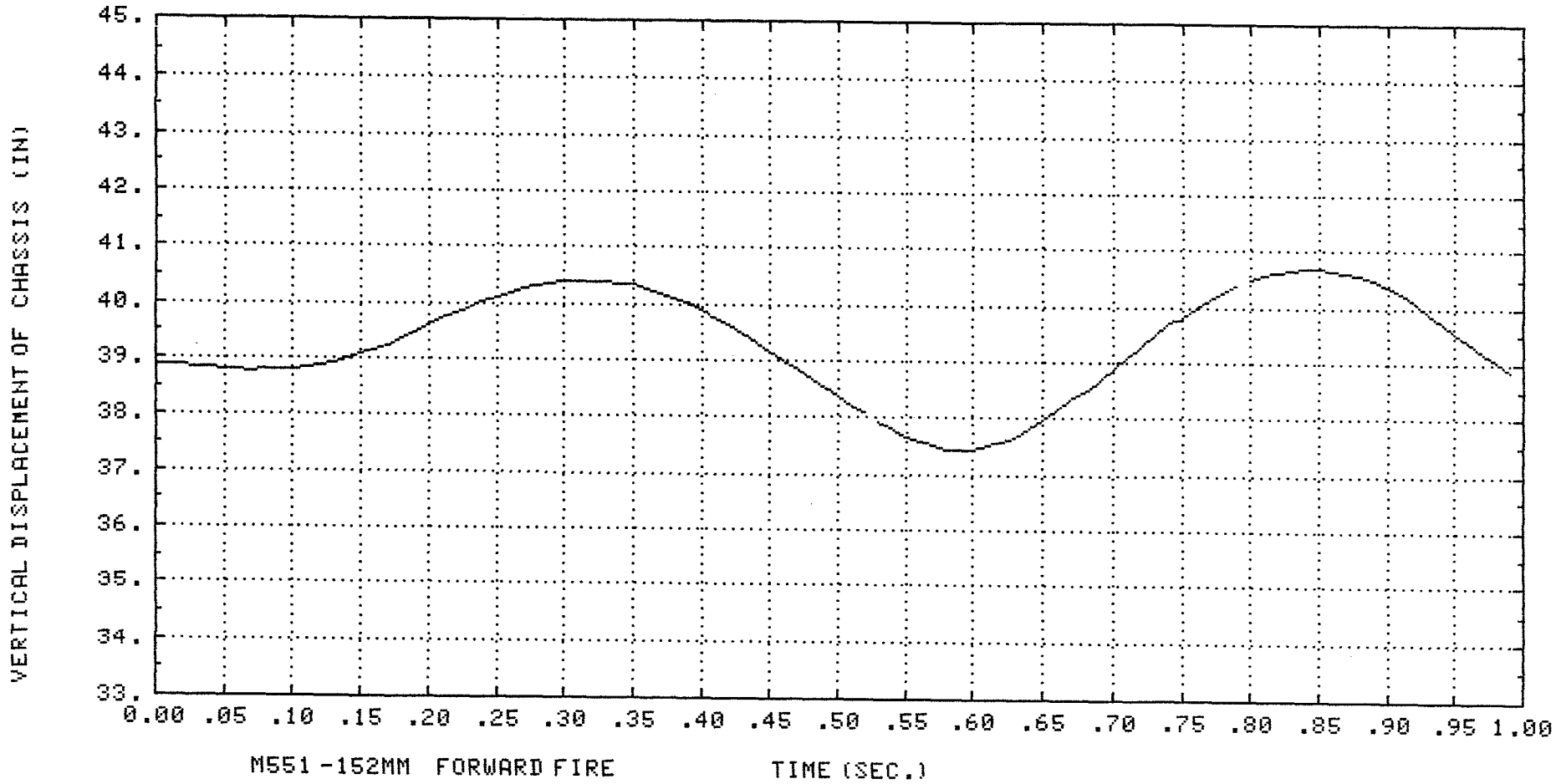
VERTICAL DISPLACEMENT OF CHASSIS (IN)
45.
44.
43.
42.
41.
40.
39.
38.
37.
36.
35.
34.
33.
0.00 .05 .10 .15 .20 .25 .30 .35 .40 .45 .50 .55 .60 .65 .70 .75 .80 .85 .90 .95 1.00
M551 -152MM FORWARD FIRE
TIME (SEC.)

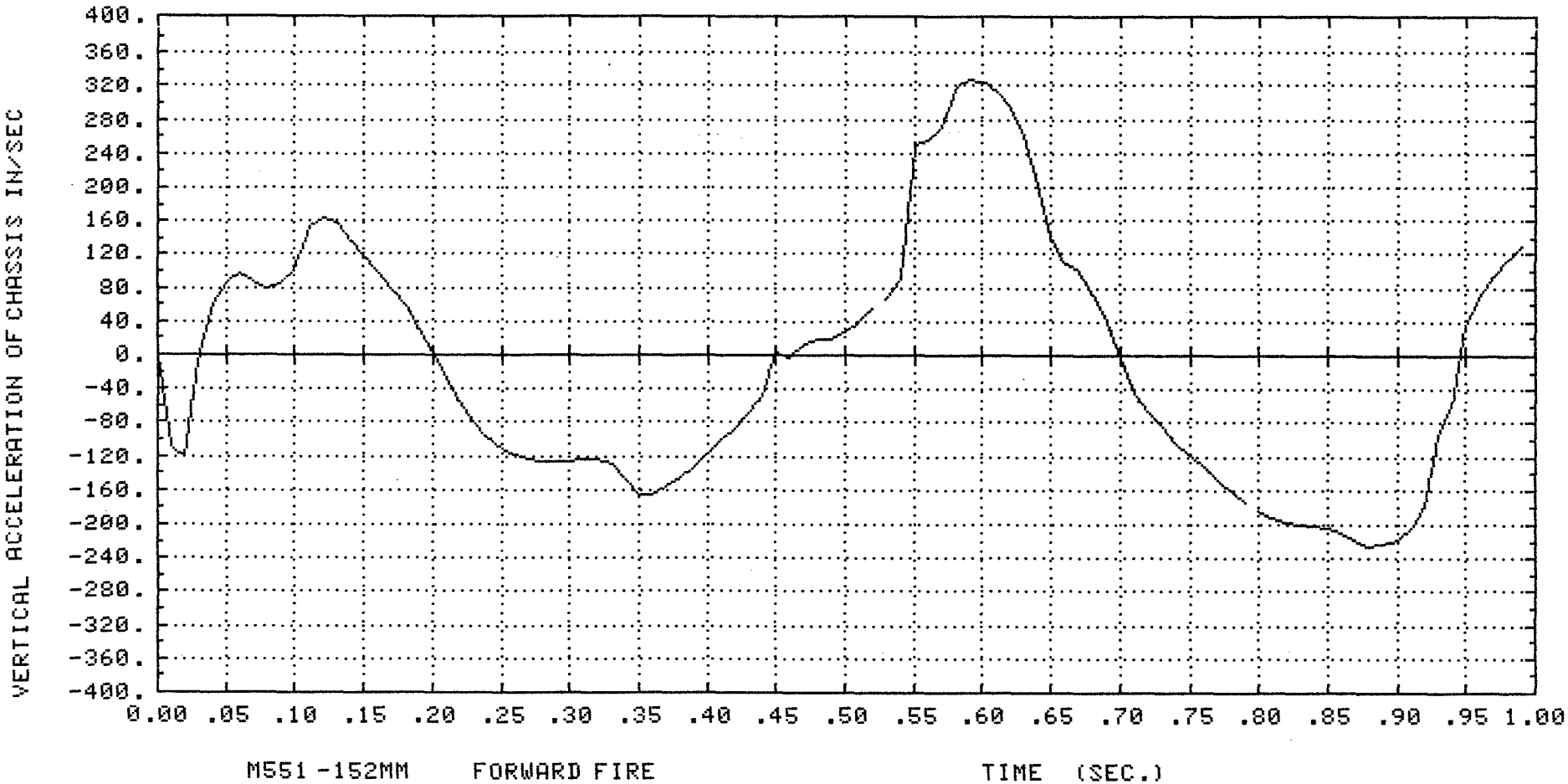
VERTICAL ACCELERATION OF CHASSIS IN/SEC
400.
360.
320.
280.
240.
200.
160.
120.
80.
40.
0.
-40.
-80.
-120.
-160.
-200.
-240.
-280.
-320.
-360.
-400.
0.00 .05 .10 .15 .20 .25 .30 .35 .40 .45 .50 .55 .60 .65 .70 .75 .80 .85 .90 .95 1.00
M551 -152MM FORWARD FIRE
TIME (SEC.)

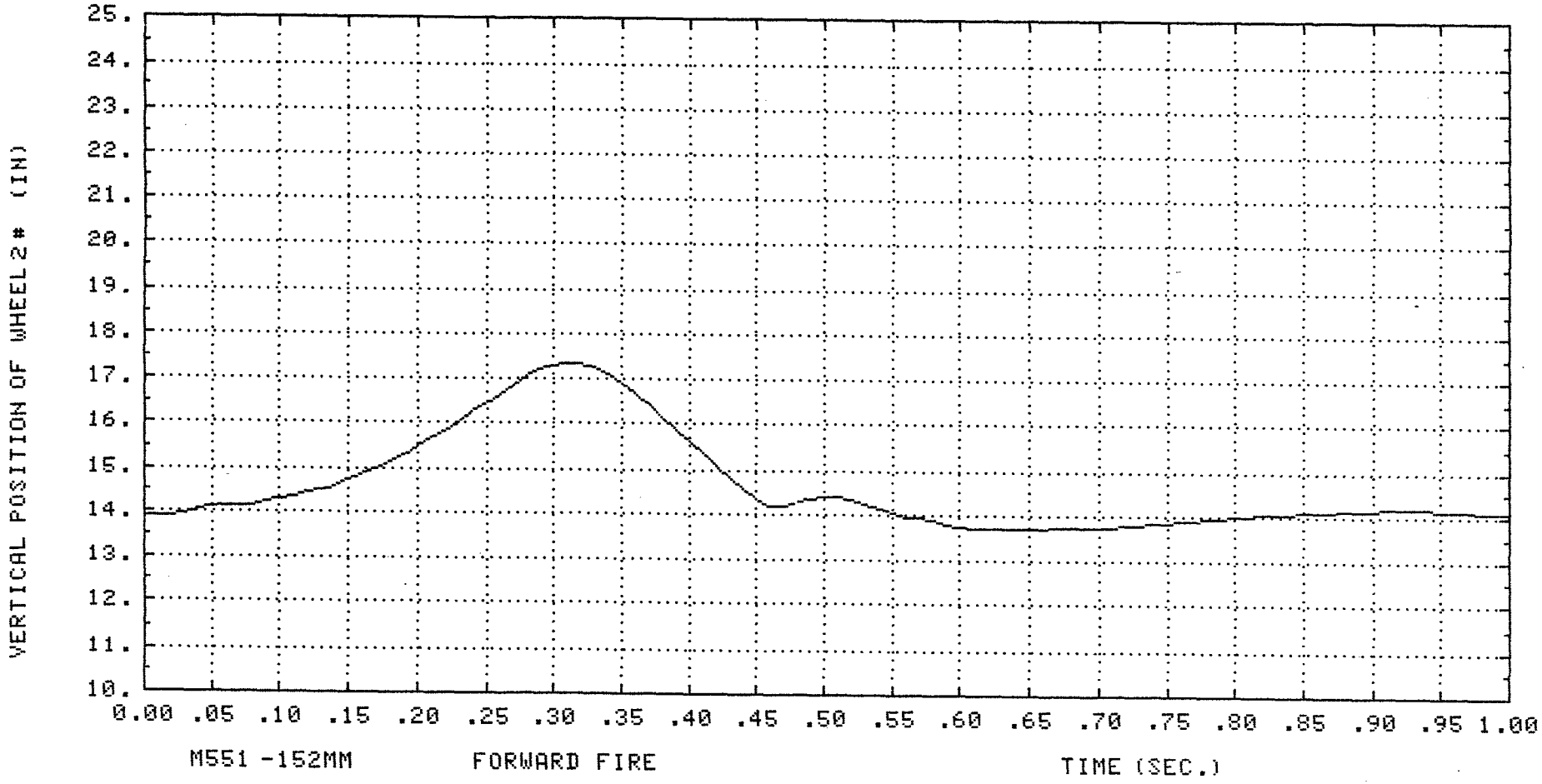
VERTICAL POSITION OF WHEEL 2# (IN)
25.
24.
23.
22.
21.
20.
19.
18.
17.
16.
15.
14.
13.
12.
11.
10.
0.00 .05 .10 .15 .20 .25 .30 .35 .40 .45 .50 .55 .60 .65 .70 .75 .80 .85 .90 .95 1.00
M551 -152MM
FORWARD FIRE
TIME (SEC.)

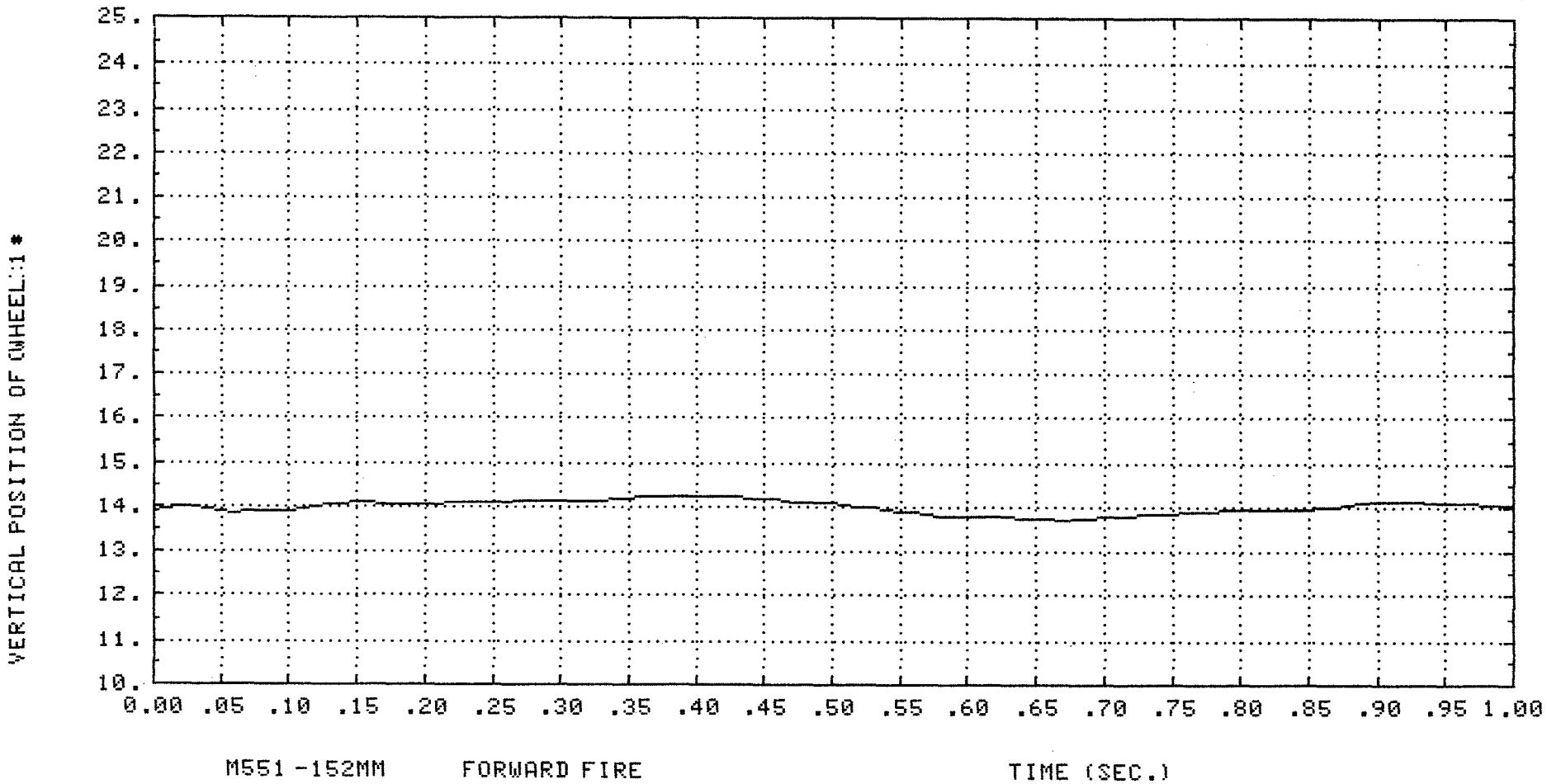
VERTICAL POSITION OF (WHEEL:1 *
25.
24.
23.
22.
21.
20.
19.
18.
17.
16.
15.
14.
13.
12.
11.
10.
0.00 .05 .10 .15 .20 .25 .30 .35 .40 .45 .50 .55 .60 .65 .70 .75 .80 .85 .90 .95 1.00
M551 -152MM FORWARD FIRE
TIME (SEC.)

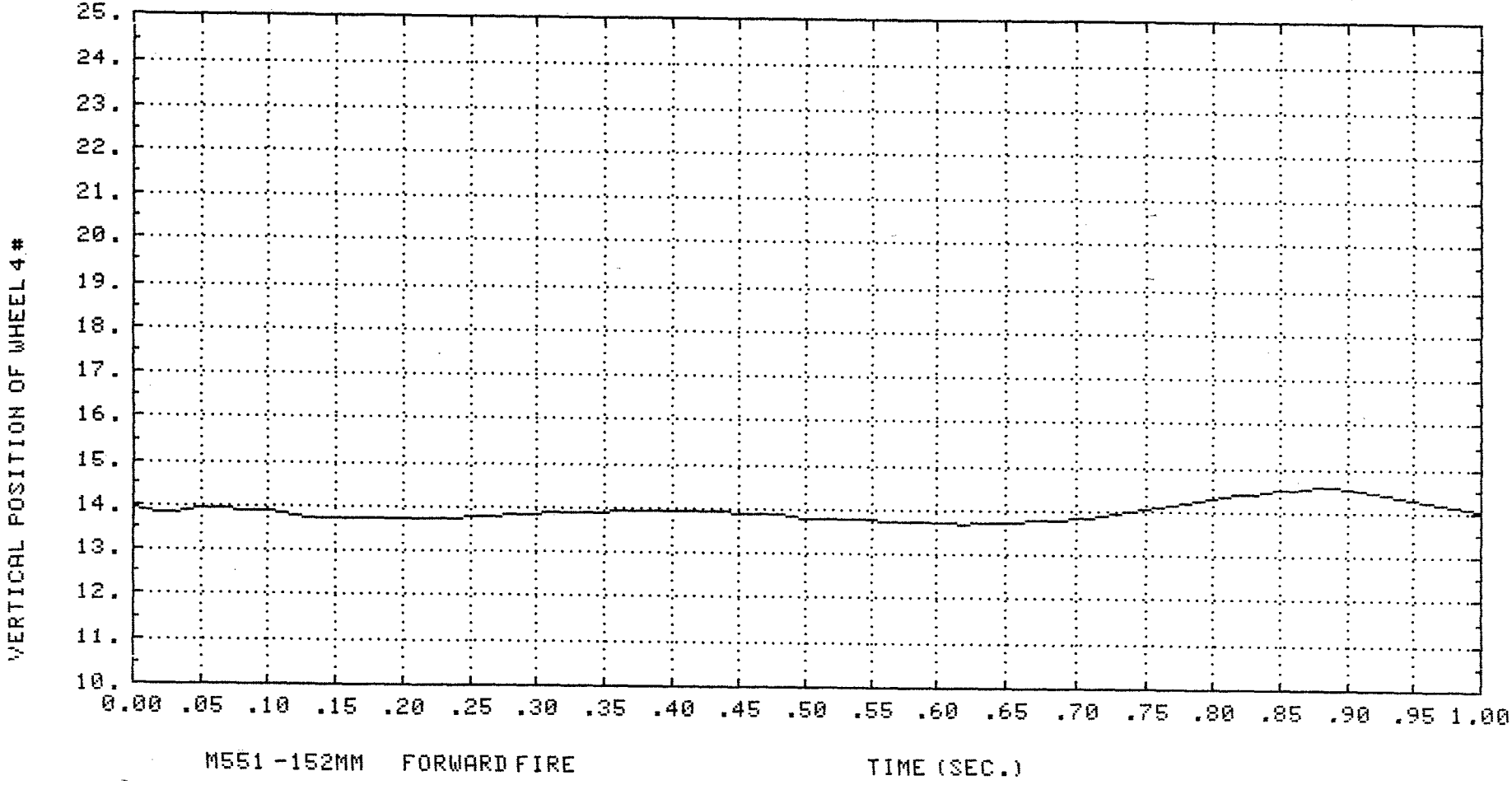
VERTICAL POSITION OF WHEEL 4 #
25.
24.
23.
22.
21.
20.
19.
18.
17.
16.
15.
14.
13.
12.
11.
10.
0.00 .05 .10 .15 .20 .25 .30 .35 .40 .45 .50 .55 .60 .65 .70 .75 .80 .85 .90 .95 1.00
M551 -152MM FORWARD FIRE
TIME (SEC.)

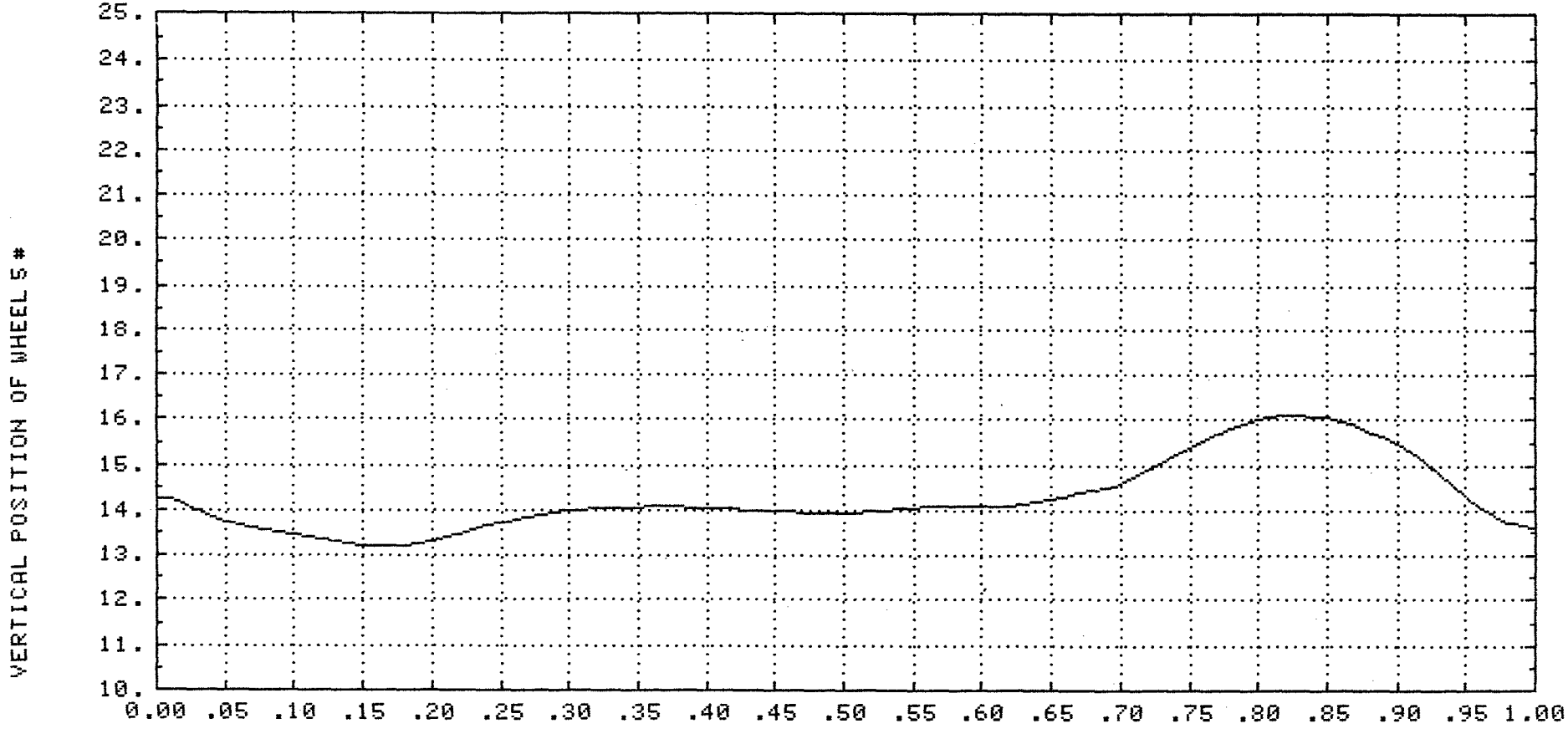
VERTICAL POSITION OF WHEEL 5 #
25.
24.
23.
22.
21.
20.
19.
18.
17.
16.
15.
14.
13.
12.
11.
10.
0.00 .05 .10 .15 .20 .25 .30 .35 .40 .45 .50 .55 .60 .65 .70 .75 .80 .85 .90 .95 1.00

M551 -1§2MM

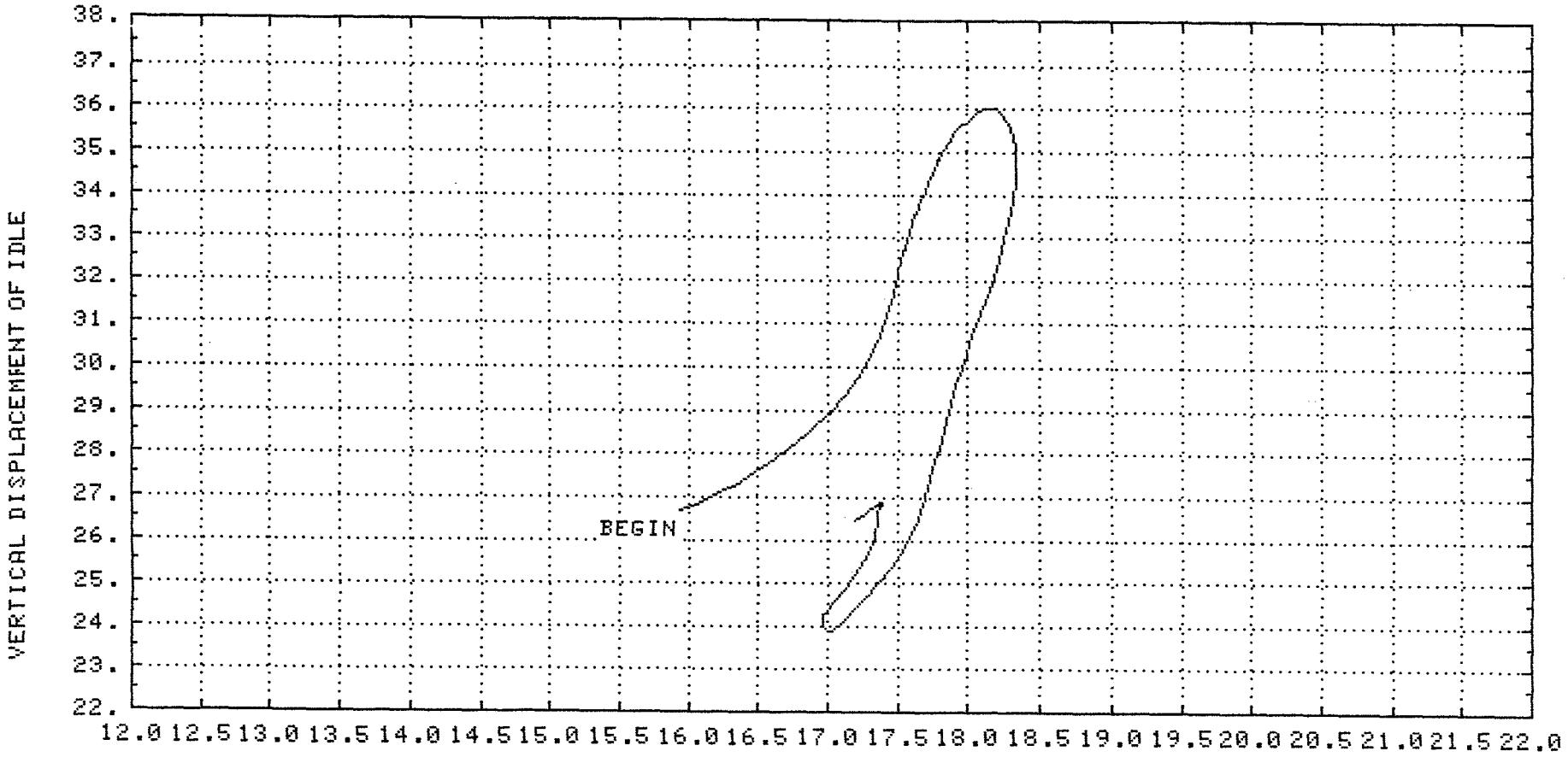

M551 -152MM FORWARD FIRE LONGITUDIAL-DISPLACEMENT OF IDLE

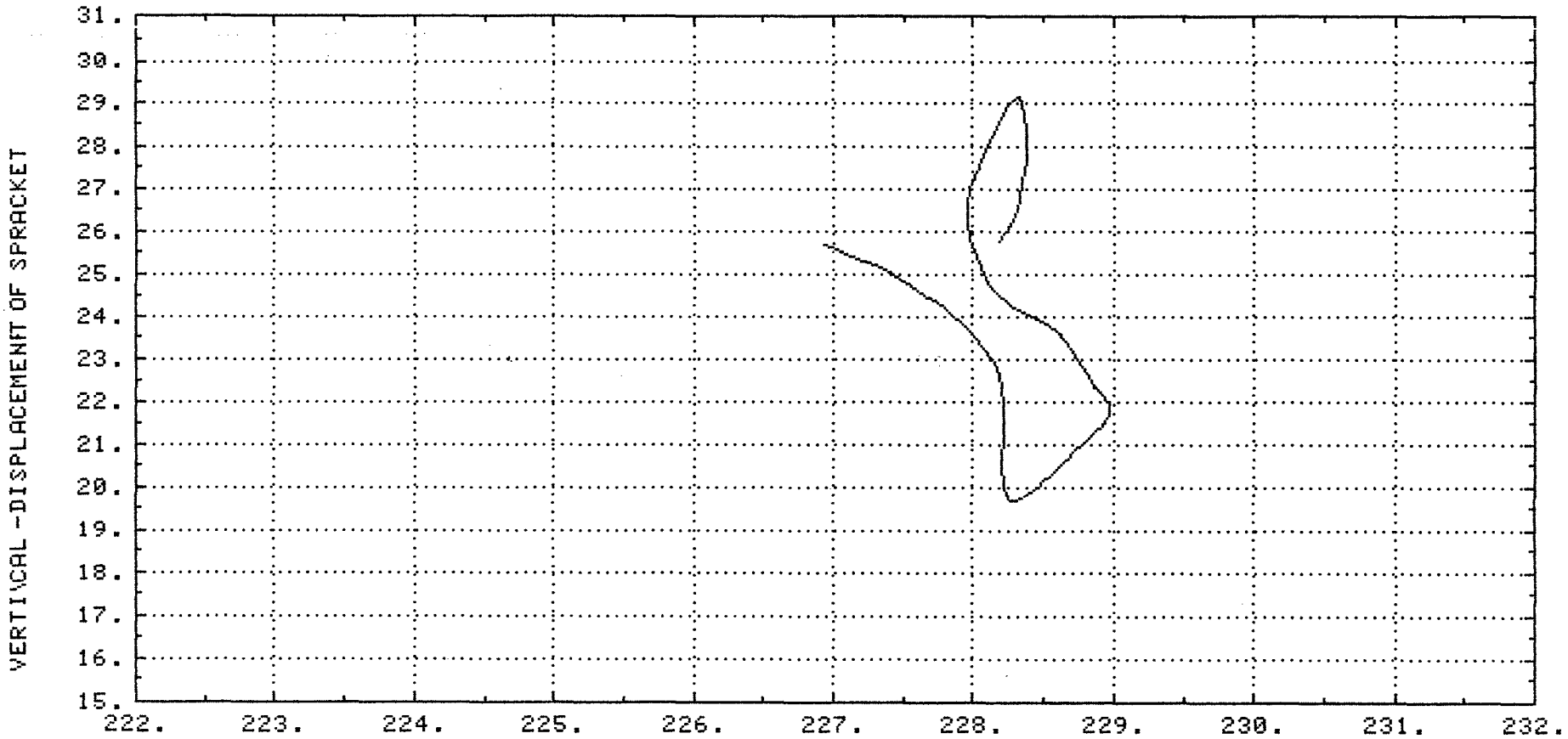

M551-152MM FORWARD FIRE LONGITUDIAL -DISPLACEMENT OF SPRACKET

Appendix B

Response Plots for Platform Stability Analysis

45° Fire Simulation

* Coulomb friction
* Coefficient of friction = 0.5
* 1.0 second simulation
* CPU time on PRIME - 750 ≈ 6500 sec.

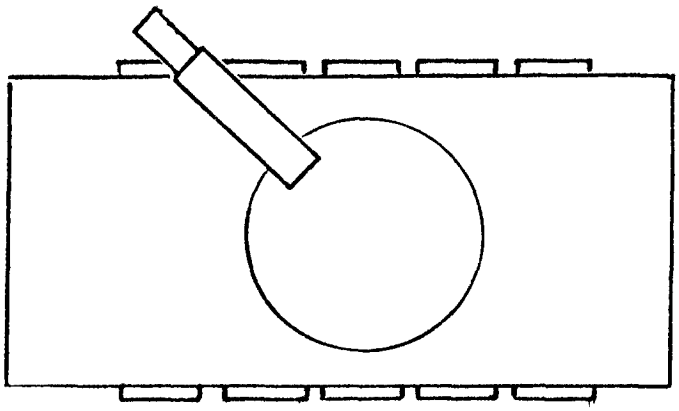

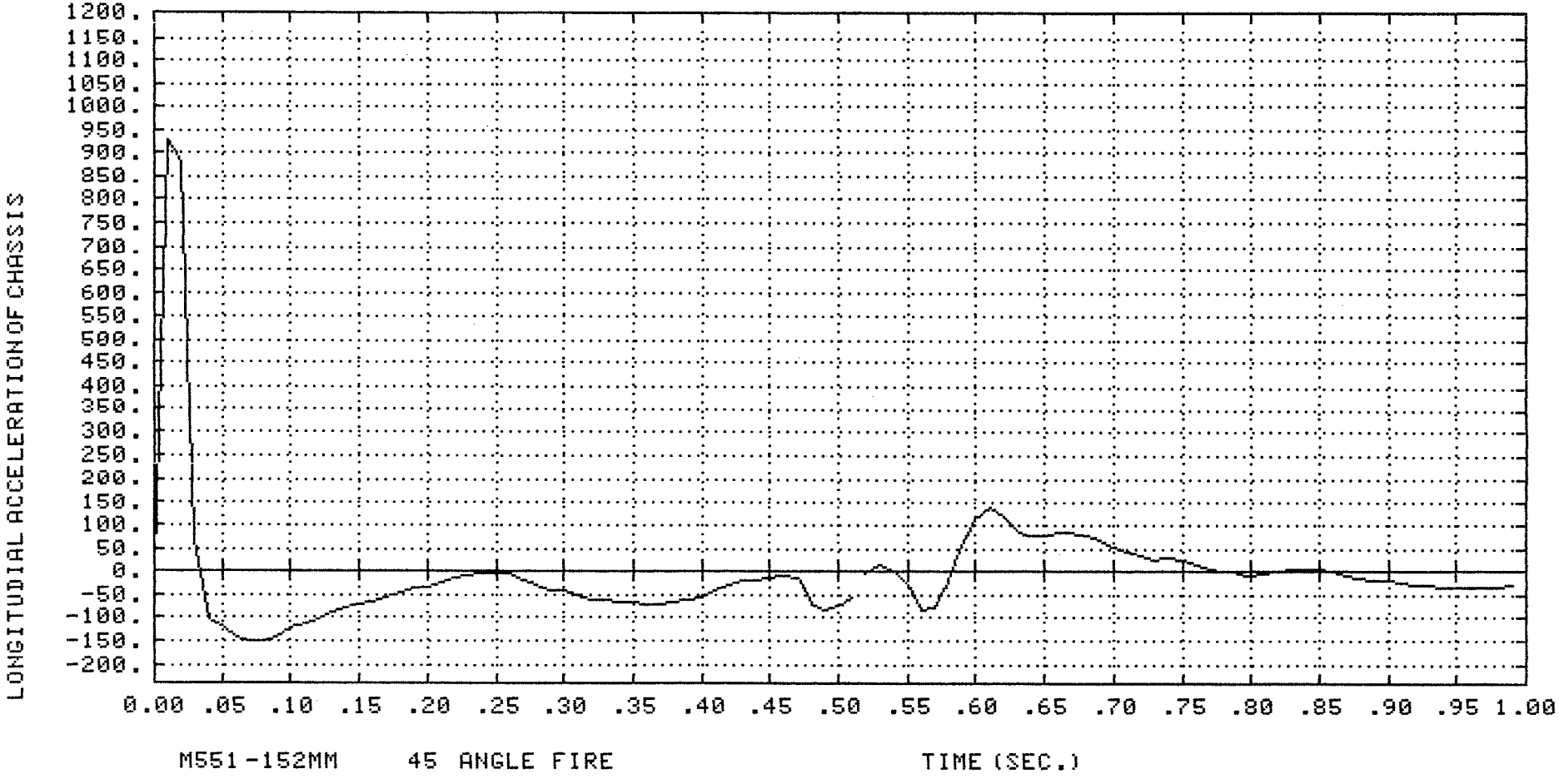
LONGITUDIAL ACCELERATION OF CHASSIS
1200.
1150.
1100.
1050.
1000.
950.
900.
850.
800.
750.
700.
650.
600.
550.
500.
450.
400.
350.
300.
250.
200.
150.
100.
50.
0.
-50.
-100.
-150.
-200.
0.00 .05 .10 .15 .20 .25 .30 .35 .40 .45 .50 .55 .60 .65 .70 .75 .80 .85 .90 .95 1.00
M551-152MM 45 ANGLE FIRE
TIME (SEC.)

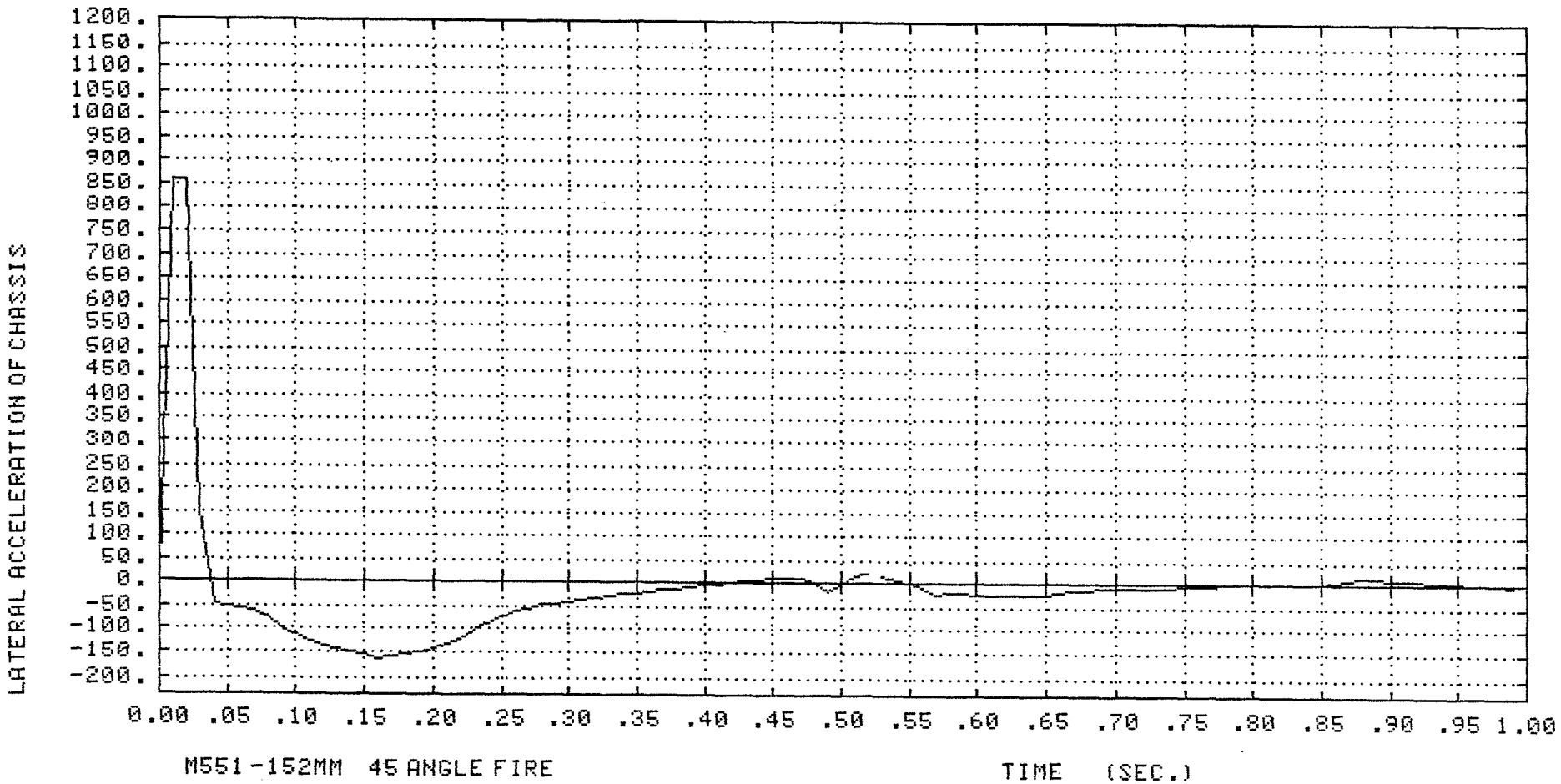
LATERAL ACCELERATION OF CHASSIS
1200.
1150.
1100.
1050.
1000.
950.
900.
850.
800.
750.
700.
650.
600.
550.
500.
450.
400.
350.
300.
250.
200.
150.
100.
50.
0.
-50.
-100.
-150.
-200.
0.00 .05 .10 .15 .20 .25 .30 .35 .40 .45 .50 .55 .60 .65 .70 .75 .80 .85 .90 .95 1.00
M551-152MM 45 ANGLE FIRE
TIME (SEC.)

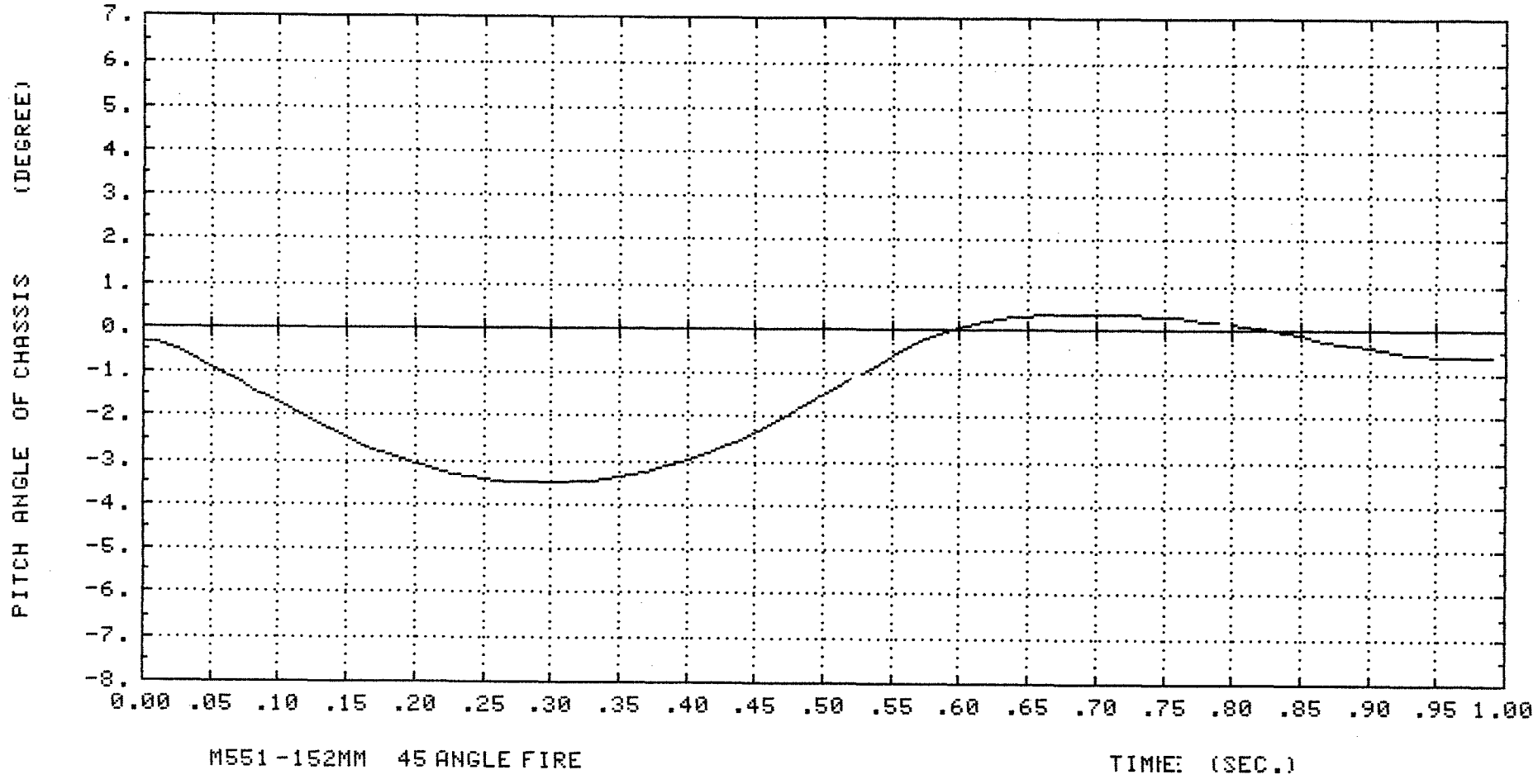

M551-152MM 45 ANGLE FIRE

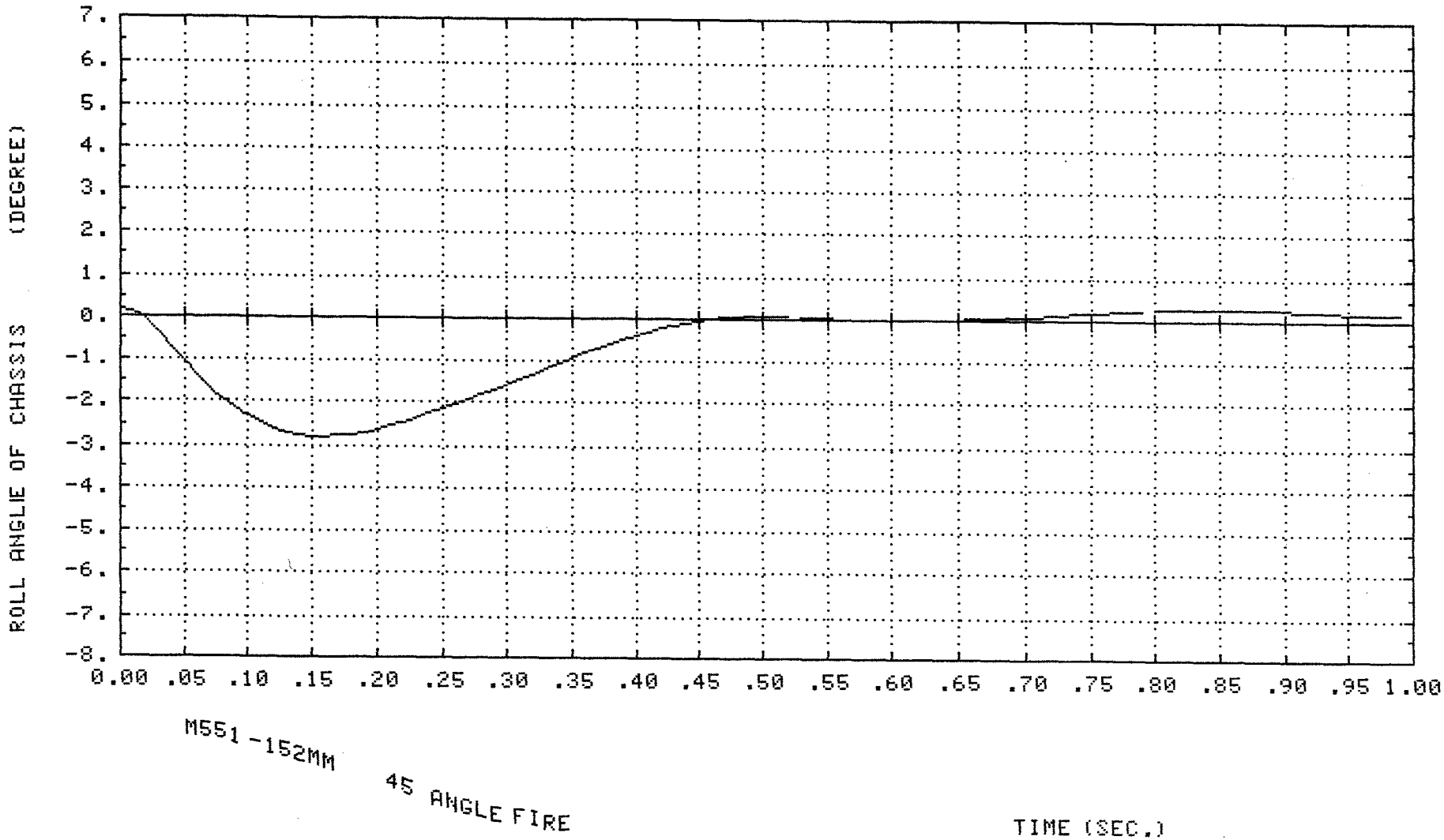
ROLL ANGLIE OF CHASSIS (DEGREE)
7.
6.
5.
4.
3.
2.
1.
0.
-1.
-2.
-3.
-4.
-5.
-6.
-7.
-8.
0.00 .05 .10 .15 .20 .25 .30 .35 .40 .45 .50 .55 .60 .65 .70 .75 .80 .85 .90 .95 1.00
M551 -152MM
45 ANGLE FIRE
TIME (SEC.)

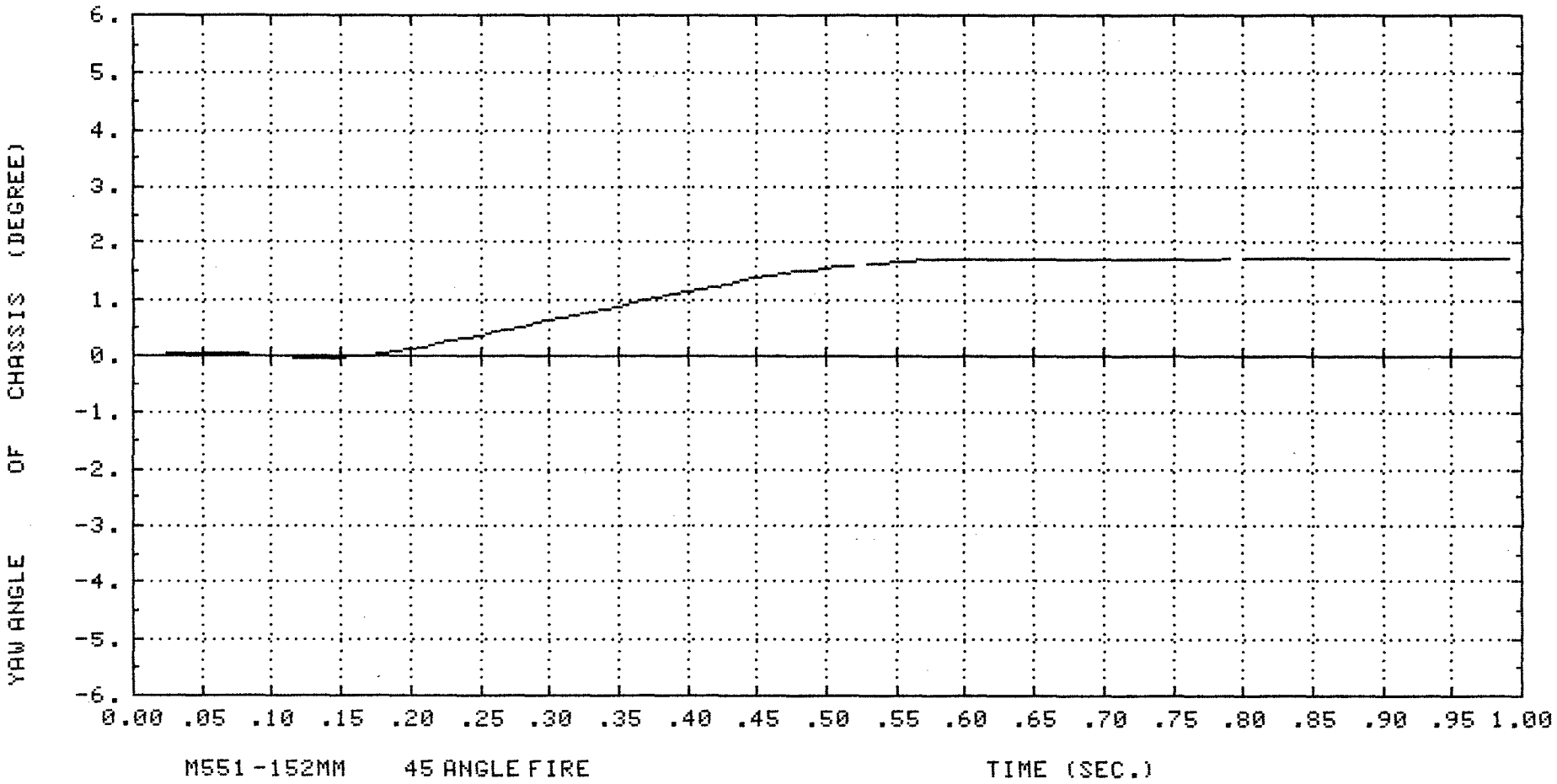
YAW ANGLE OF CHASSIS (DEGREE)
6.
5.
4.
3.
2.
1.
0.
-1.
-2.
-3.
-4.
-5.
-6.
0.00 .05 .10 .15 .20 .25 .30 .35 .40 .45 .50 .55 .60 .65 .70 .75 .80 .85 .90 .95 1.00
M551-152MM 45 ANGLE FIRE
TIME (SEC.)

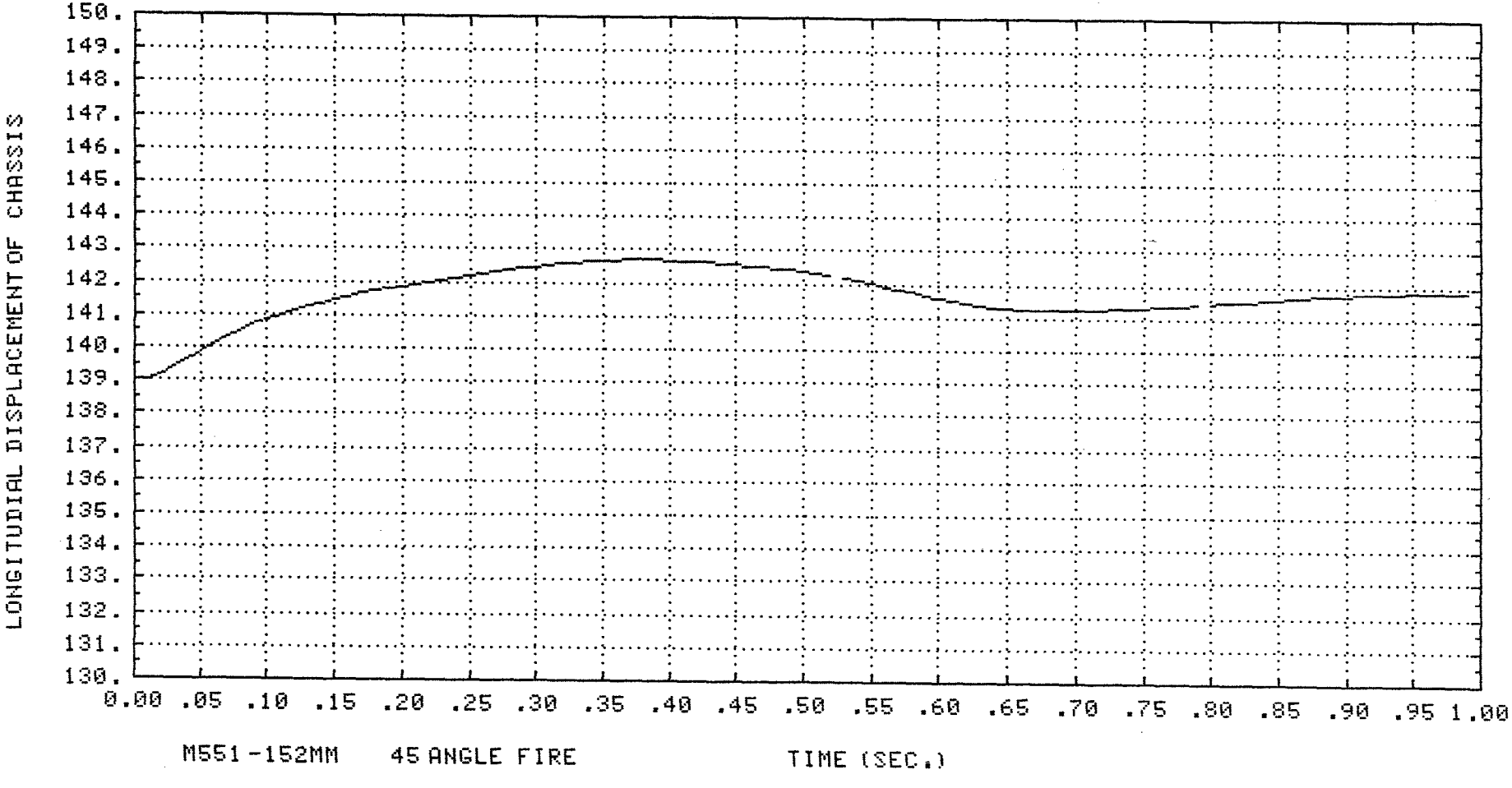
LONGITUDIAL DISPLACEMENT OF CHASSIS
150.
149.
148.
147.
146.
145.
144.
143.
142.
141.
140.
139.
138.
137.
136.
135.
134.
133.
132.
131.
130.
0.00 .05 .10 .15 .20 .25 .30 .35 .40 .45 .50 .55 .60 .65 .70 .75 .80 .85 .90 .95 1.00
M551-152MM 45 ANGLE FIRE
TIME (SEC.)

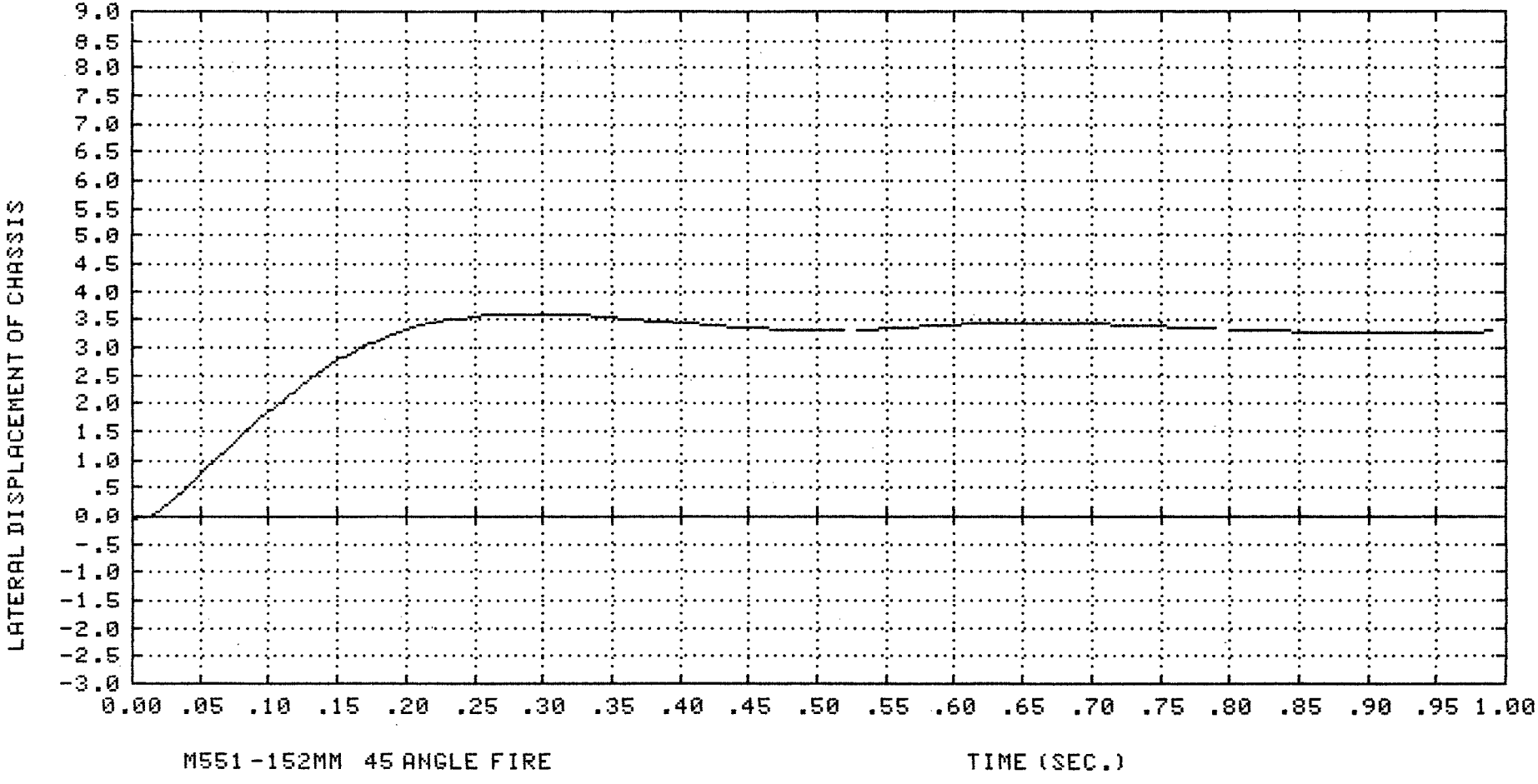
LATERAL DISPLACEMENT OF CHASSIS
9.0
8.5
8.0
7.5
7.0
6.5
6.0
5.5
5.0
4.5
4.0
3.5
3.0
2.5
2.0
1.5
1.0
.5
0.0
-.5
-1.0
-1.5
-2.0
-2.5
-3.0
0.00 .05 .10 .15 .20 .25 .30 .35 .40 .45 .50 .55 .60 .65 .70 .75 .80 .85 .90 .95 1.00
M551-152MM 45 ANGLE FIRE
TIME (SEC.)

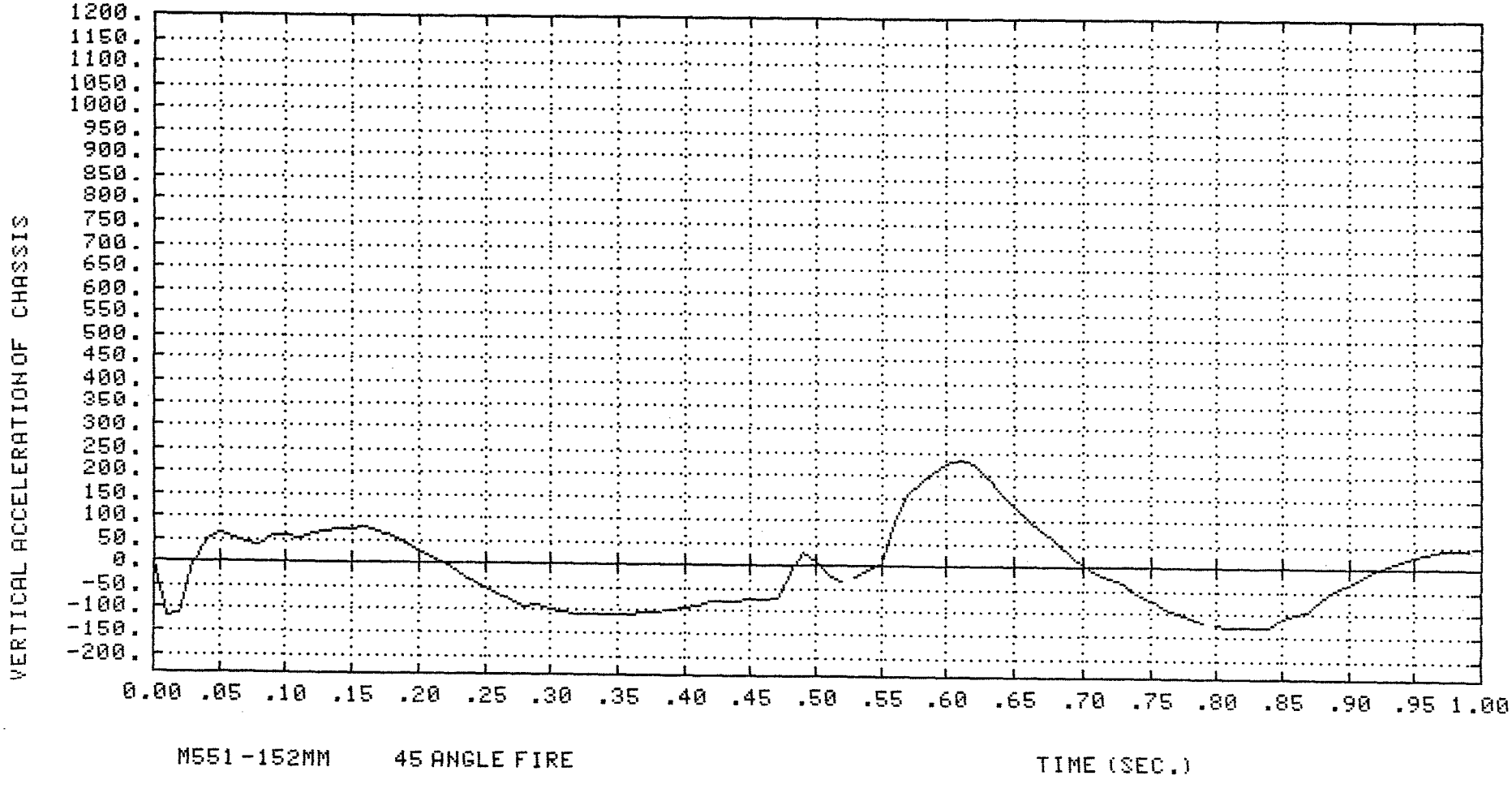

M551-152MM 45 ANGLE FIRE

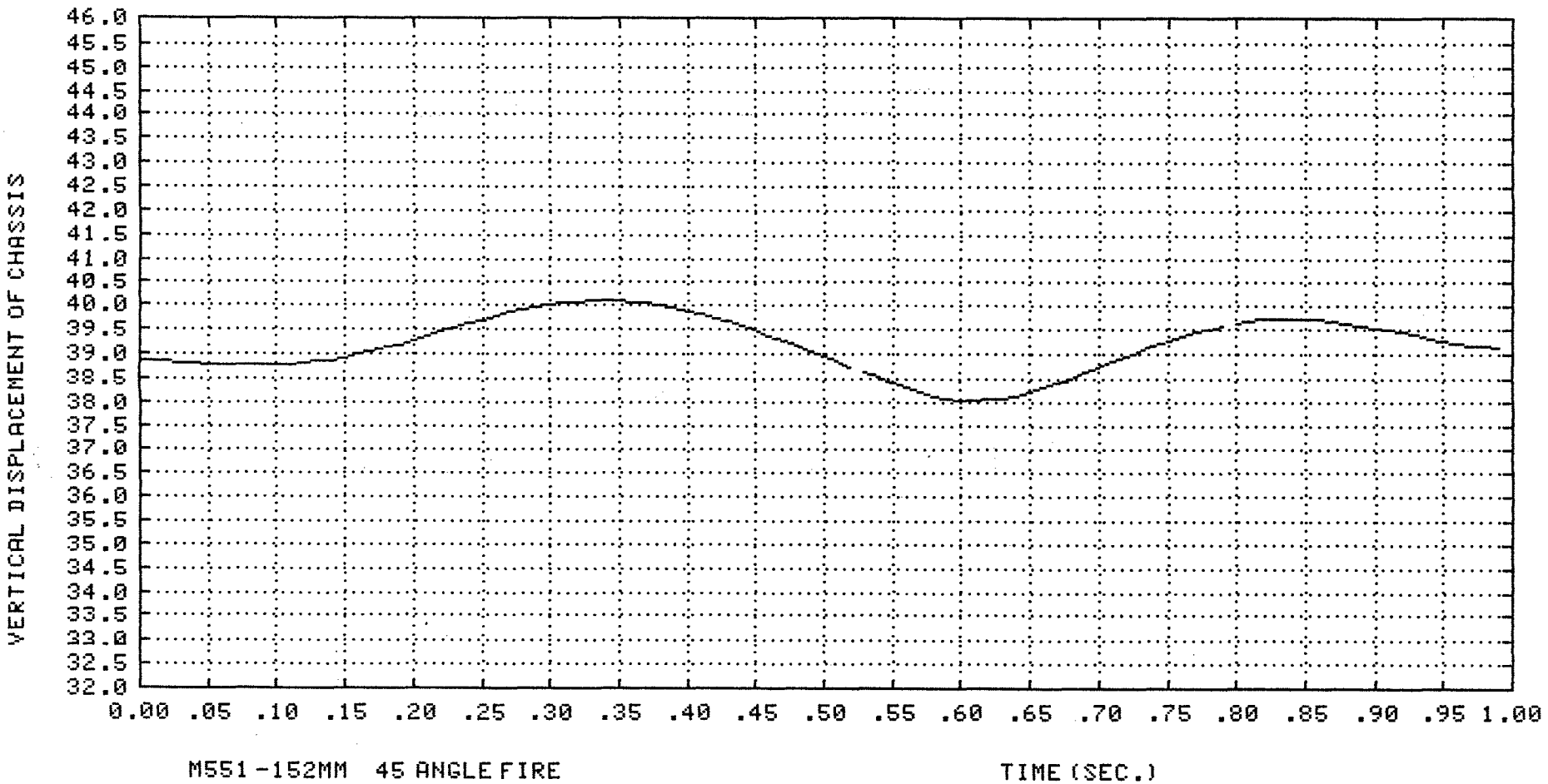
VERTICAL DISPLACEMENT OF CHASSIS
46.0
45.5
45.0
44.5
44.0
43.5
43.0
42.5
42.0
41.5
41.0
40.5
40.0
39.5
39.0
38.5
38.0
37.5
37.0
36.5
36.0
35.5
35.0
34.5
34.0
33.5
33.0
32.5
32.0
0.00 .05 .10 .15 .20 .25 .30 .35 .40 .45 .50 .55 .60 .65 .70 .75 .80 .85 .90 .95 1.00
M551-152MM 45 ANGLE FIRE
TIME (SEC.)

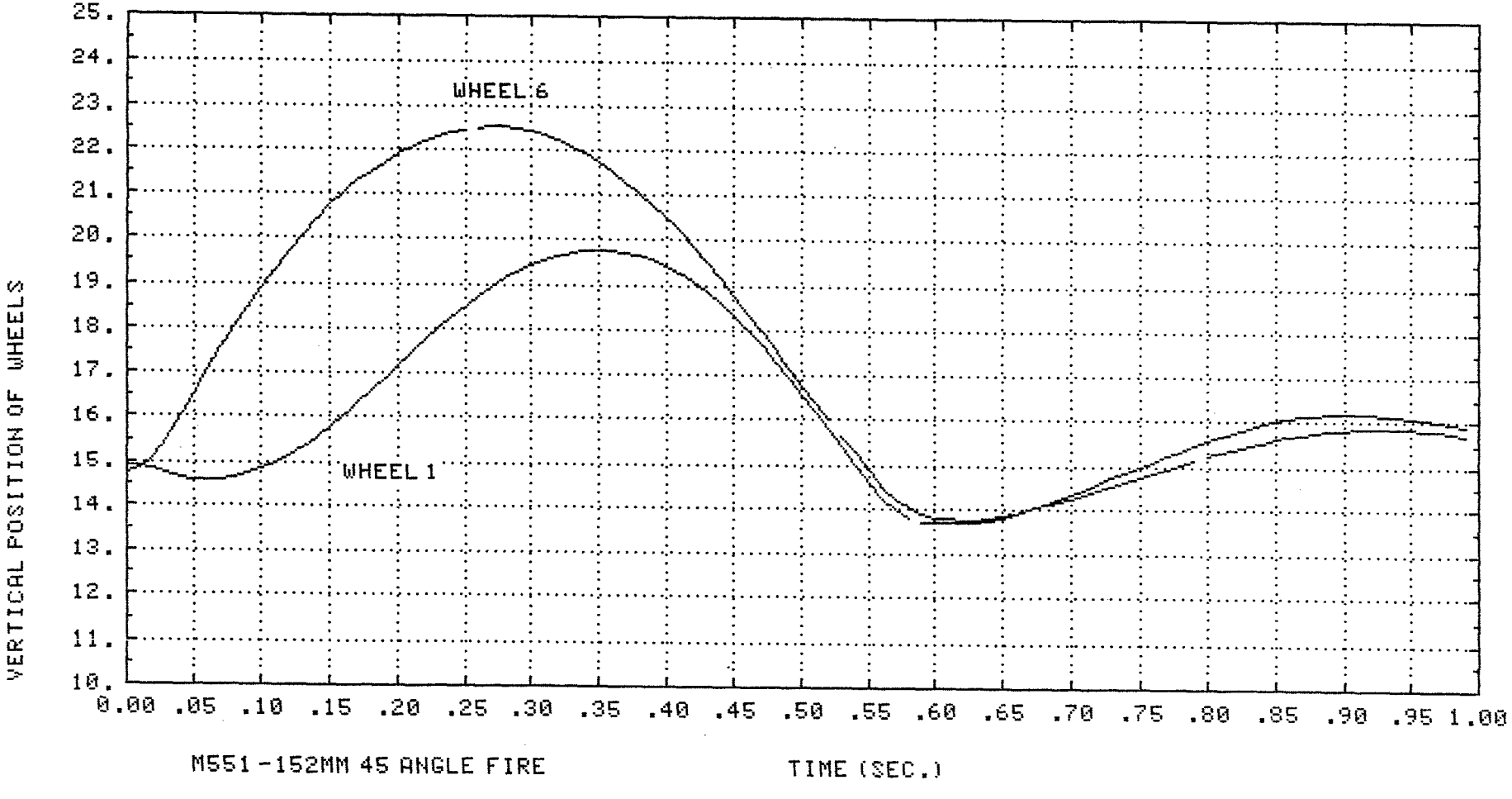

M551-152MM 45 ANGLE FIRE

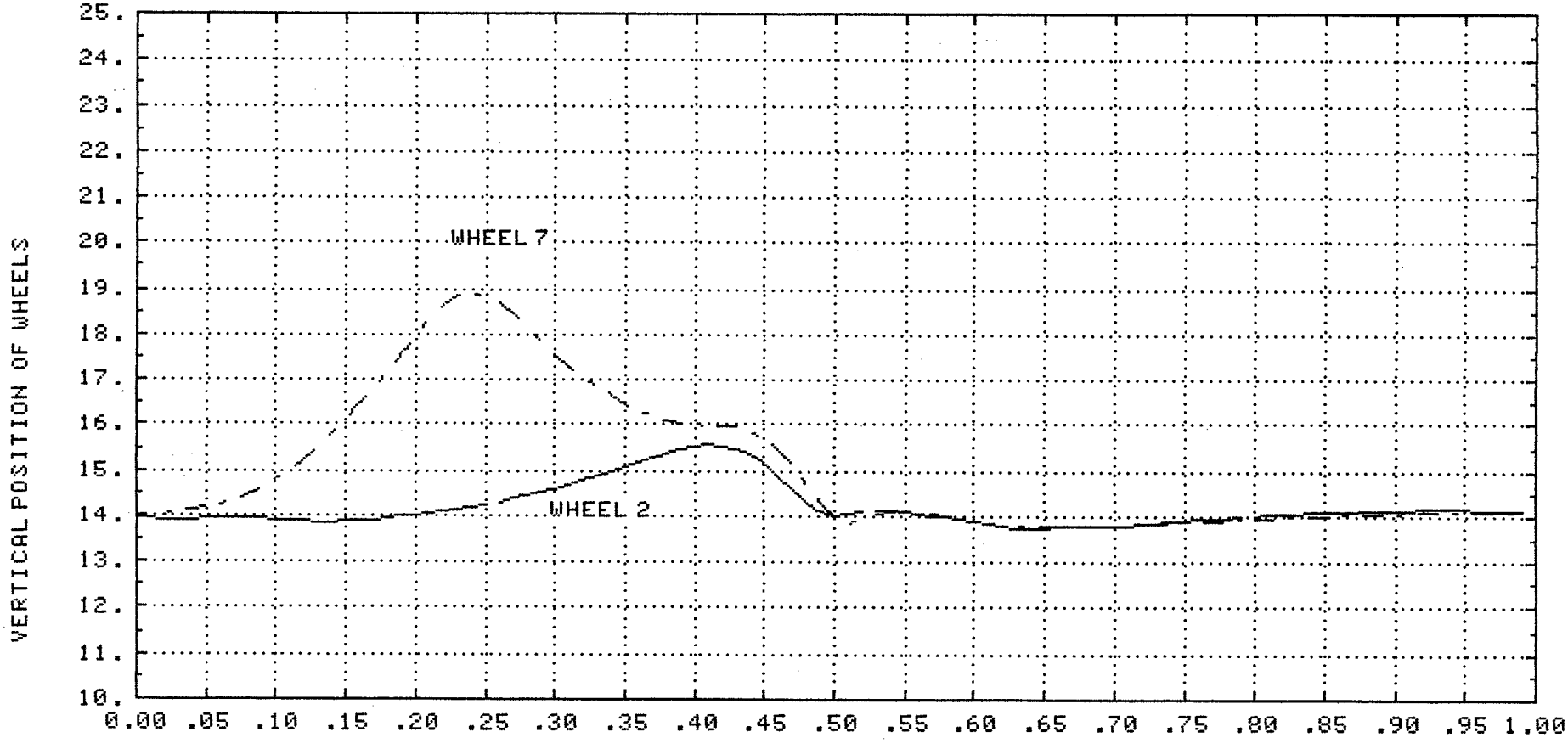

M551 -152MM 45 ANGLE FIRE

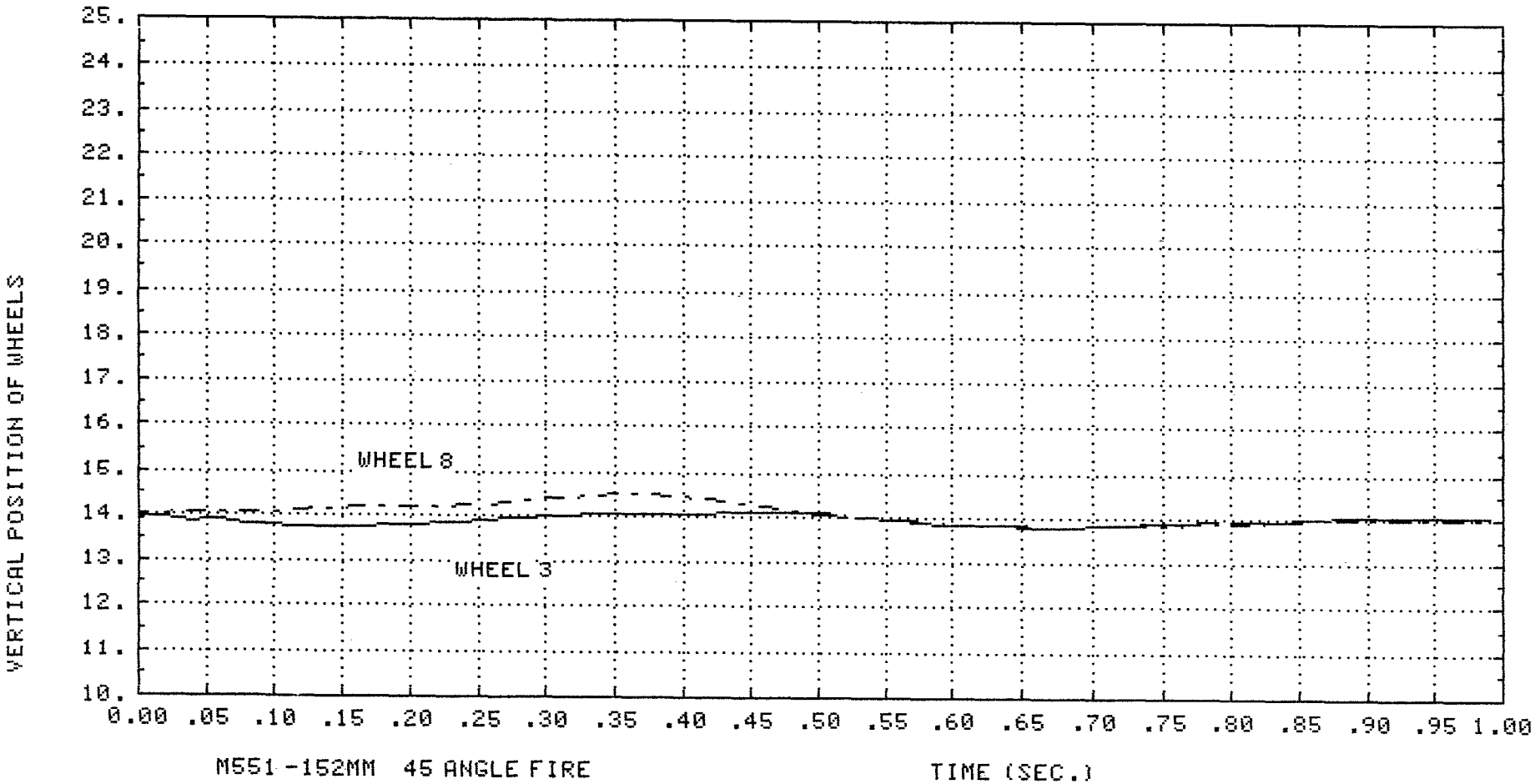
VERTICAL POSITION OF WHEELS
25.
24.
23.
22.
21.
20.
19.
18.
17.
16.
15.
14.
13.
12.
11.
10.
WHEEL 8
WHEEL 3
0.00 .05 .10 .15 .20 .25 .30 .35 .40 .45 .50 .55 .60 .65 .70 .75 .80 .85 .90 .95 1.00
M551 -152MM 45 ANGLE FIRE
TIME (SEC.)

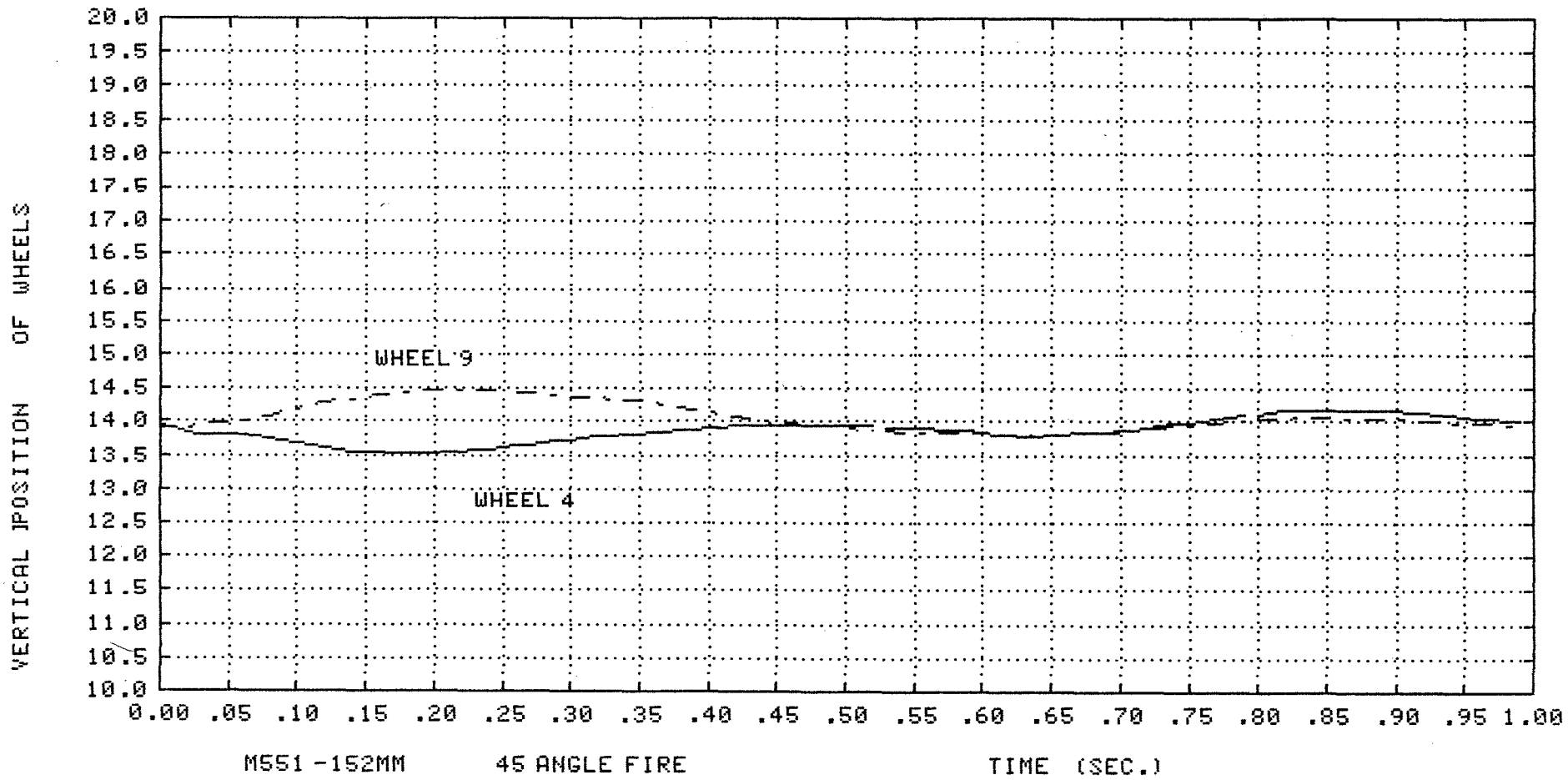
VERTICAL POSITION OF WHEELS
20.0
19.5
19.0
18.5
18.0
17.5
17.0
16.5
16.0
15.5
15.0
14.5
14.0
13.5
13.0
12.5
12.0
11.5
11.0
10.5
10.0
WHEEL 9
WHEEL 4
0.00 .05 .10 .15 .20 .25 .30 .35 .40 .45 .50 .55 .60 .65 .70 .75 .80 .85 .90 .95 1.00
M551 -152MM 45 ANGLE FIRE
TIME (SEC.)

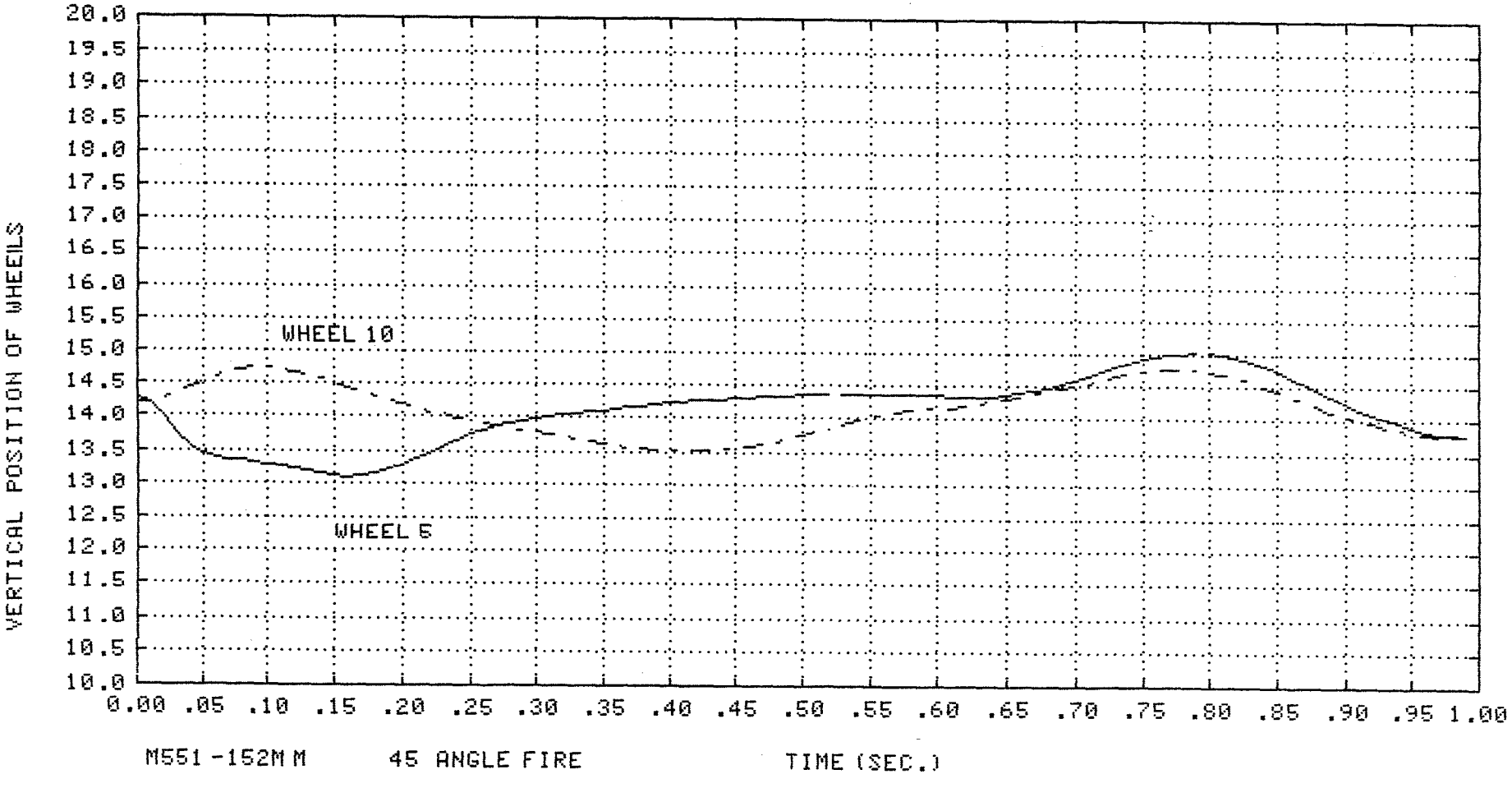
VERTICAL POSITION OF WHEELS
20.0
19.5
19.0
18.5
18.0
17.5
17.0
16.5
16.0
15.5
15.0
14.5
14.0
13.5
13.0
12.5
12.0
11.5
11.0
10.5
10.0
WHEEL 10
WHEEL 6
0.00 .05 .10 .15 .20 .25 .30 .35 .40 .45 .50 .55 .60 .65 .70 .75 .80 .85 .90 .95 1.00
M551-152M M
45 ANGLE FIRE
TIME (SEC.)

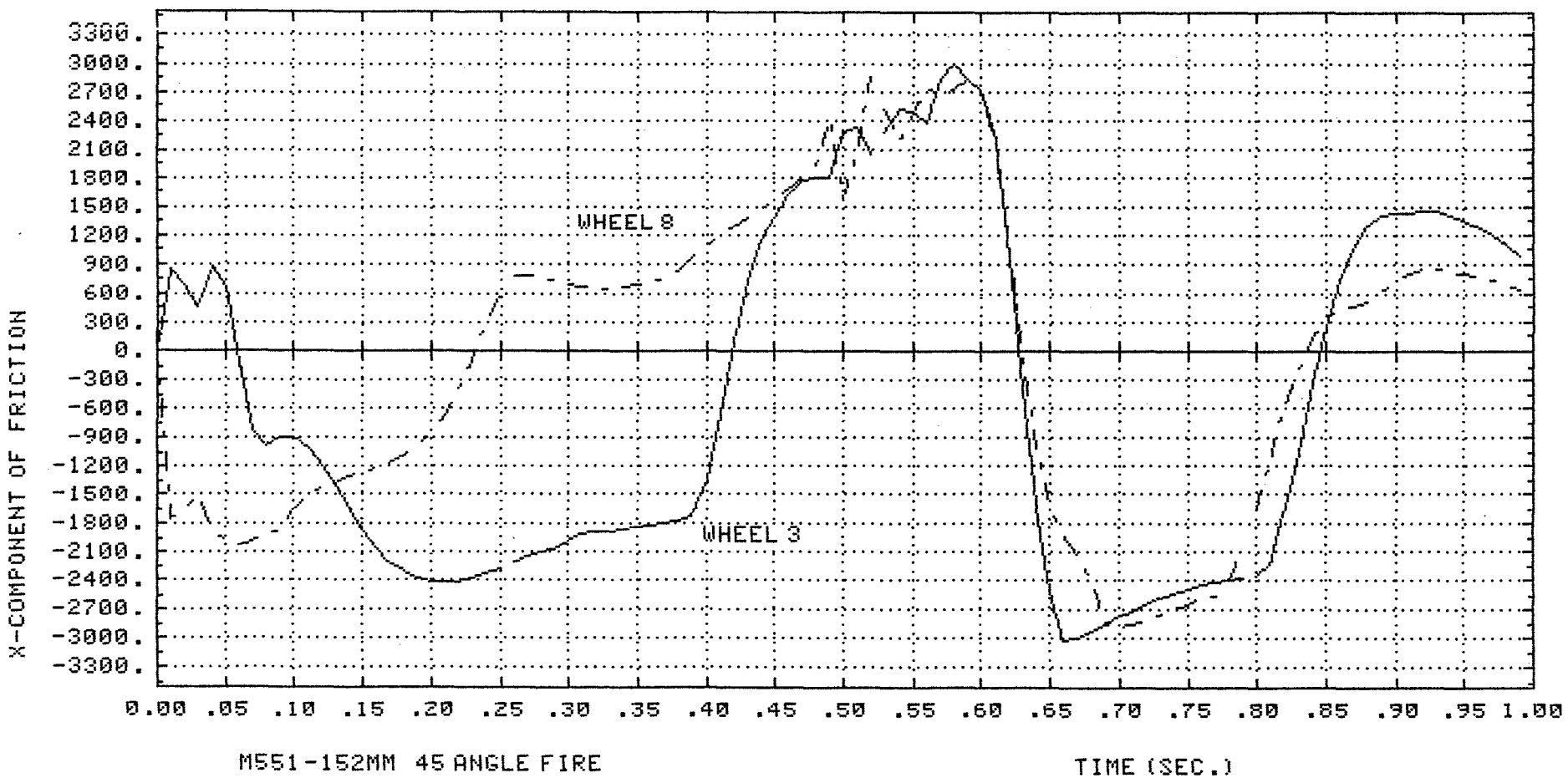
X-COMPONENT OF FRICTION
3300.
3000.
2700.
2400.
2100.
1800.
1500.
1200.
900.
600.
300.
0.
-300.
-600.
-900.
-1200.
-1500.
-1800.
-2100.
-2400.
-2700.
-3000.
-3300.
WHEEL 8
WHEEL 3
0.00 .05 .10 .15 .20 .25 .30 .35 .40 .45 .50 .55 .60 .65 .70 .75 .80 .85 .90 .95 1.00
M551-152MM 45 ANGLE FIRE
TIME (SEC.)

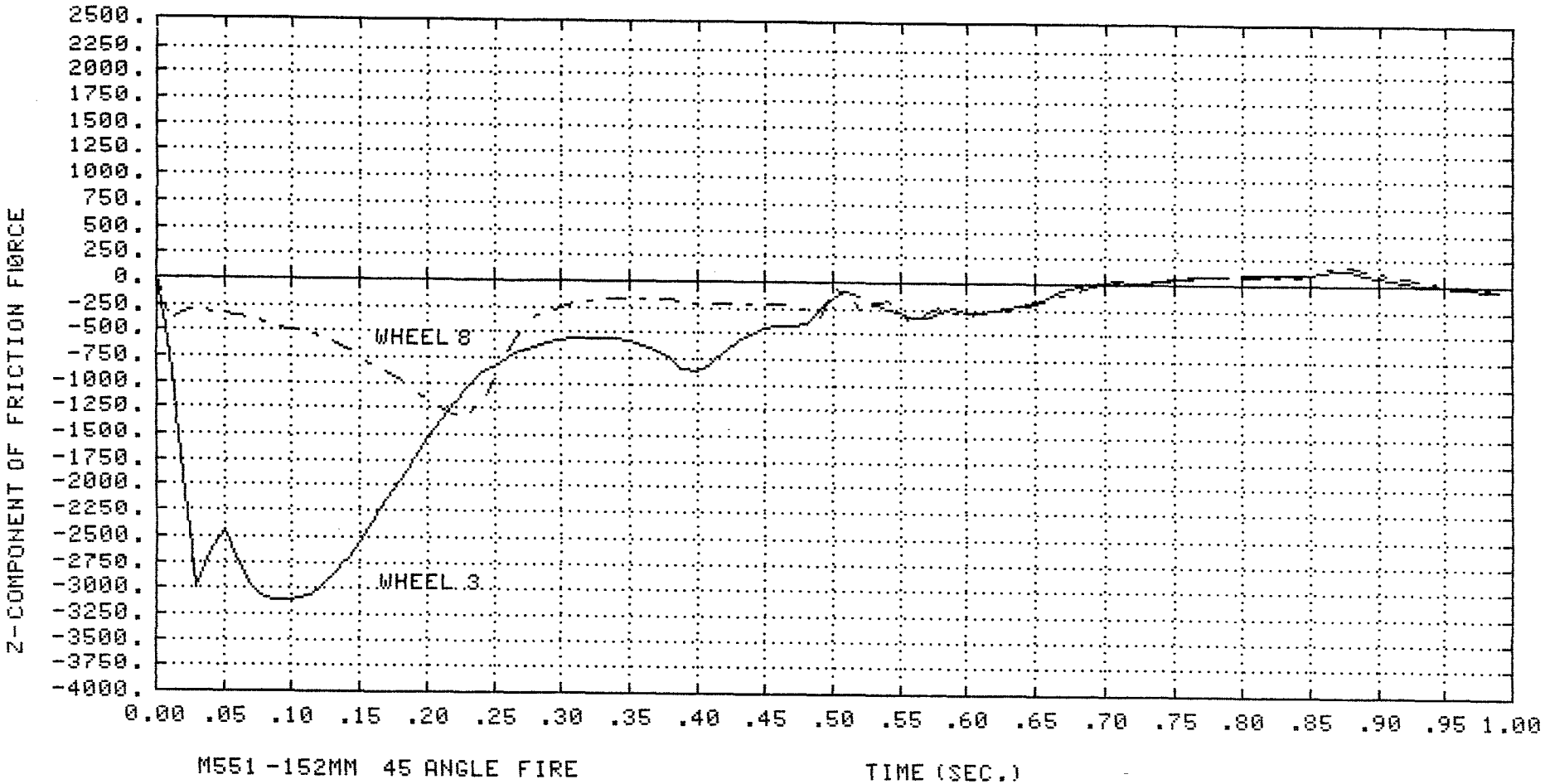

M551 -152MM 45 ANGLE FIRE

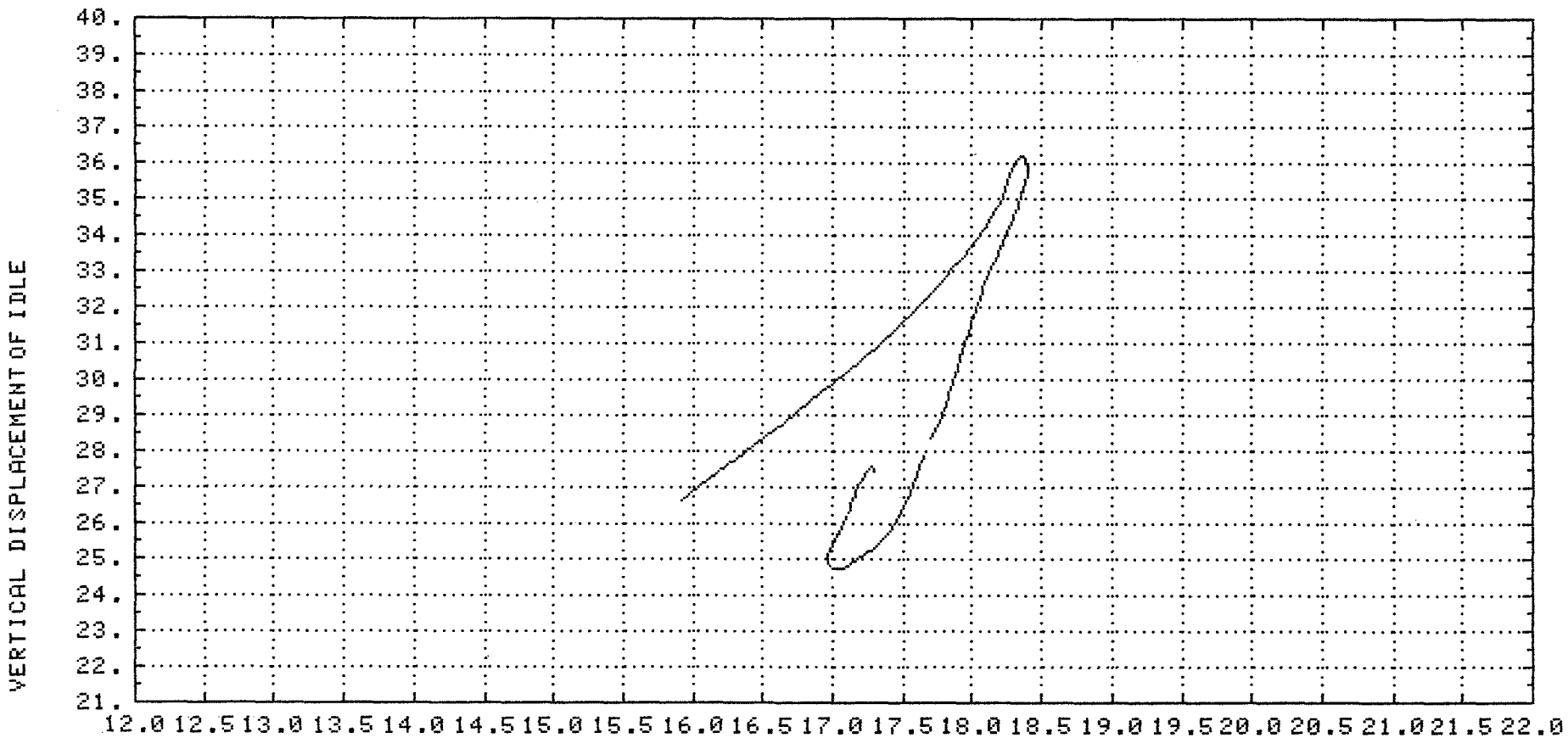

M551-152MM 45 ANGLE FIRE LONGITUDIAL DISPLACEMENT OF IDLE (F~~RONT~~ SIDE)
REAR

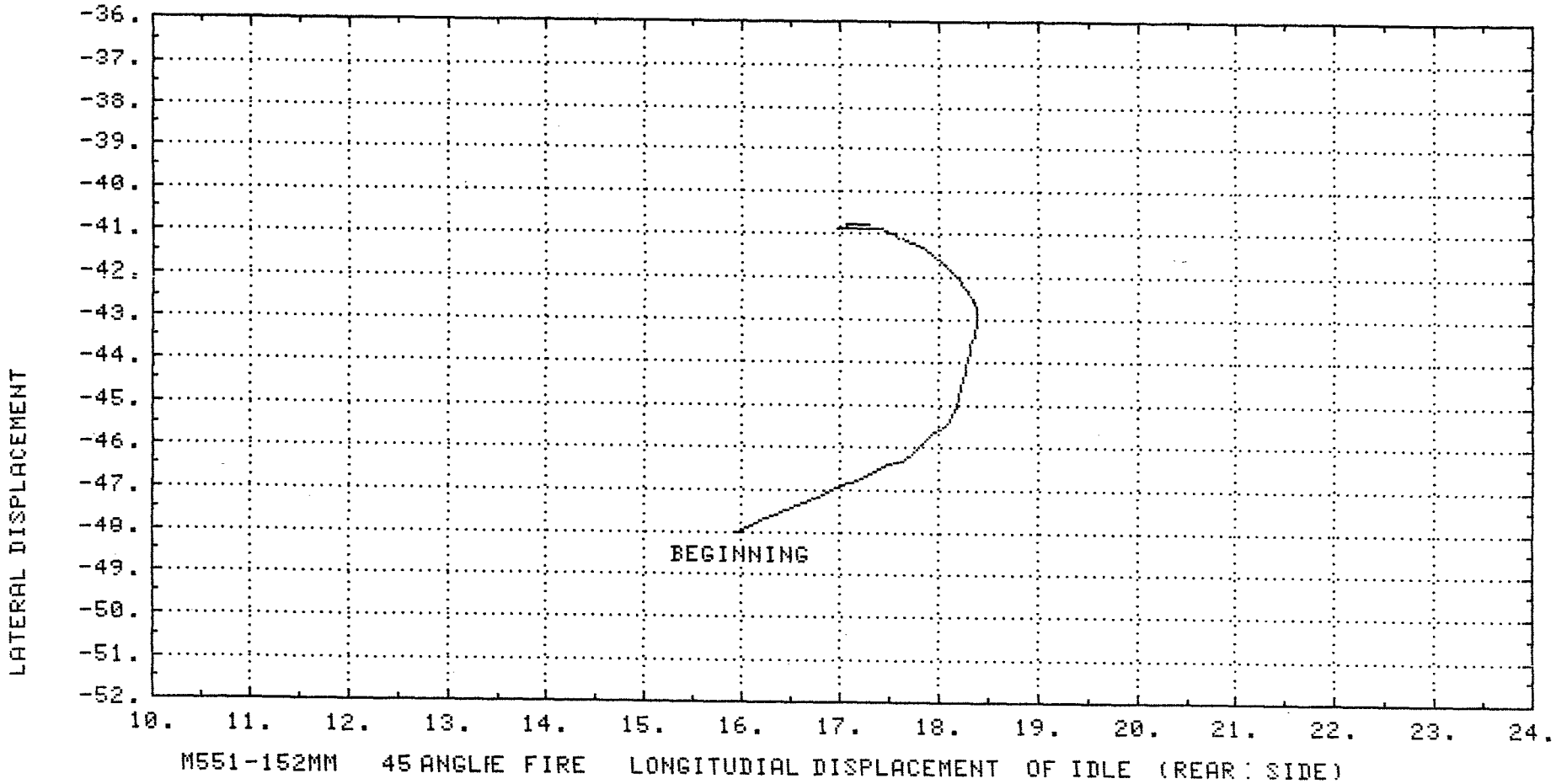
LATERAL DISPLACEMENT
-36.
-37.
-38.
-39.
-40.
-41.
-42.
-43.
-44.
-45.
-46.
-47.
-48.
-49.
-50.
-51.
-52.
10.
11.
12.
13.
14.
15.
16.
17.
18.
19.
20.
21.
22.
23.
24.
BEGINNING
M551-152MM 45 ANGLE FIRE LONGITUDIAL DISPLACEMENT OF IDLE (REAR SIDE)

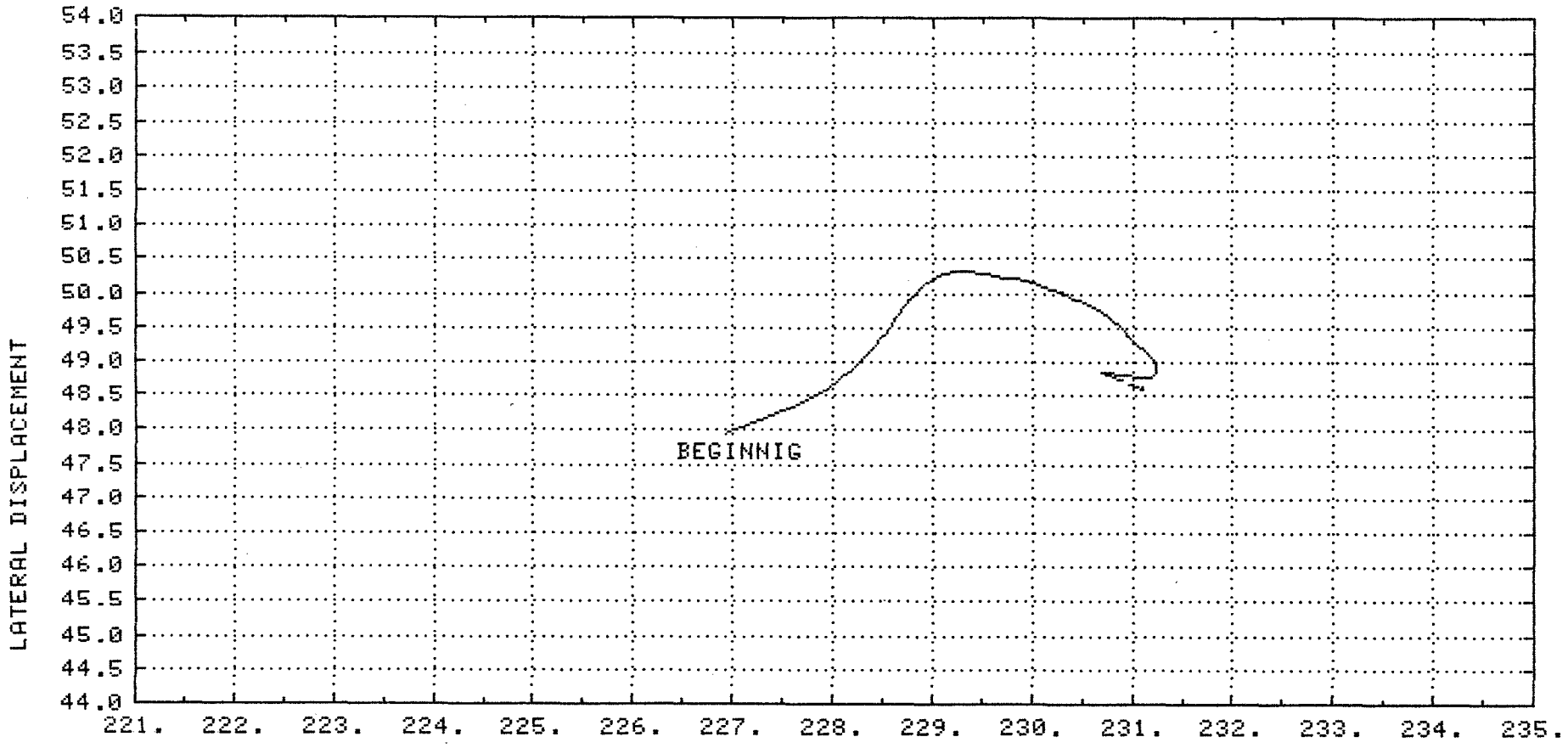

M551-152MM 45 ANGLE FIRE LONGITUDIAL DISPLACEMENT OF SPRACKET (FRONT SIDE)

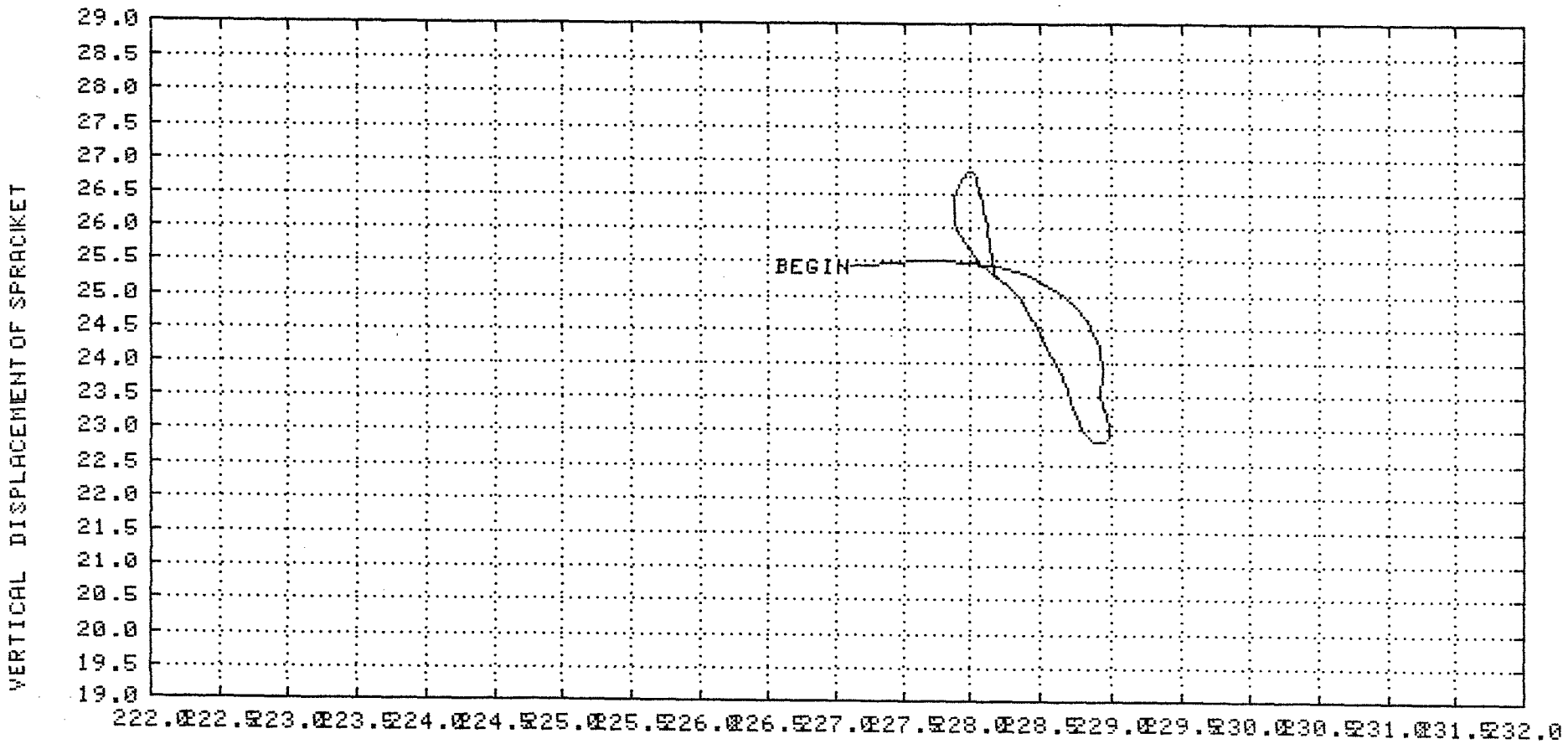

M551-152MM 45 ANGLE FIRE LONGITUDIAL DISPLACEMENT OF SPRACT (REAR SIDE)

Appendix C

Response Plots for Platform Stability Analysis

Side Fire Simulation

* Coulomb friction
* Coefficient of friction = 0.5
* 1.0 second simulation
* CPU time on PRIME - 750 ≈ 5800 sec.

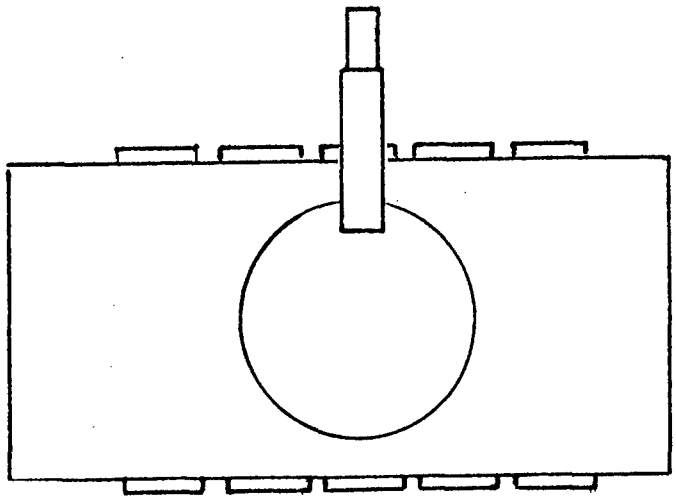

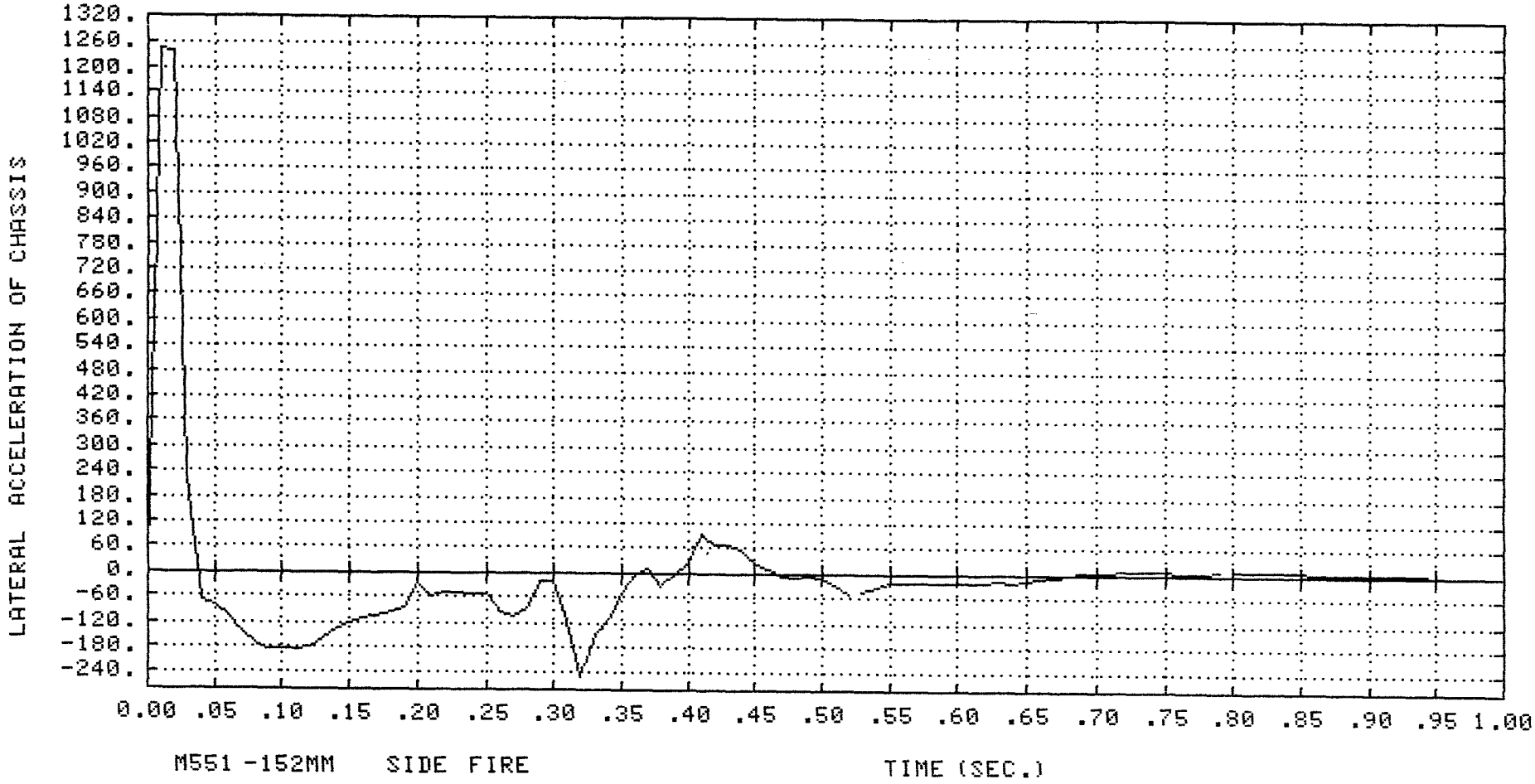
LATERAL ACCELERATION OF CHASSIS
1320.
1260.
1200.
1140.
1080.
1020.
960.
900.
840.
780.
720.
660.
600.
540.
480.
420.
360.
300.
240.
180.
120.
60.
0.
-60.
-120.
-180.
-240.
0.00 .05 .10 .15 .20 .25 .30 .35 .40 .45 .50 .55 .60 .65 .70 .75 .80 .85 .90 .95 1.00
M551 -152MM SIDE FIRE
TIME (SEC.)

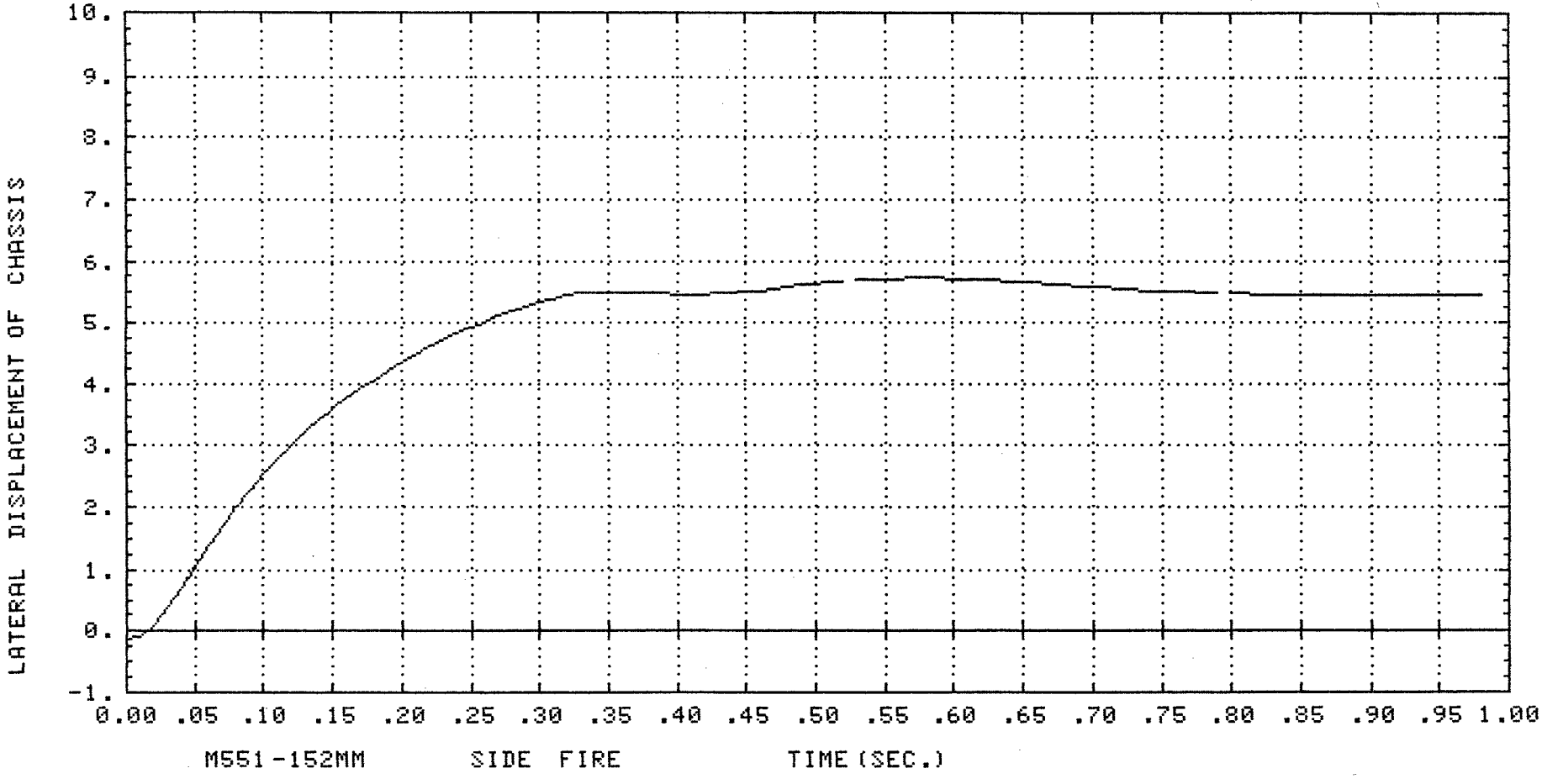
LATERAL DISPLACEMENT OF CHASSIS
10.
9.
8.
7.
6.
5.
4.
3.
2.
1.
0.
-1.
0.00 .05 .10 .15 .20 .25 .30 .35 .40 .45 .50 .55 .60 .65 .70 .75 .80 .85 .90 .95 1.00
M551-152MM SIDE FIRE
TIME (SEC.)

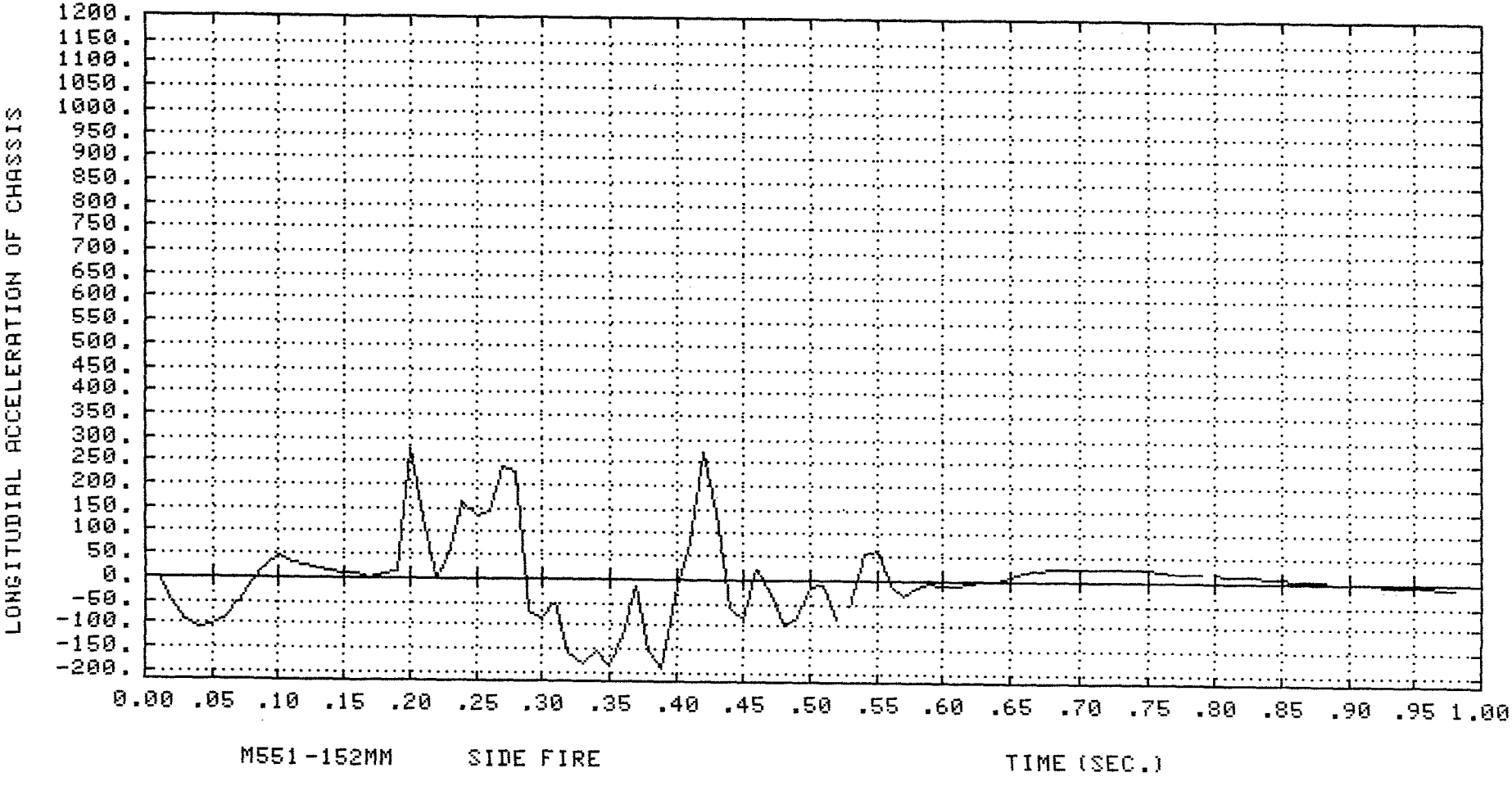
LONGITUDIAL ACCELERATION OF CHASSIS
1200.
1150.
1100.
1050.
1000.
950.
900.
850.
800.
750.
700.
650.
600.
550.
500.
450.
400.
350.
300.
250.
200.
150.
100.
50.
0.
-50.
-100.
-150.
-200.
0.00 .05 .10 .15 .20 .25 .30 .35 .40 .45 .50 .55 .60 .65 .70 .75 .80 .85 .90 .95 1.00
M551-152MM SIDE FIRE
TIME (SEC.)

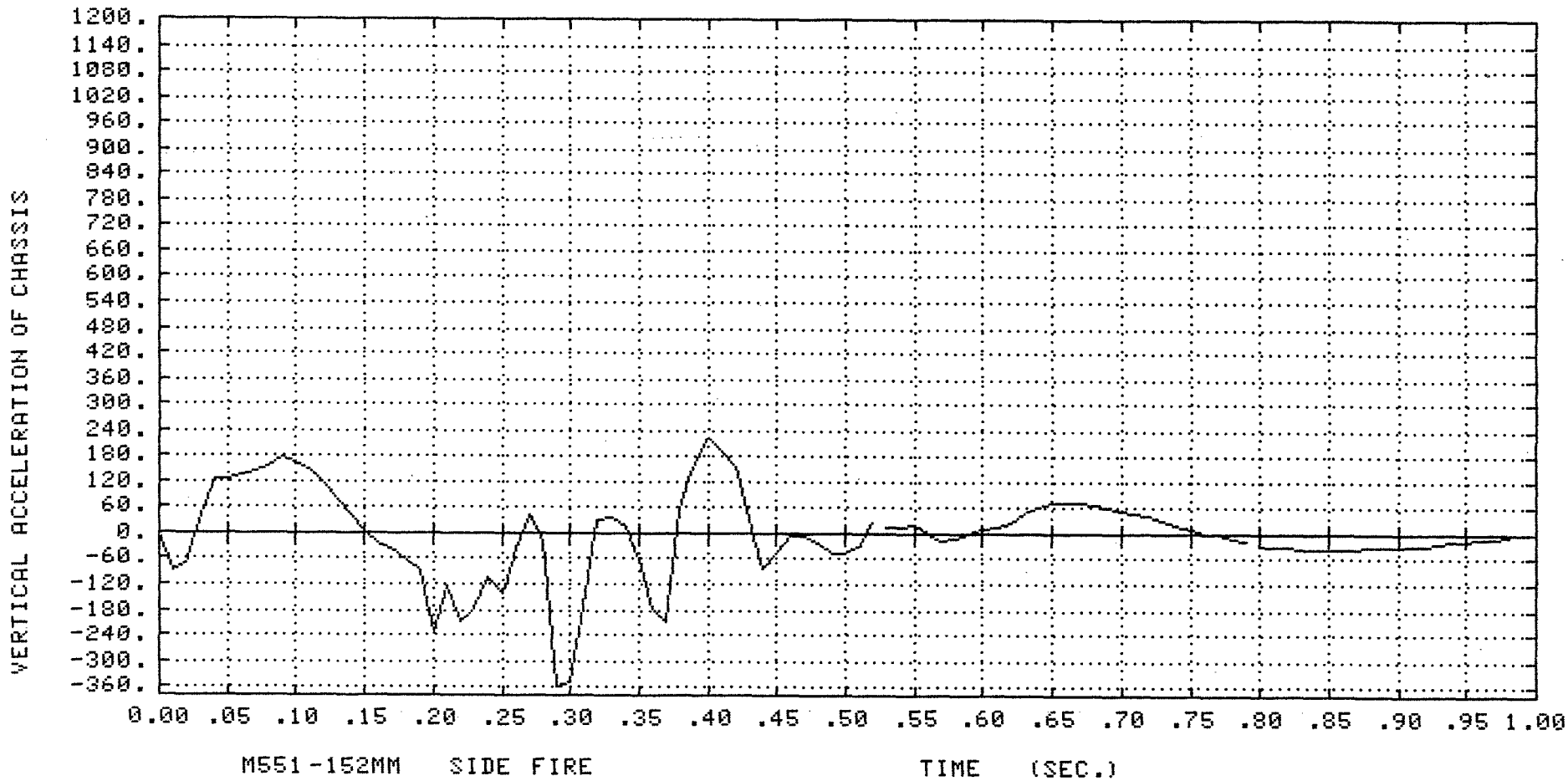
VERTICAL ACCELERATION OF CHASSIS
1200.
1140.
1080.
1020.
960.
900.
840.
780.
720.
660.
600.
540.
480.
420.
360.
300.
240.
180.
120.
60.
0.
-60.
-120.
-180.
-240.
-300.
-360.
0.00 .05 .10 .15 .20 .25 .30 .35 .40 .45 .50 .55 .60 .65 .70 .75 .80 .85 .90 .95 1.00
M551-152MM SIDE FIRE
TIME (SEC.)

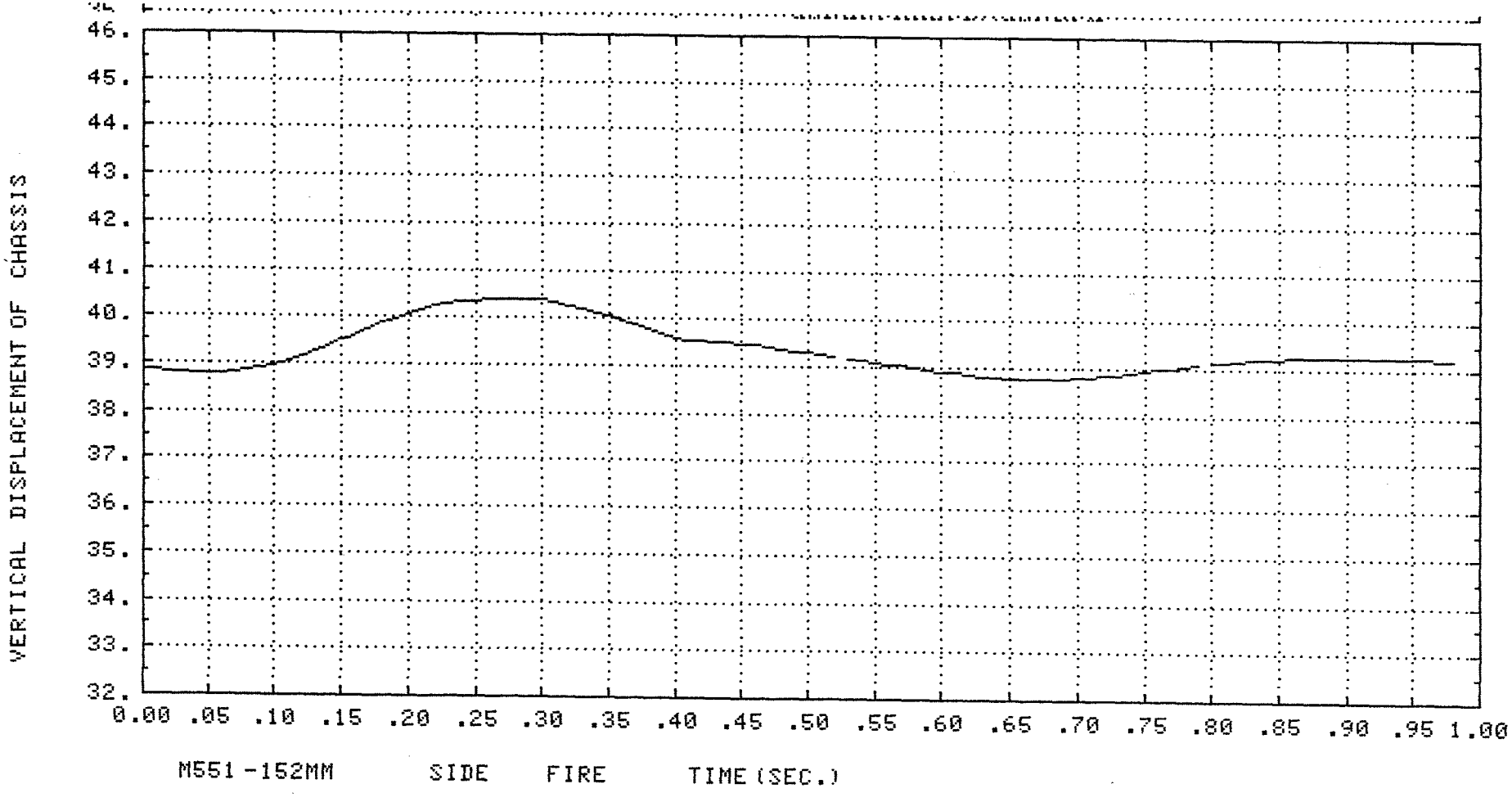
VERTICAL DISPLACEMENT OF CHASSIS
46.
45.
44.
43.
42.
41.
40.
39.
38.
37.
36.
35.
34.
33.
32.
0.00 .05 .10 .15 .20 .25 .30 .35 .40 .45 .50 .55 .60 .65 .70 .75 .80 .85 .90 .95 1.00
M551-152MM SIDE FIRE TIME (SEC.)

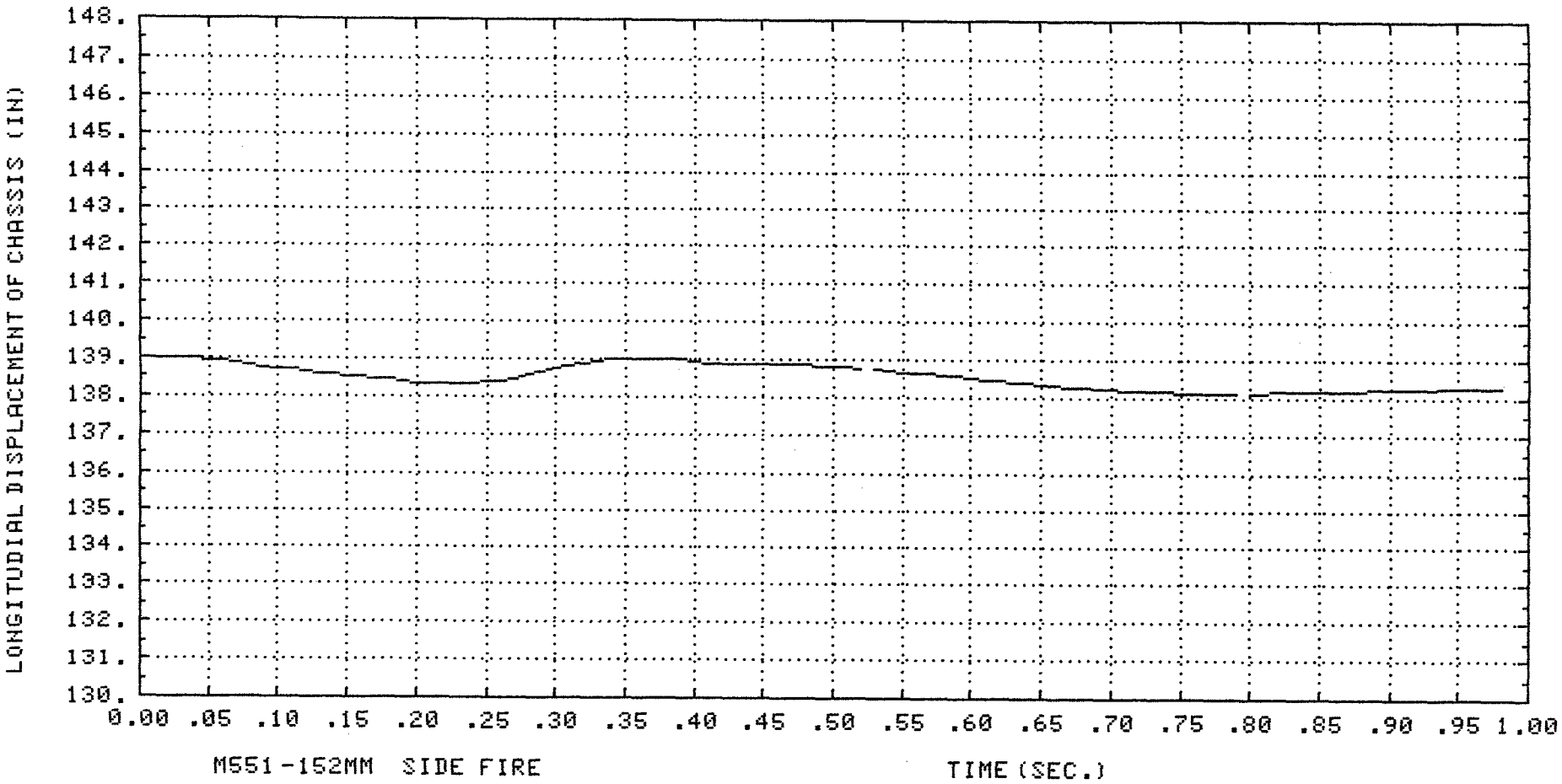
LONGITUDIAL DISPLACEMENT OF CHASSIS (IN)
148.
147.
146.
145.
144.
143.
142.
141.
140.
139.
138.
137.
136.
135.
134.
133.
132.
131.
130.
0.00 .05 .10 .15 .20 .25 .30 .35 .40 .45 .50 .55 .60 .65 .70 .75 .80 .85 .90 .95 1.00
M551-152MM SIDE FIRE
TIME (SEC.)

M551 - 152MM SIDE FIRE

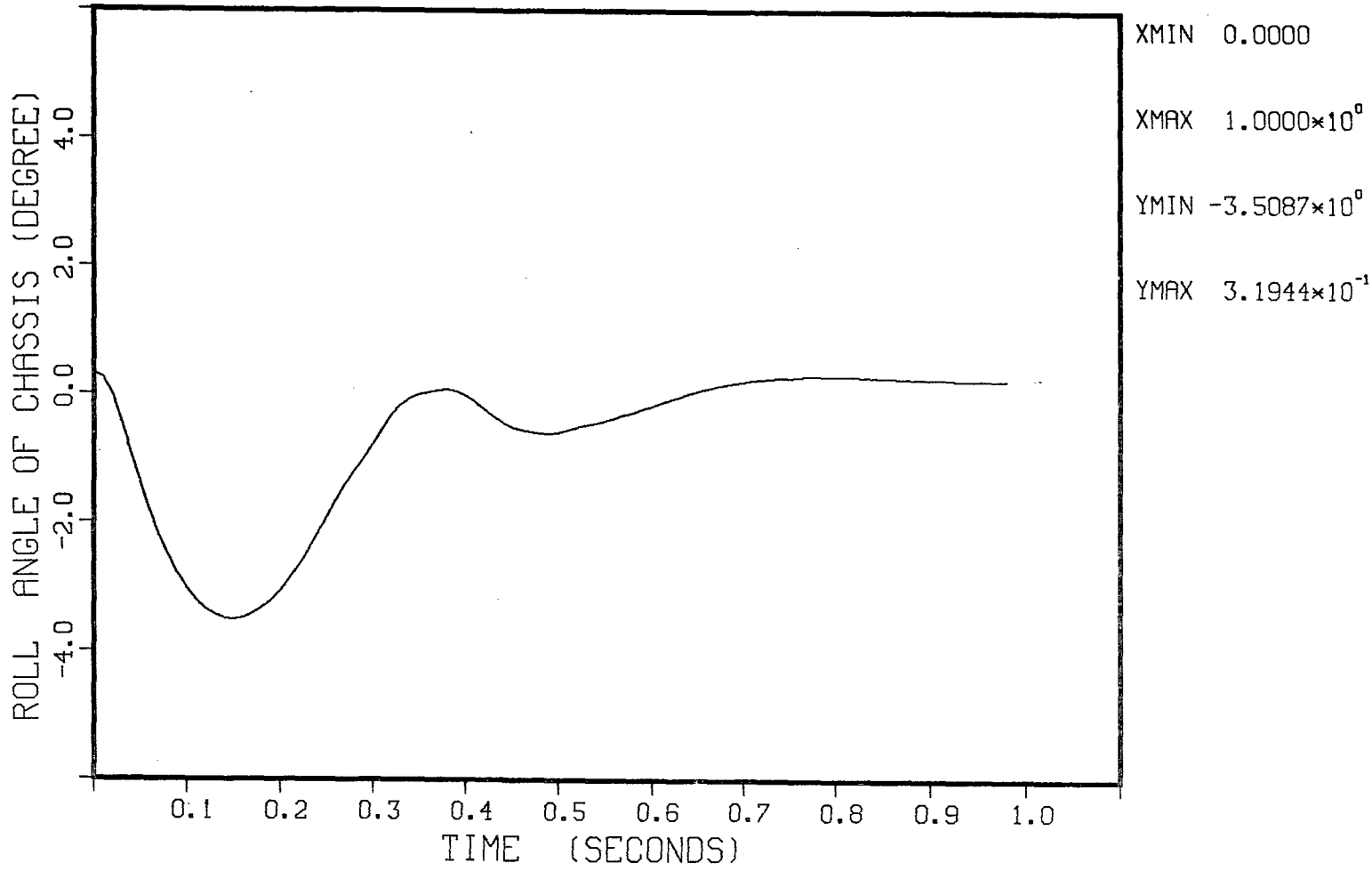

(NOTE : ' - ' MEANS GOING UP)

M551 - 152MM SIDE FIRE

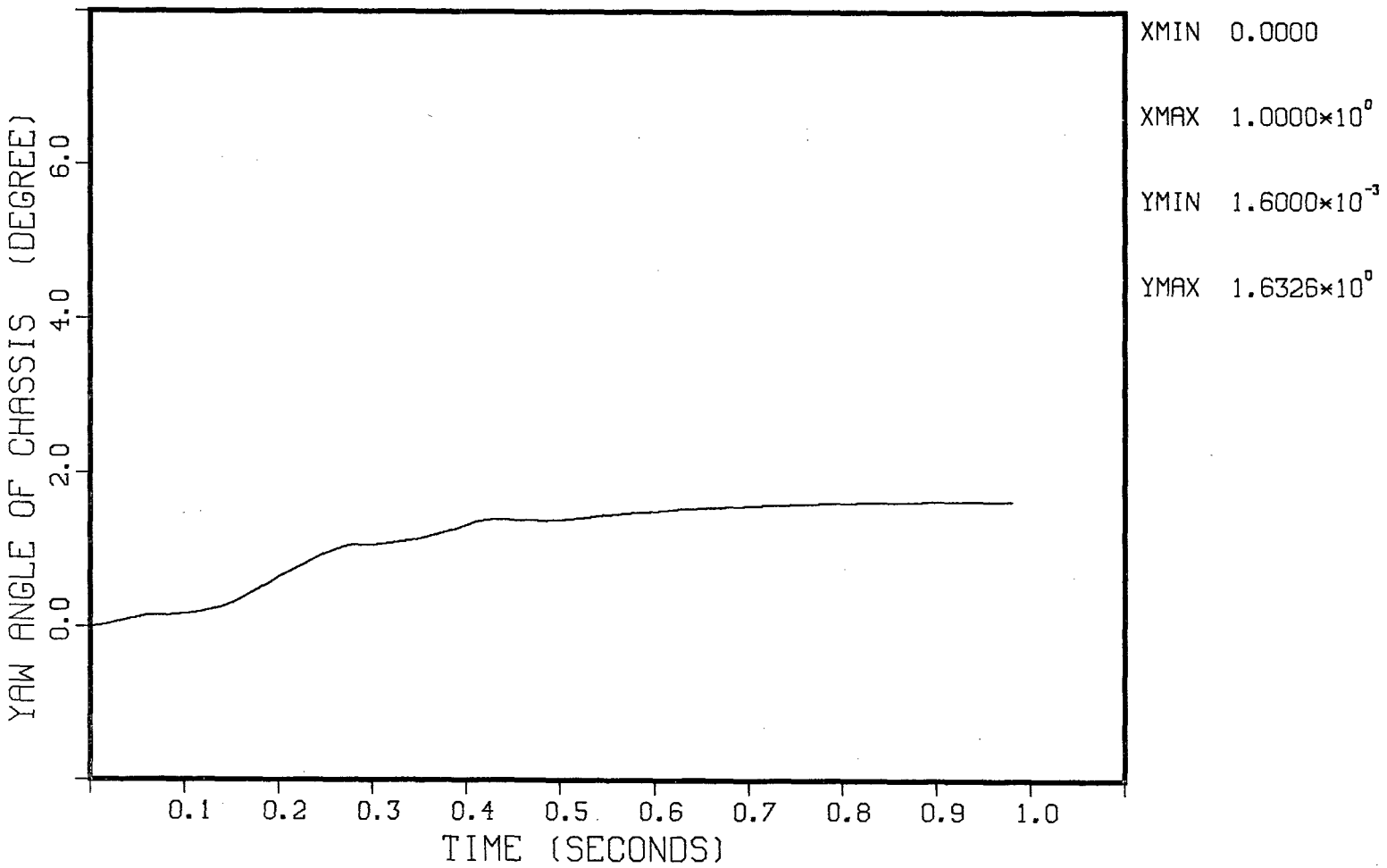

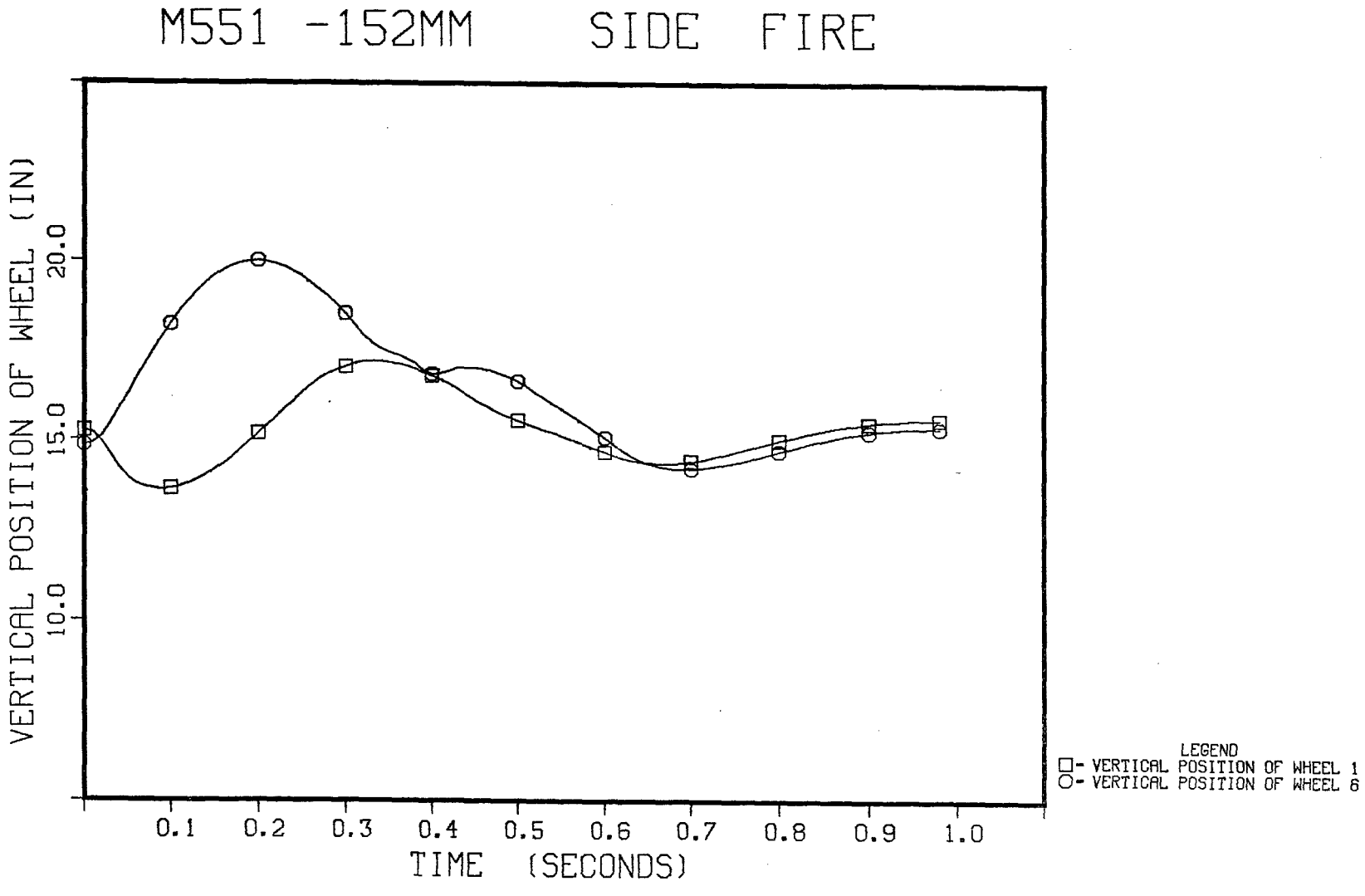
M551 -152MM SIDE FIRE
VERTICAL POSITION OF WHEEL (IN)
20.0
15.0
10.0
0.1
0.2
0.3
0.4
0.5
0.6
0.7
0.8
0.9
1.0
TIME (SECONDS)
LEGEND
□- VERTICAL POSITION OF WHEEL 1
○- VERTICAL POSITION OF WHEEL 6

M551 - 152MM SIDE FIRE

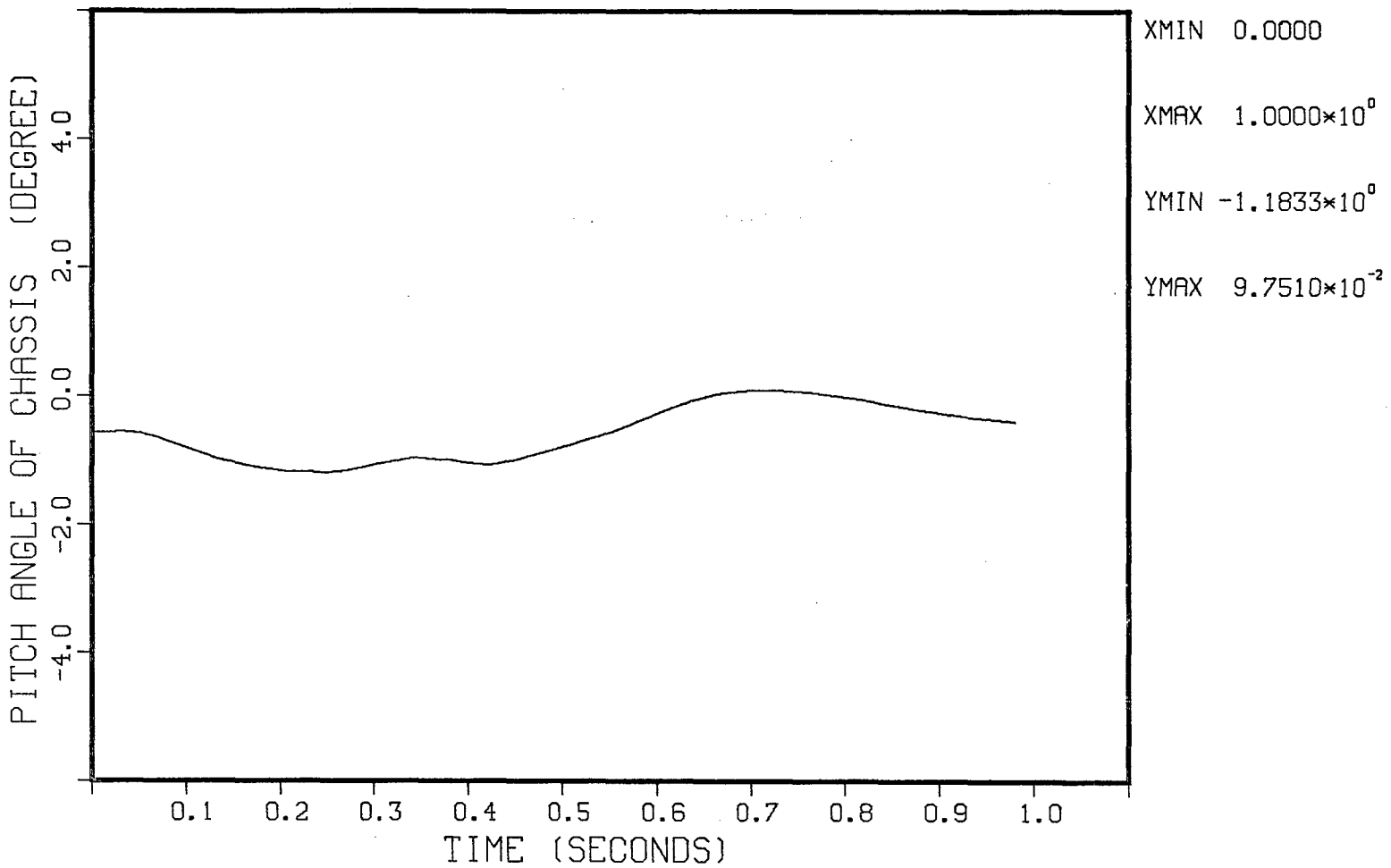

(NOTE : ' - ' MEANS GOING UP)

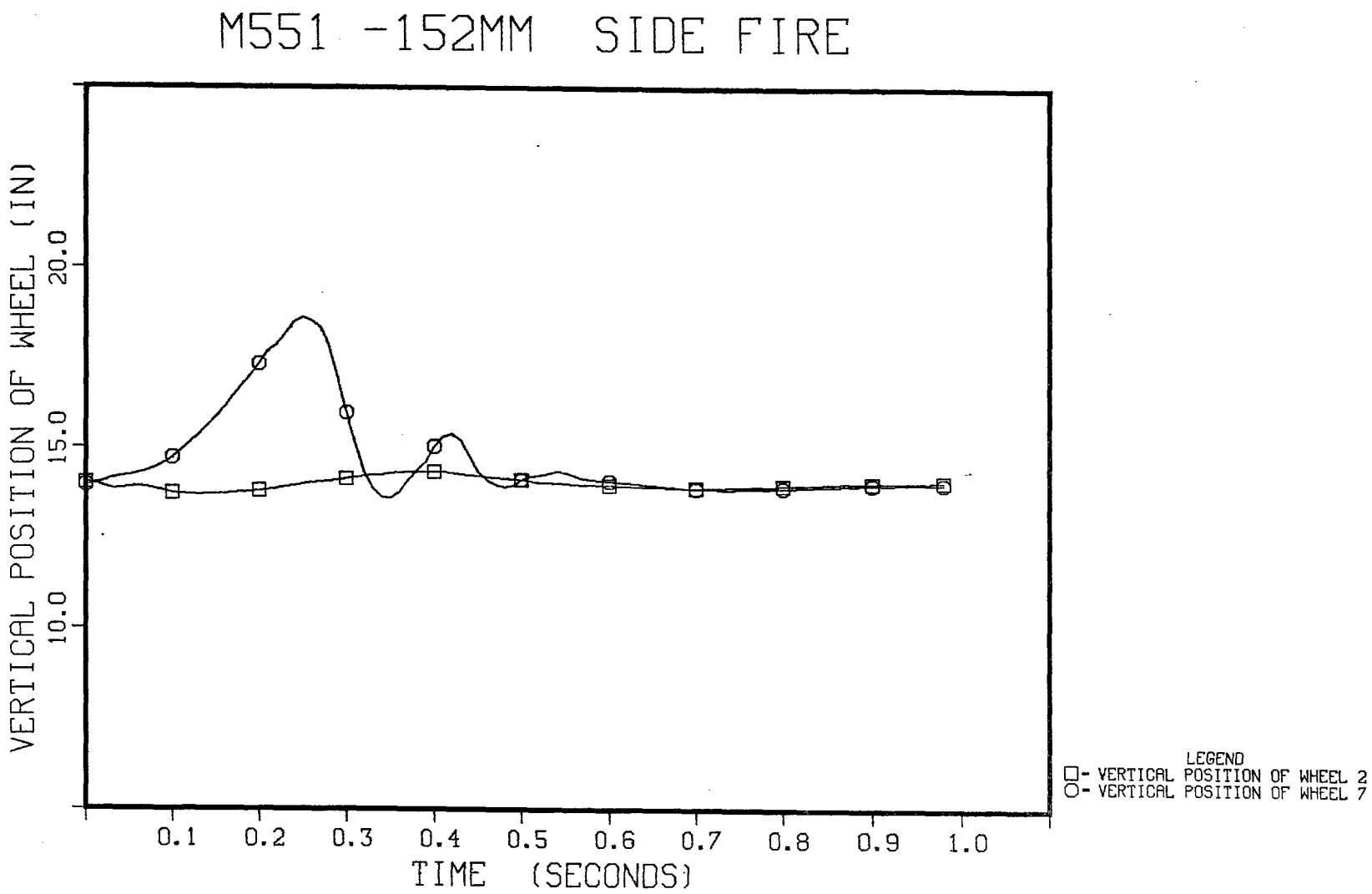
M551 -152MM SIDE FIRE
VERTICAL POSITION OF WHEEL (IN)
20.0
15.0
10.0
0.1
0.2
0.3
0.4
0.5
0.6
0.7
0.8
0.9
1.0
TIME (SECONDS)
LEGEND
□- VERTICAL POSITION OF WHEEL 2
○- VERTICAL POSITION OF WHEEL 7

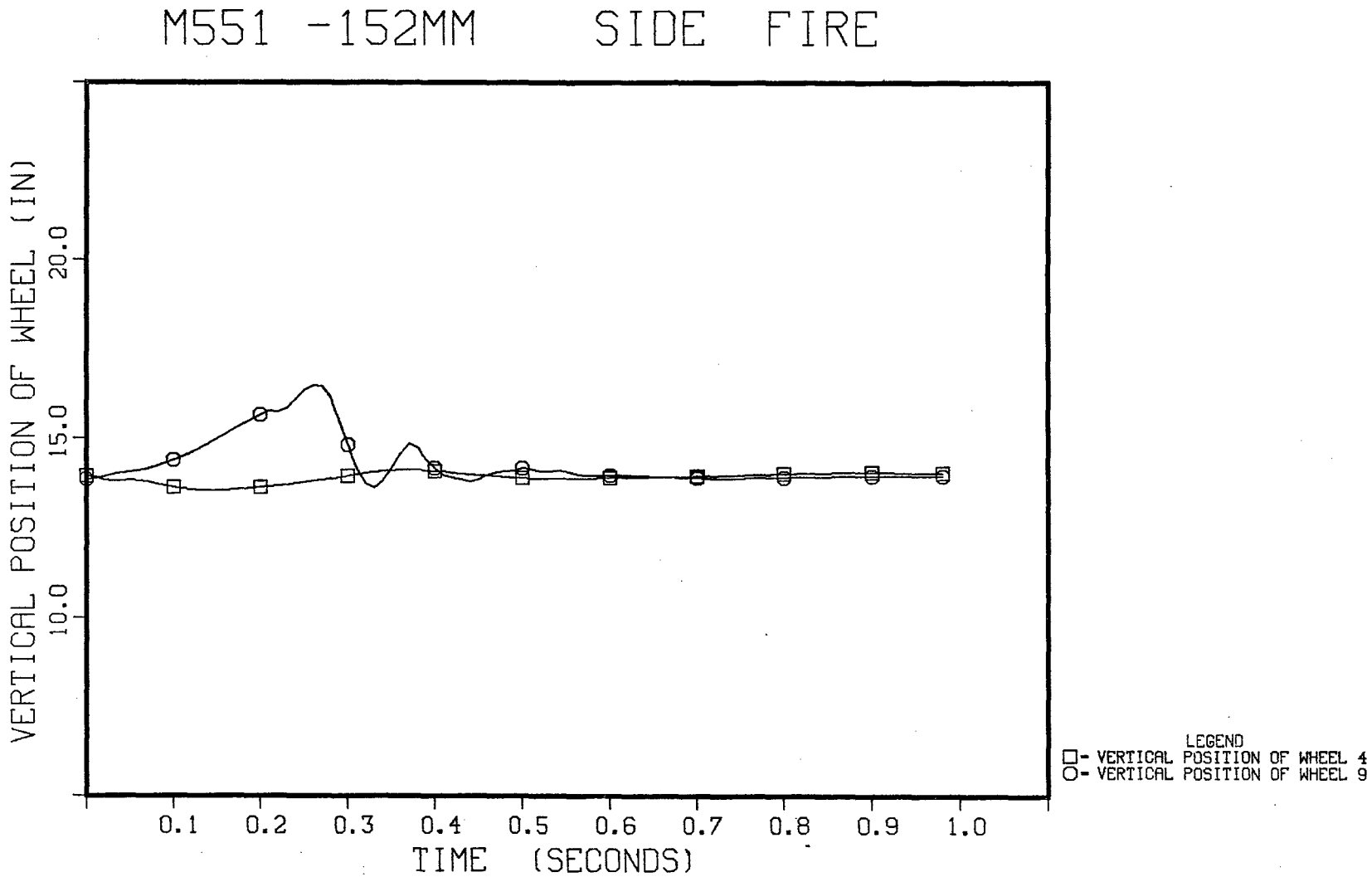
M551 -152MM SIDE FIRE
VERTICAL POSITION OF WHEEL (IN)
20.0
15.0
10.0
0.1
0.2
0.3
0.4
0.5
0.6
0.7
0.8
0.9
1.0
TIME (SECONDS)
LEGEND
□- VERTICAL POSITION OF WHEEL 4
○- VERTICAL POSITION OF WHEEL 9

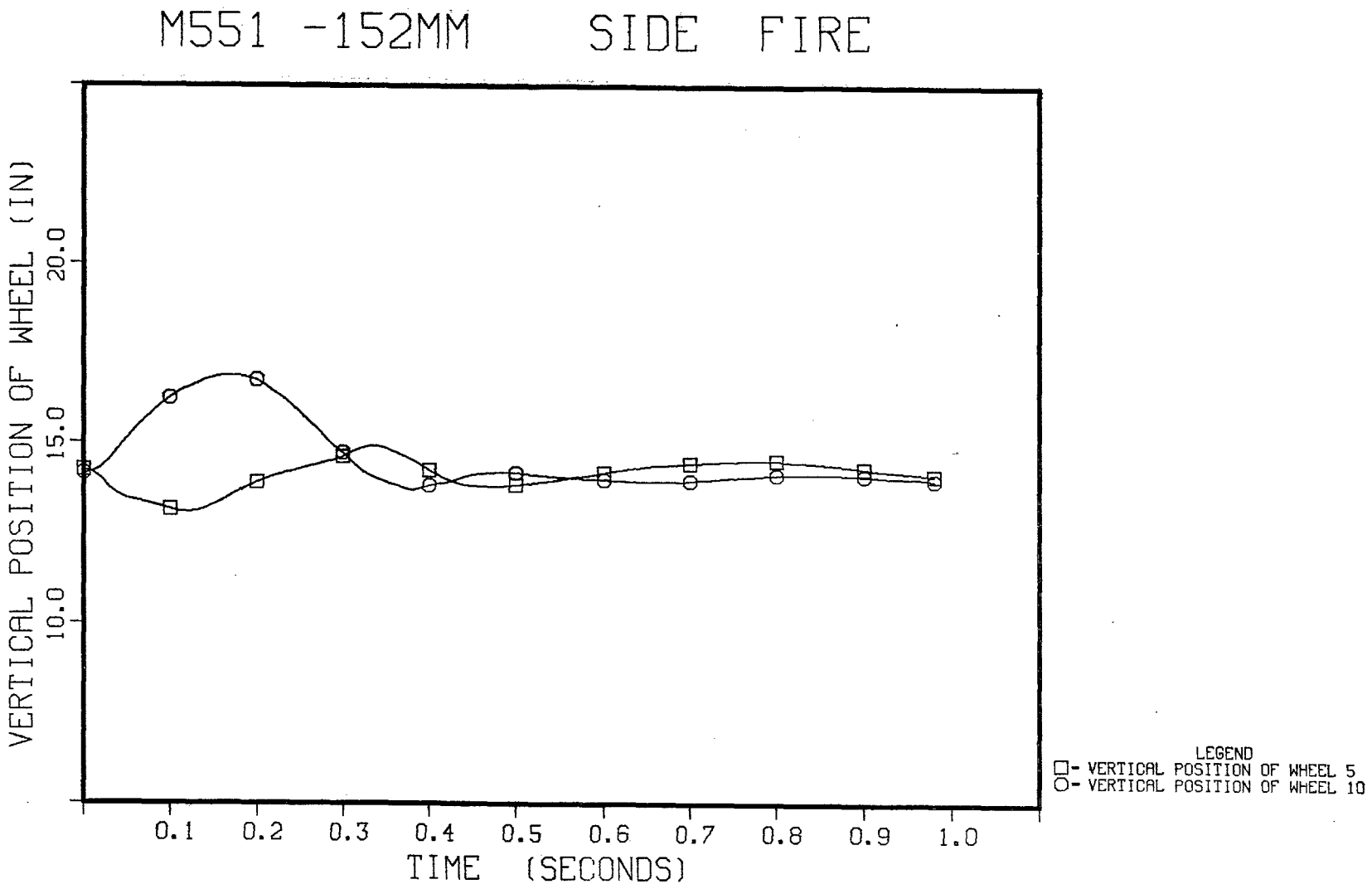
M551 -152MM SIDE FIRE
VERTICAL POSITION OF WHEEL (IN)
20.0
15.0
10.0
0.1
0.2
0.3
0.4
0.5
0.6
0.7
0.8
0.9
1.0
TIME (SECONDS)
LEGEND
□- VERTICAL POSITION OF WHEEL 5
○- VERTICAL POSITION OF WHEEL 10

Appendix D

Response Plots for Platform Stability Analysis

45° Fire Simulation

* Output time internal = 0.0025
* Coulomb friction
* Ground-track shear deformation (ref. point: bottom of the wheels)
* Coefficient of friction =
* 1.0 second of simulation
* CPU time on PRIME - 750 ≈ 9 hr.

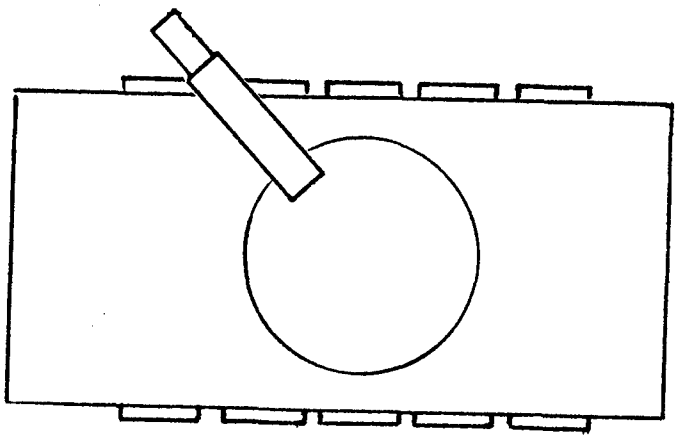

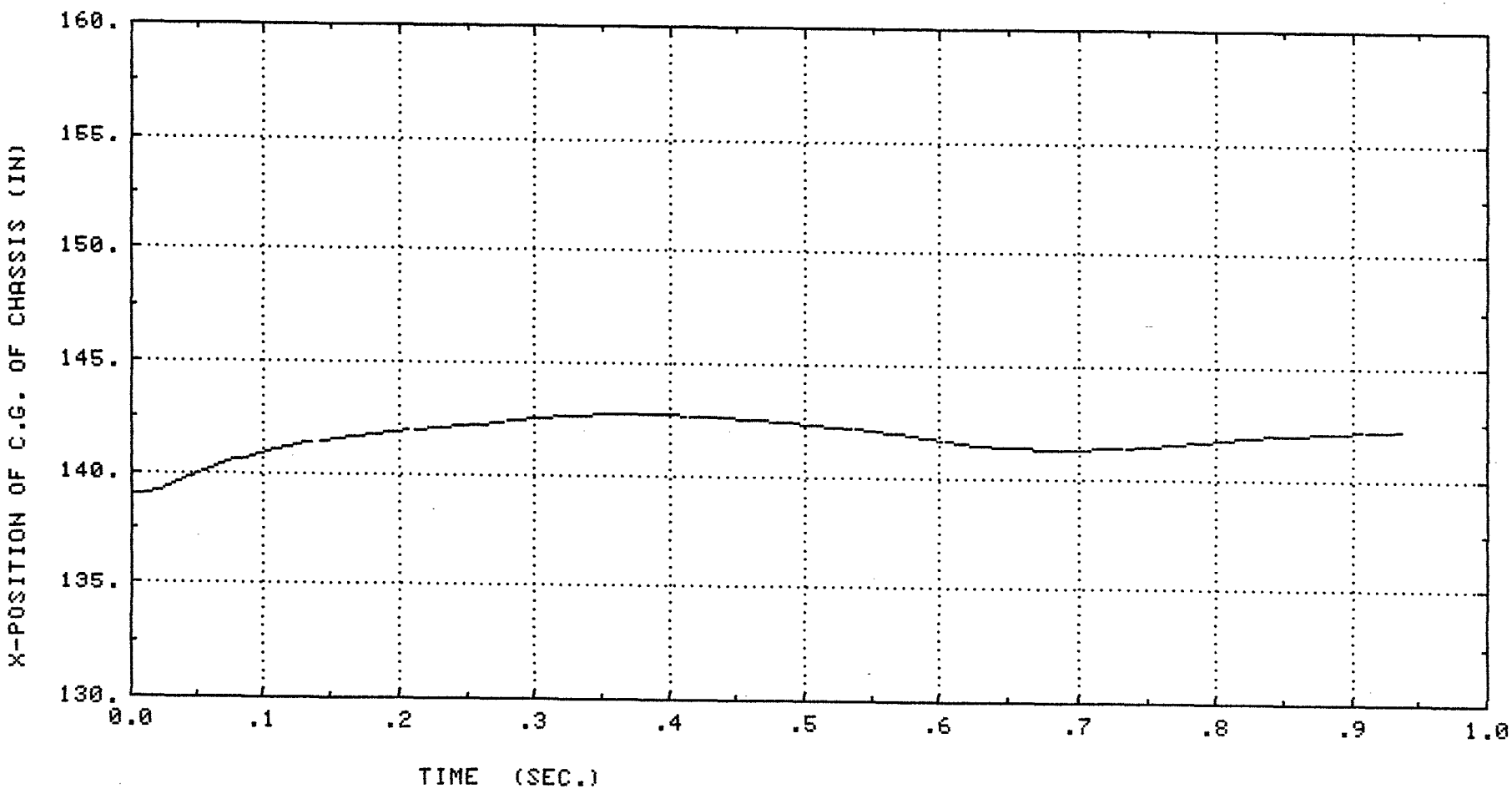
160.
155.
150.
145.
140.
135.
130.
X-POSITION OF C.G. OF CHASSIS (IN)
0.0
.1
.2
.3
.4
.5
.6
.7
.8
.9
1.0
TIME (SEC.)

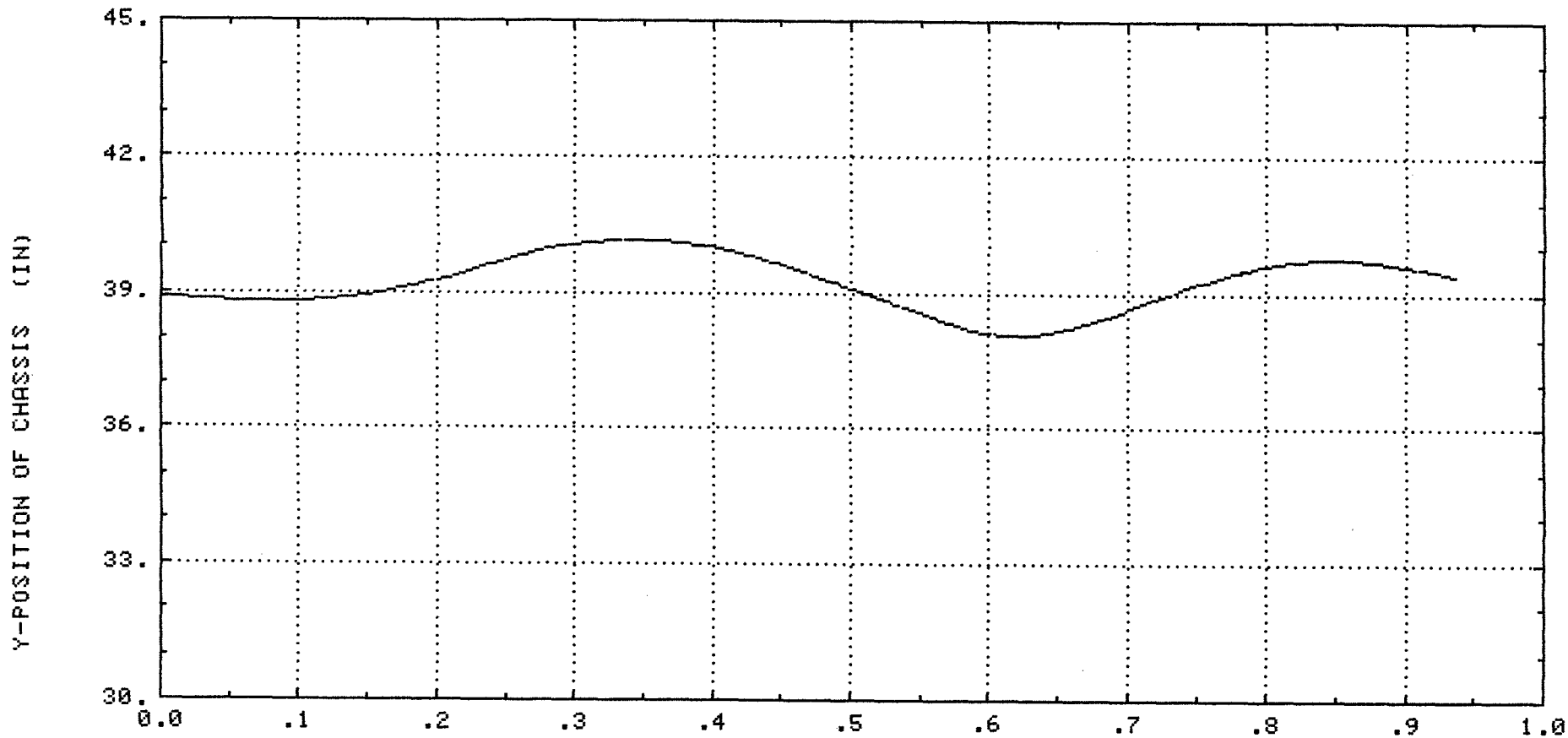
Y-POSITION OF CHASSIS (IN)
45.
42.
39.
36.
33.
30.
0.0
.1
.2
.3
.4
.5
.6
.7
.8
.9
1.0

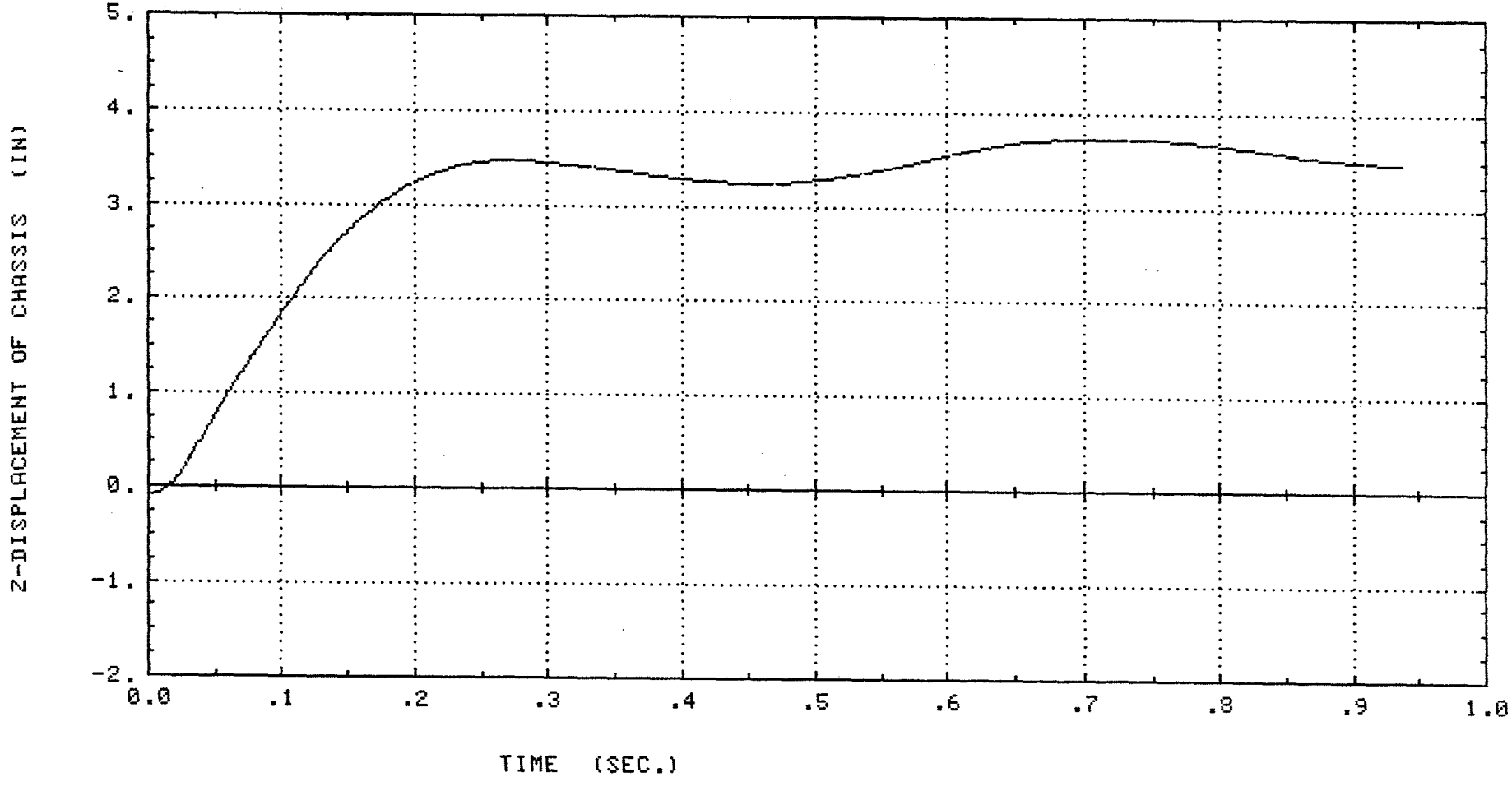
Z-DISPLACEMENT OF CHASSIS (IN)
5.
4.
3.
2.
1.
0.
-1.
-2.
0.0
.1
.2
.3
.4
.5
.6
.7
.8
.9
1.0
TIME (SEC.)

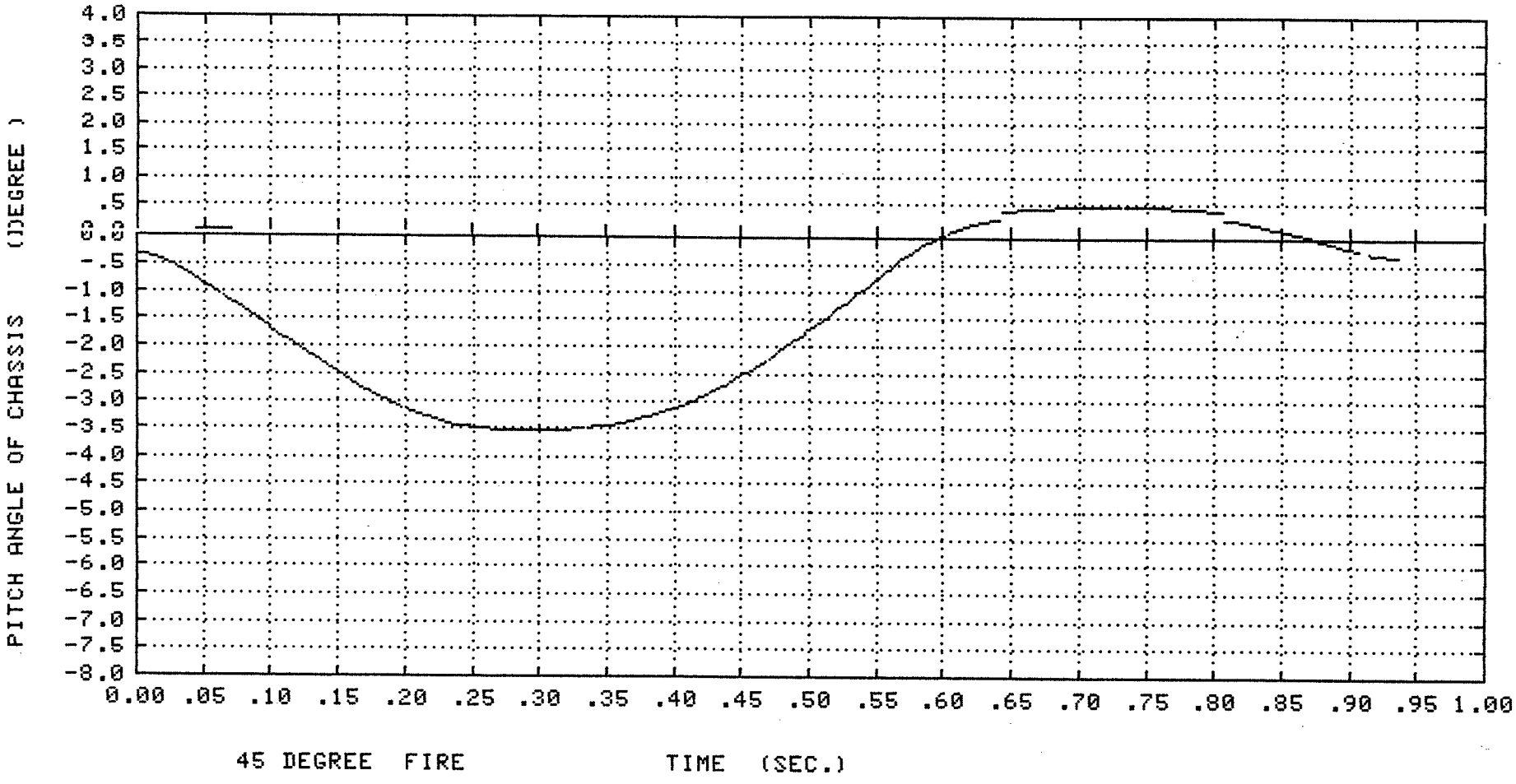

45 DEGREE FIRE

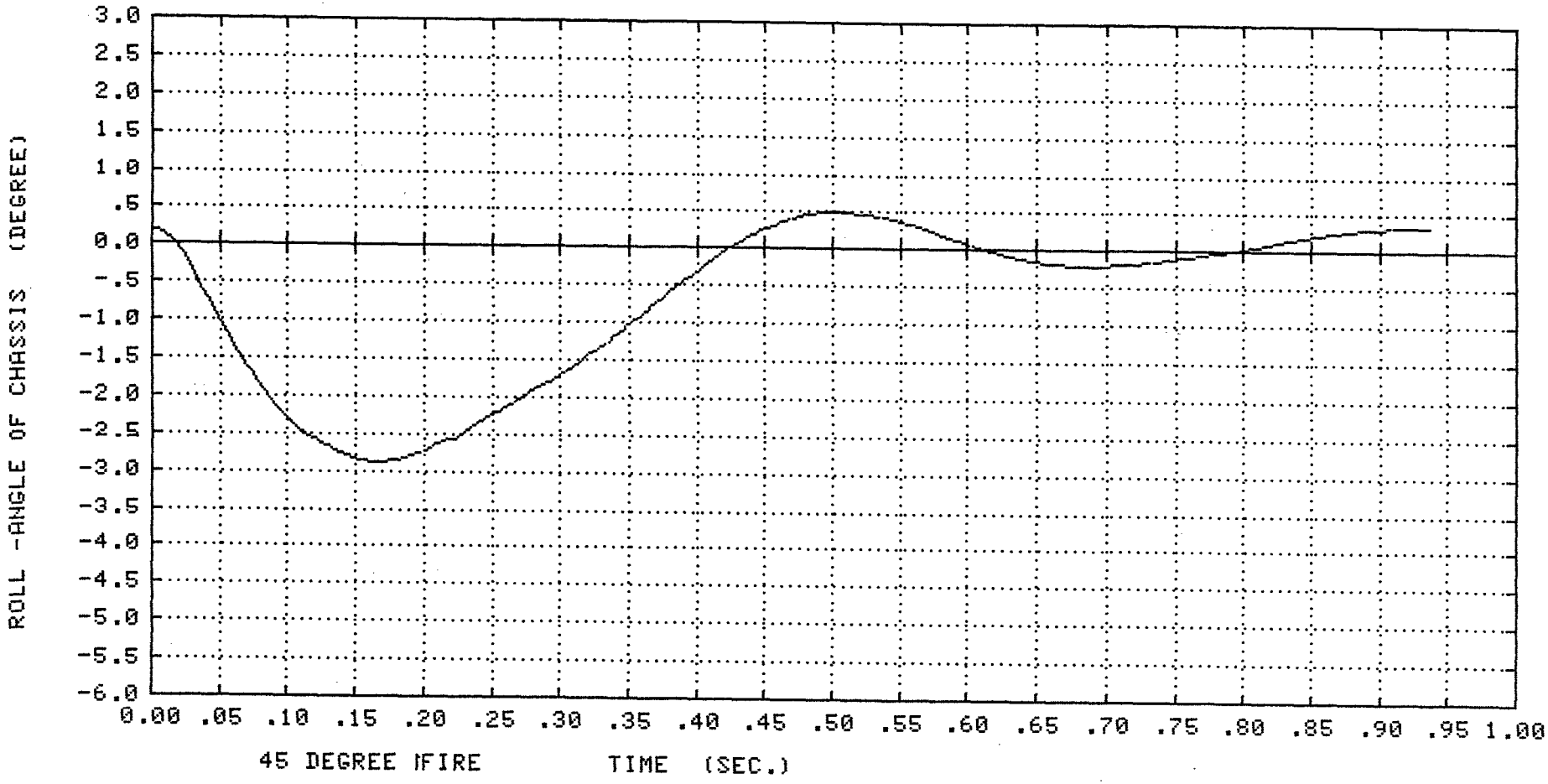
ROLL -ANGLE OF CHASSIS (DEGREE)
3.0
2.5
2.0
1.5
1.0
.5
0.0
-.5
-1.0
-1.5
-2.0
-2.5
-3.0
-3.5
-4.0
-4.5
-5.0
-5.5
-6.0
0.00 .05 .10 .15 .20 .25 .30 .35 .40 .45 .50 .55 .60 .65 .70 .75 .80 .85 .90 .95 1.00
45 DEGREE FIRE
TIME (SEC.)

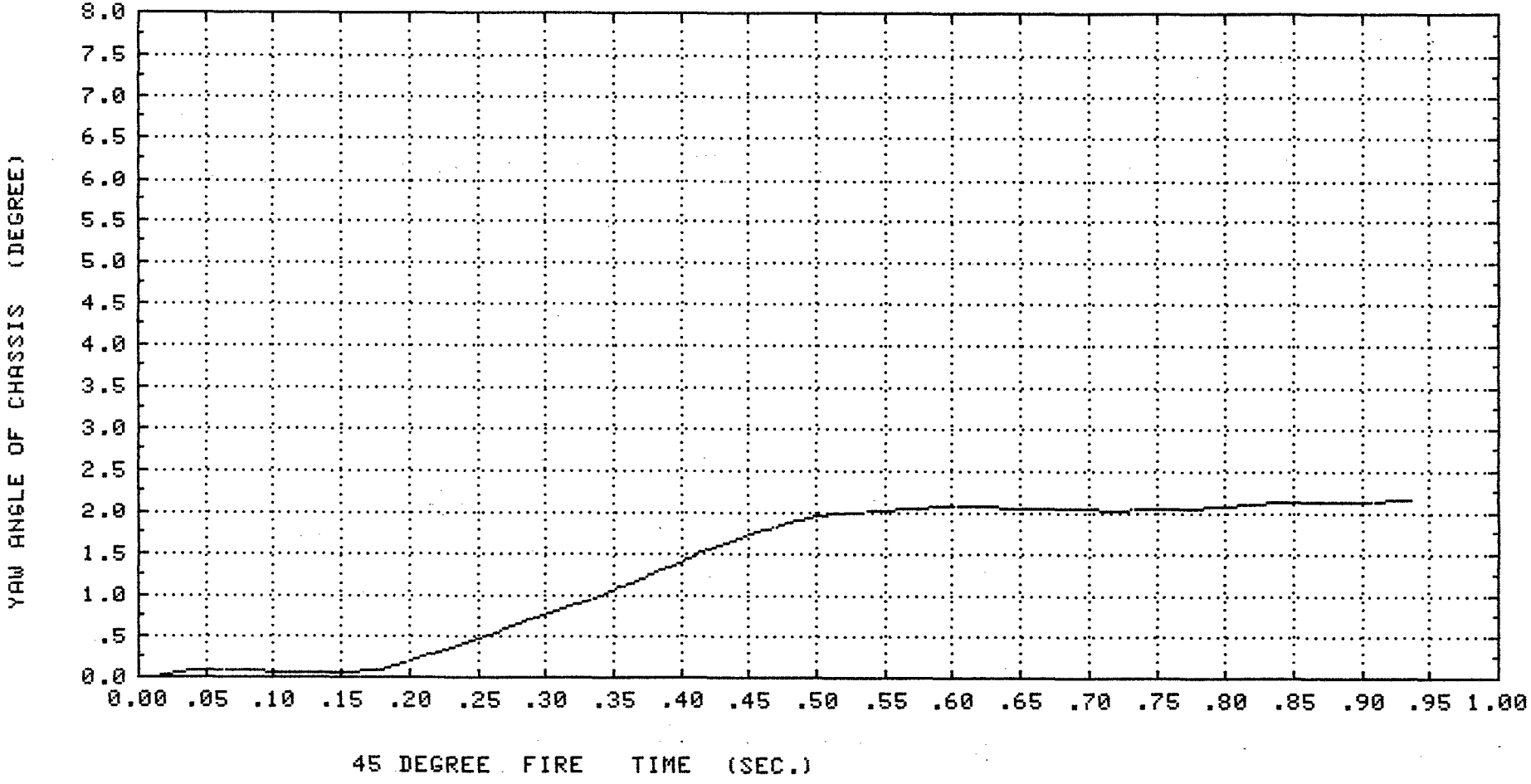
YAW ANGLE OF CHASSIS (DEGREE)
8.0
7.5
7.0
6.5
6.0
5.5
5.0
4.5
4.0
3.5
3.0
2.5
2.0
1.5
1.0
.5
0.0
0.00 .05 .10 .15 .20 .25 .30 .35 .40 .45 .50 .55 .60 .65 .70 .75 .80 .85 .90 .95 1.00
45 DEGREE FIRE TIME (SEC.)

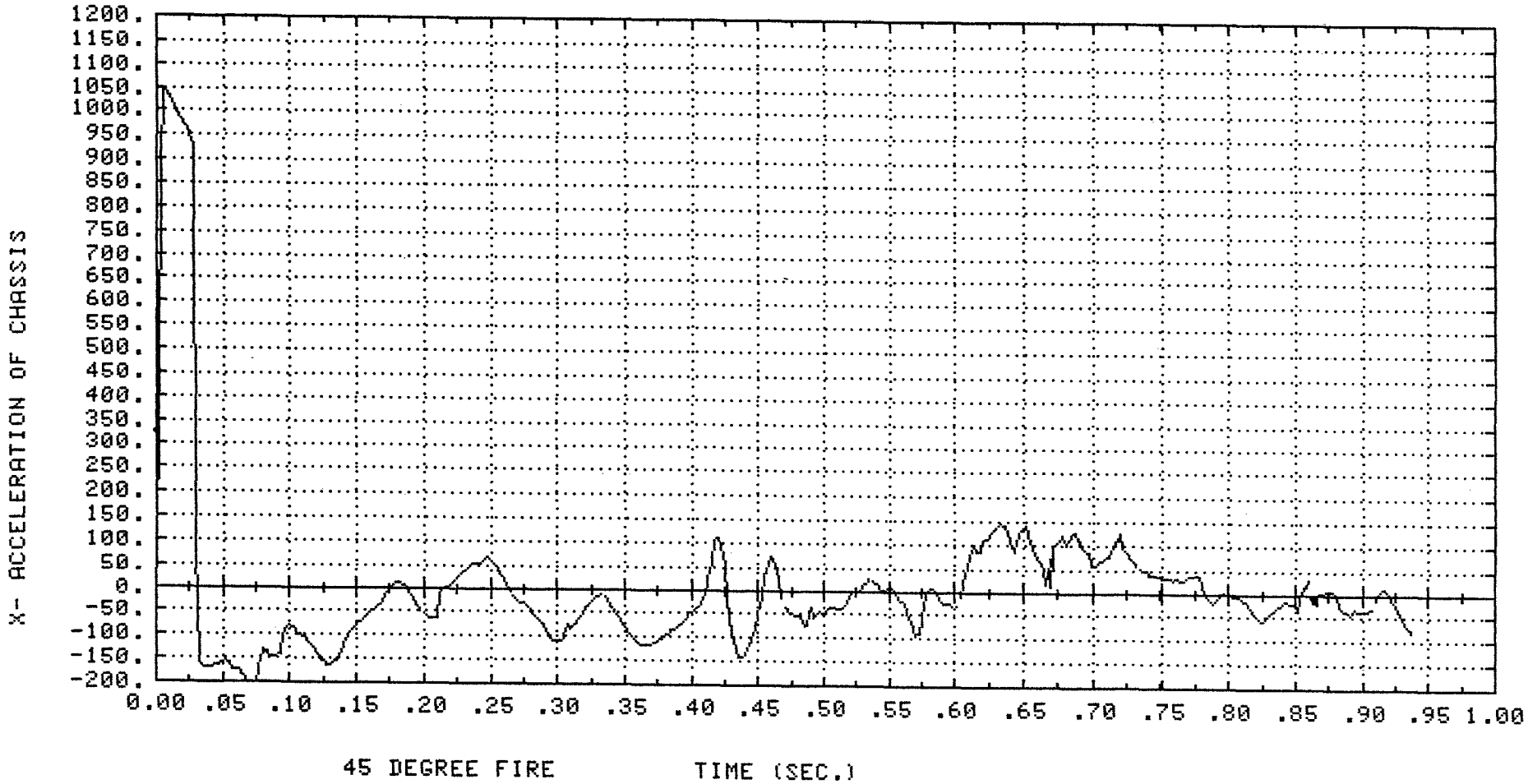
X- ACCELERATION OF CHASSIS
1200.
1150.
1100.
1050.
1000.
950.
900.
850.
800.
750.
700.
650.
600.
550.
500.
450.
400.
350.
300.
250.
200.
150.
100.
50.
0.
-50.
-100.
-150.
-200.
0.00 .05 .10 .15 .20 .25 .30 .35 .40 .45 .50 .55 .60 .65 .70 .75 .80 .85 .90 .95 1.00
45 DEGREE FIRE
TIME (SEC.)

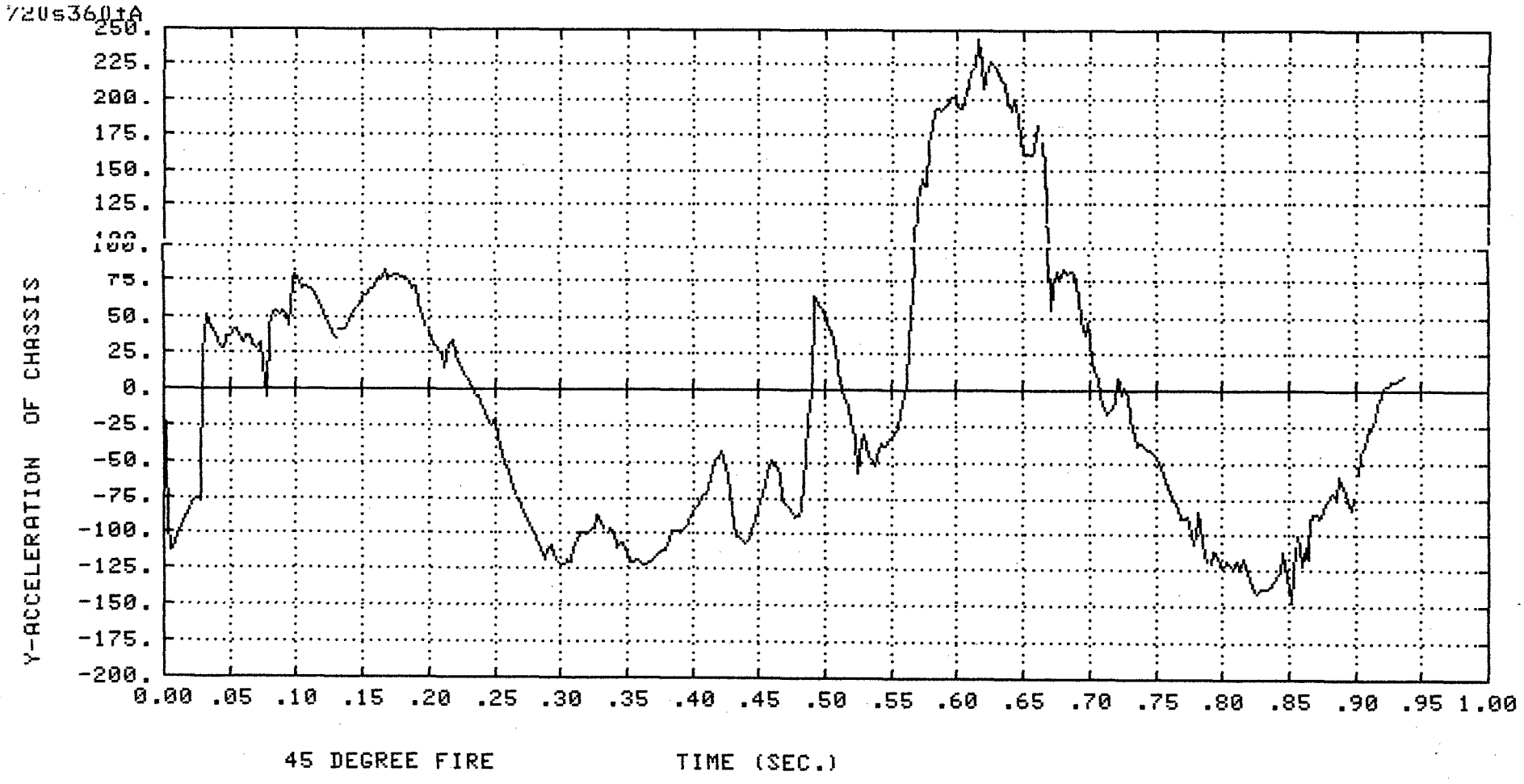

45 DEGREE FIRE

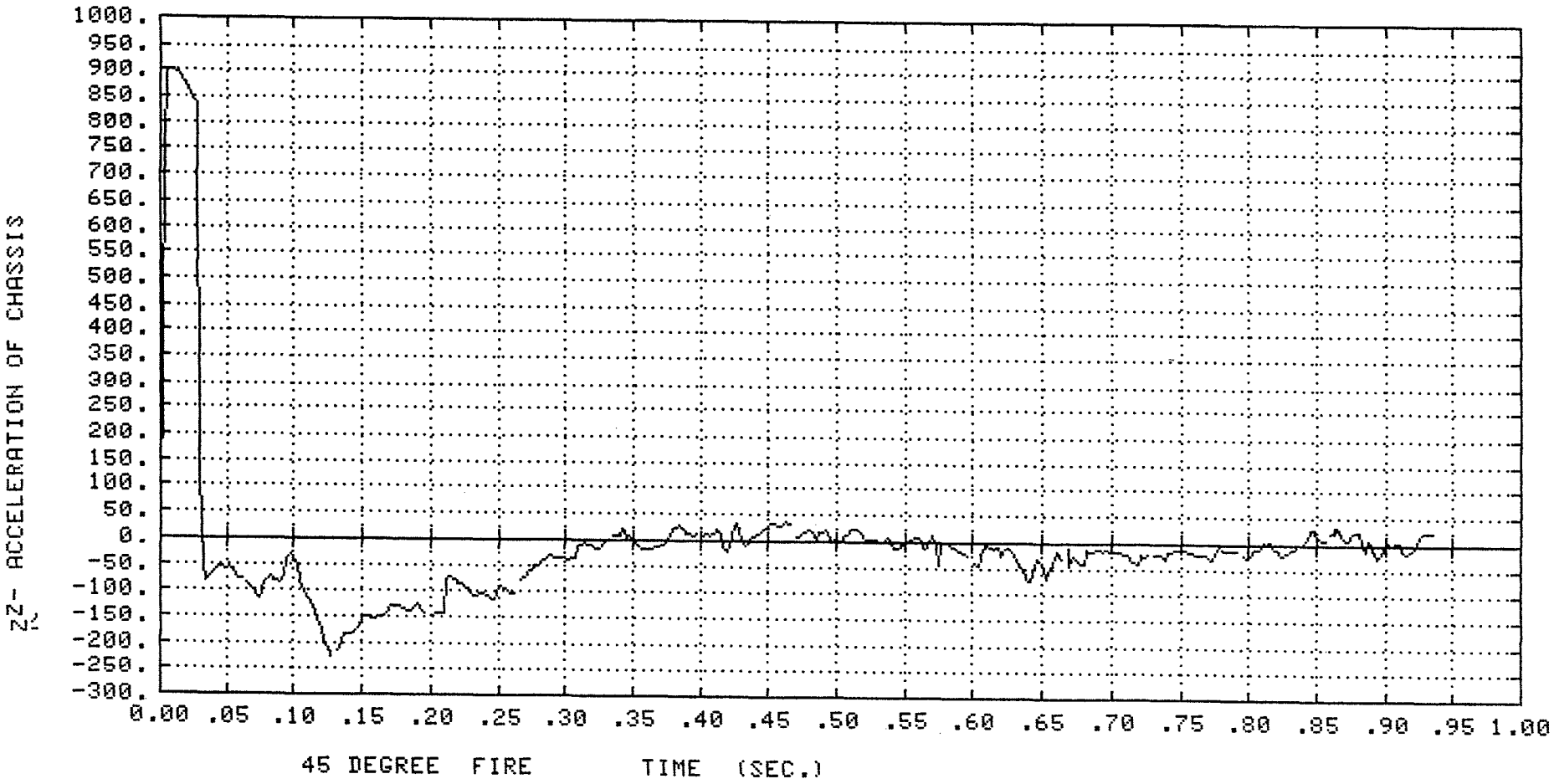
ZZ- ACCELERATION OF CHASSIS
1000.
950.
900.
850.
800.
750.
700.
650.
600.
550.
500.
450.
400.
350.
300.
250.
200.
150.
100.
50.
0.
-50.
-100.
-150.
-200.
-250.
-300.
0.00 .05 .10 .15 .20 .25 .30 .35 .40 .45 .50 .55 .60 .65 .70 .75 .80 .85 .90 .95 1.00
45 DEGREE FIRE
TIME (SEC.)

Appendix E

Response Plots for Platform Stability Analysis

Side-Fire Simulation

* Output time interval = 0.005
* Coulomb friction
* Ground-track shear deformation (ref. point: bottom of the wheels)
* Coefficient of friction =
* 1.0 second of simulation
* CPU time on PRIME - 750 ≈ 6.5 hr.

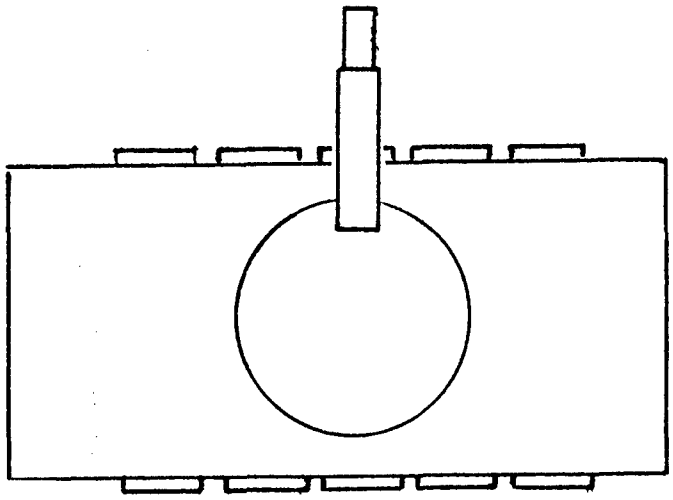

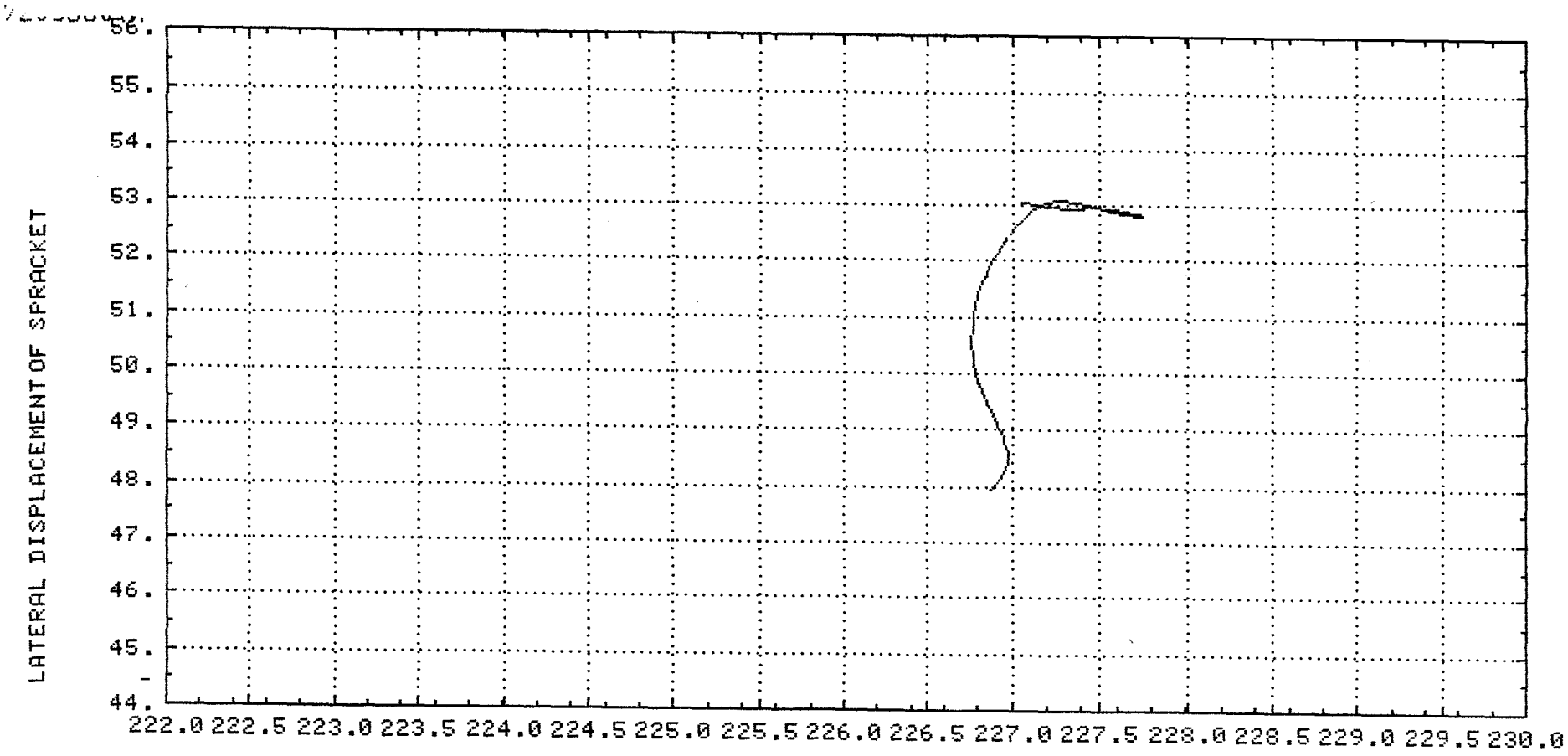

M551 -152MM SIDE FIRE LONGITUDIAL DISPLACEMENT OF SPRACKET (FRONT SIDE)

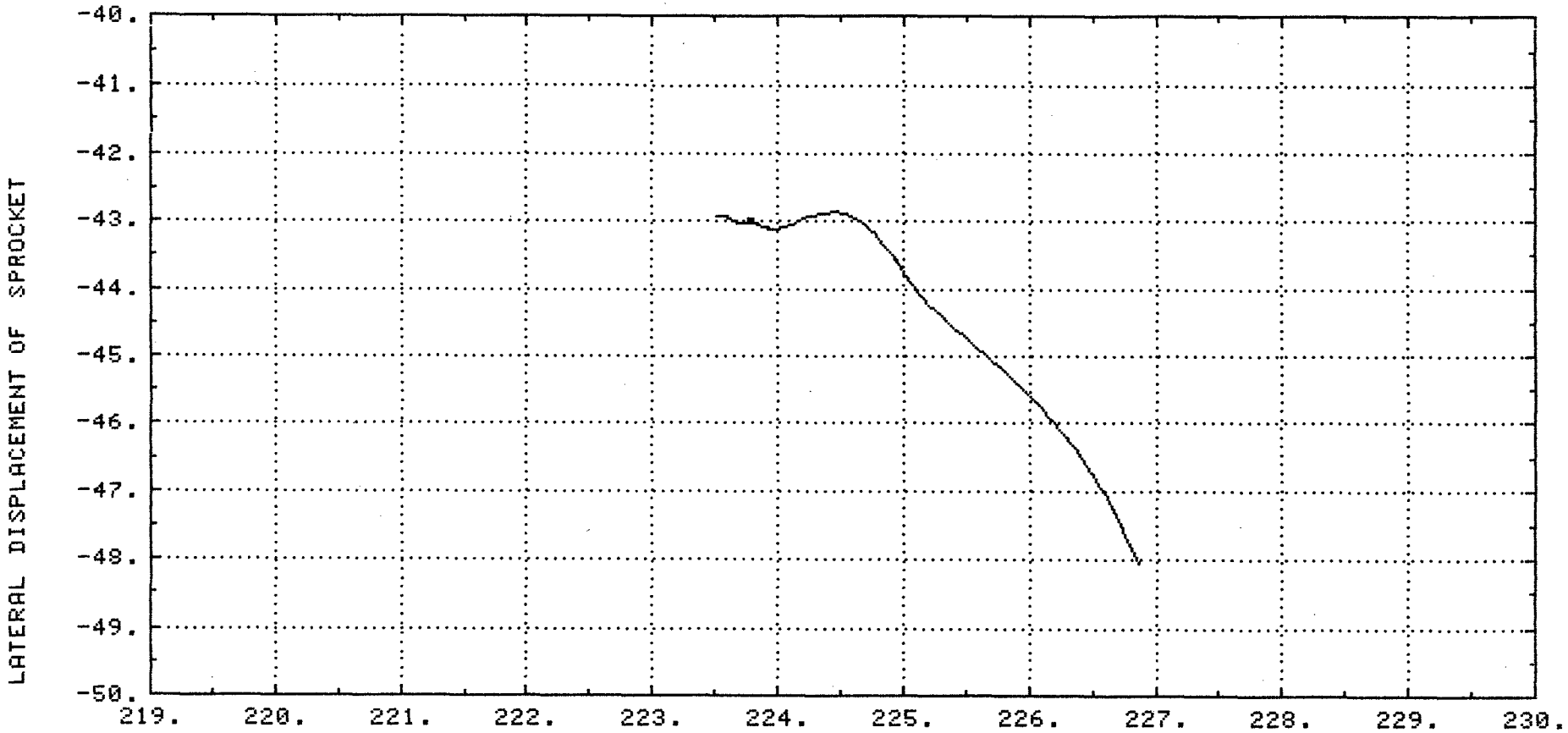

M551 -152MM SIDE FIRE LONGITUDIAL DISPLACEMENT OF SPROCKET (REAR SIDE)

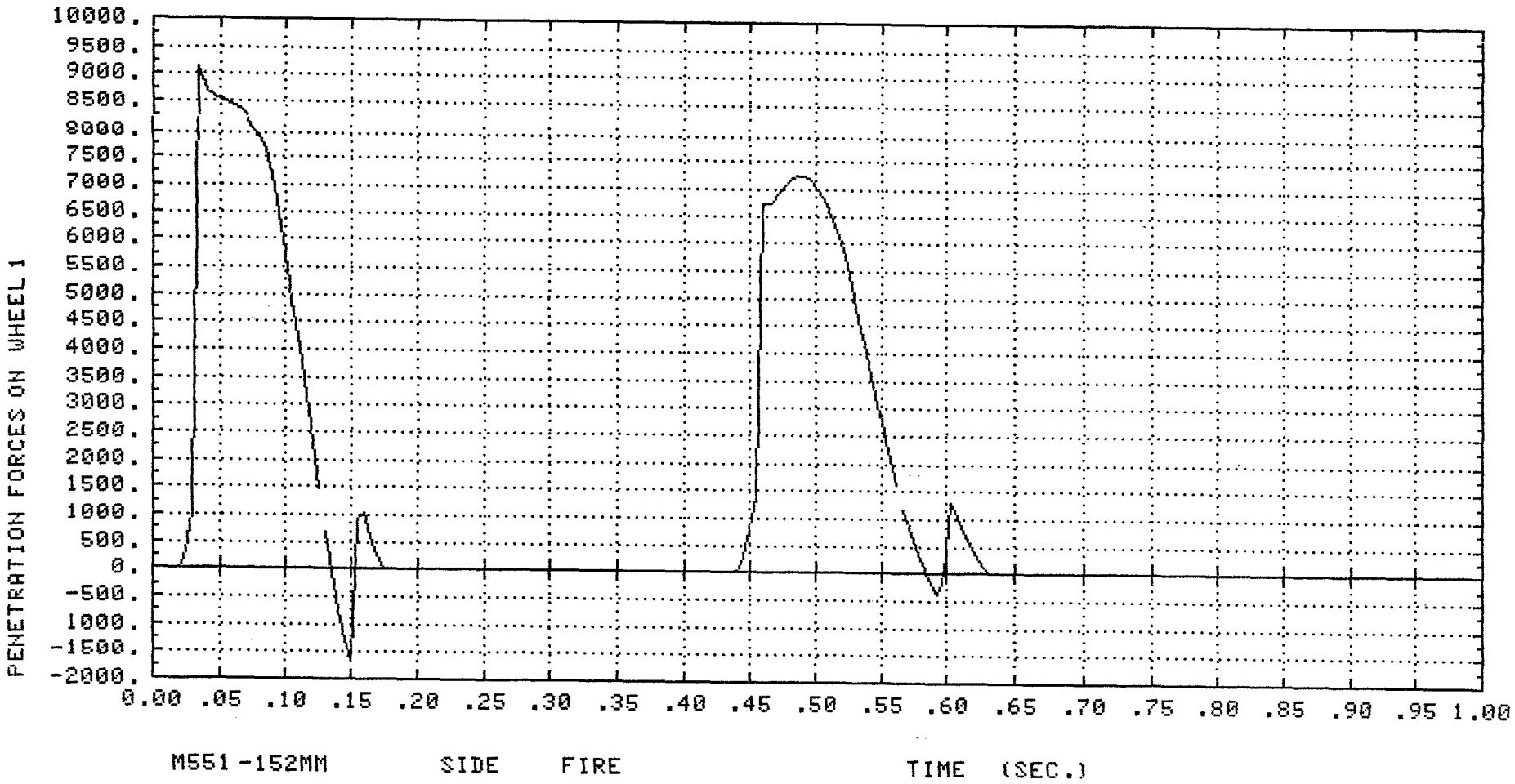
PENETRATION FORCES ON WHEEL 1
10000.
9500.
9000.
8500.
8000.
7500.
7000.
6500.
6000.
5500.
5000.
4500.
4000.
3500.
3000.
2500.
2000.
1500.
1000.
500.
0.
-500.
1000.
-1500.
-2000.
0.00 .05 .10 .15 .20 .25 .30 .35 .40 .45 .50 .55 .60 .65 .70 .75 .80 .85 .90 .95 1.00
M551 -152MM SIDE FIRE
TIME (SEC.)

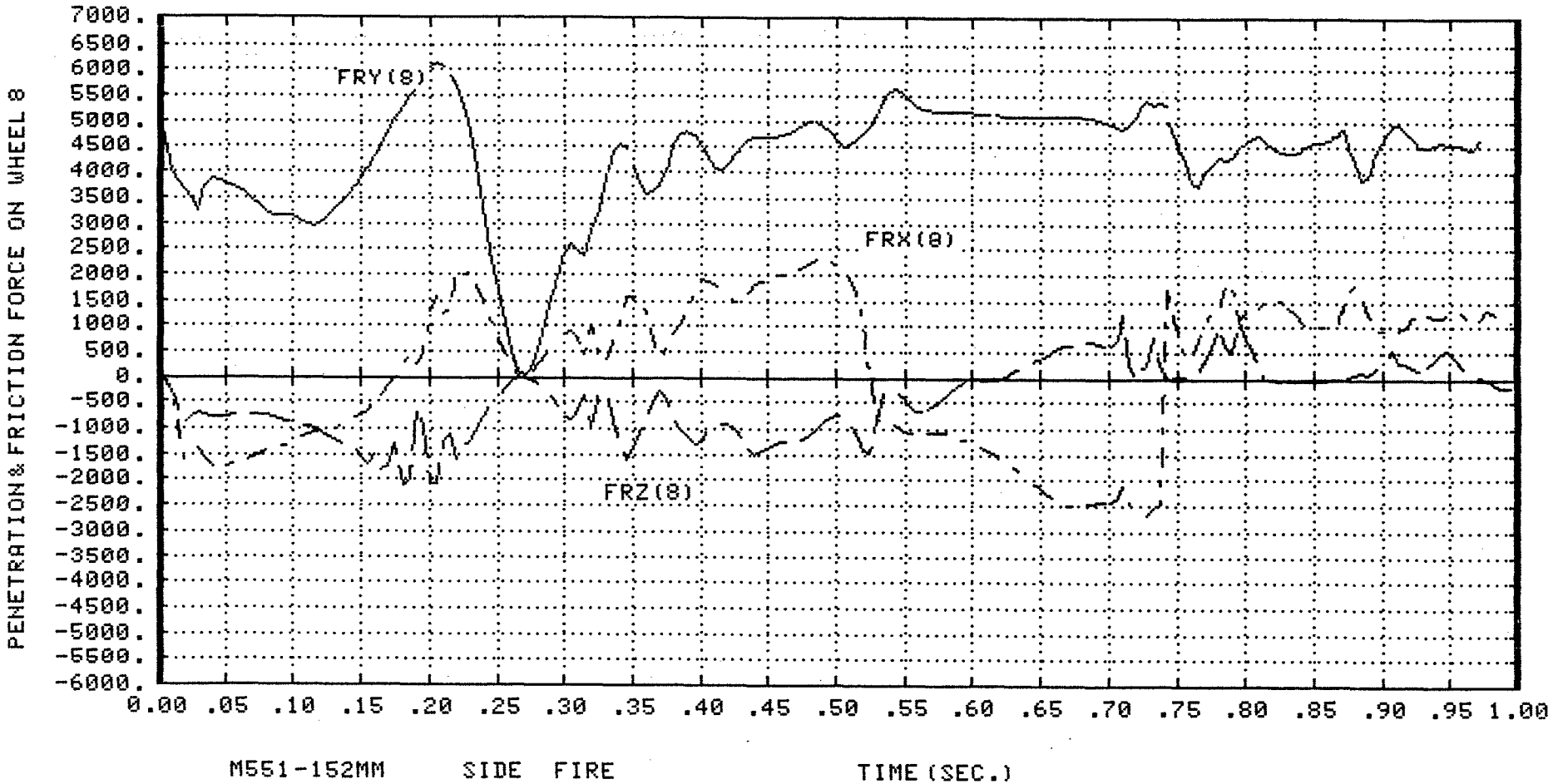
PENETRATION & FRICTION FORCE ON WHEEL 8
7000.
6500.
6000.
5500.
5000.
4500.
4000.
3500.
3000.
2500.
2000.
1500.
1000.
500.
0.
-500.
-1000.
-1500.
-2000.
-2500.
-3000.
-3500.
-4000.
-4500.
-5000.
-5500.
-6000.
FRY(8)
FRX(8)
FRZ(8)
0.00 .05 .10 .15 .20 .25 .30 .35 .40 .45 .50 .55 .60 .65 .70 .75 .80 .85 .90 .95 1.00
M551-152MM SIDE FIRE
TIME (SEC.)

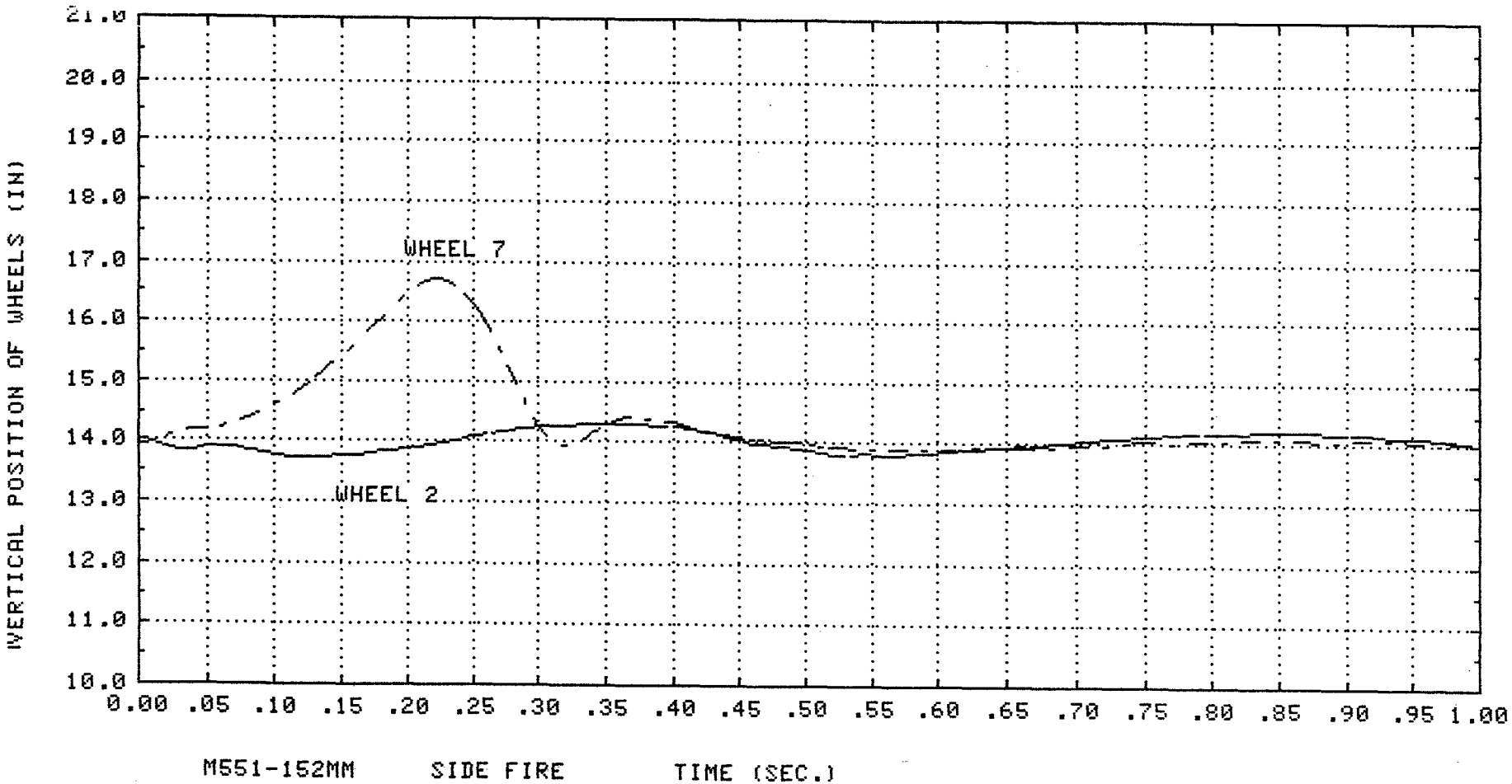
VERTICAL POSITION OF WHEELS (IN)
21.0
20.0
19.0
18.0
17.0
16.0
15.0
14.0
13.0
12.0
11.0
10.0
WHEEL 7
WHEEL 2
0.00 .05 .10 .15 .20 .25 .30 .35 .40 .45 .50 .55 .60 .65 .70 .75 .80 .85 .90 .95 1.00
M551-152MM SIDE FIRE TIME (SEC.)

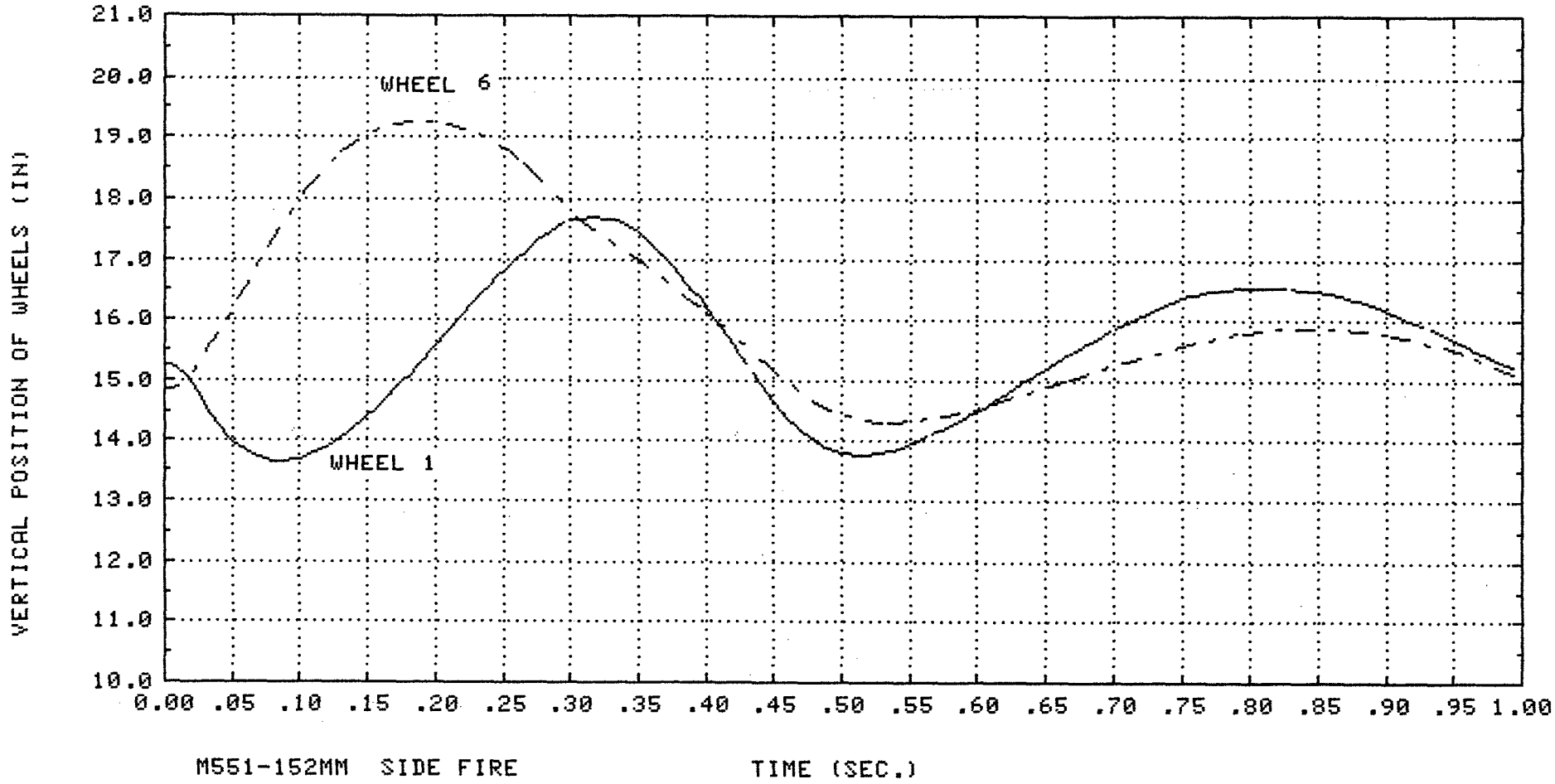
VERTICAL POSITION OF WHEELS (IN)
21.0
20.0
19.0
18.0
17.0
16.0
15.0
14.0
13.0
12.0
11.0
10.0
WHEEL 6
WHEEL 1
0.00 .05 .10 .15 .20 .25 .30 .35 .40 .45 .50 .55 .60 .65 .70 .75 .80 .85 .90 .95 1.00
M551-152MM SIDE FIRE
TIME (SEC.)

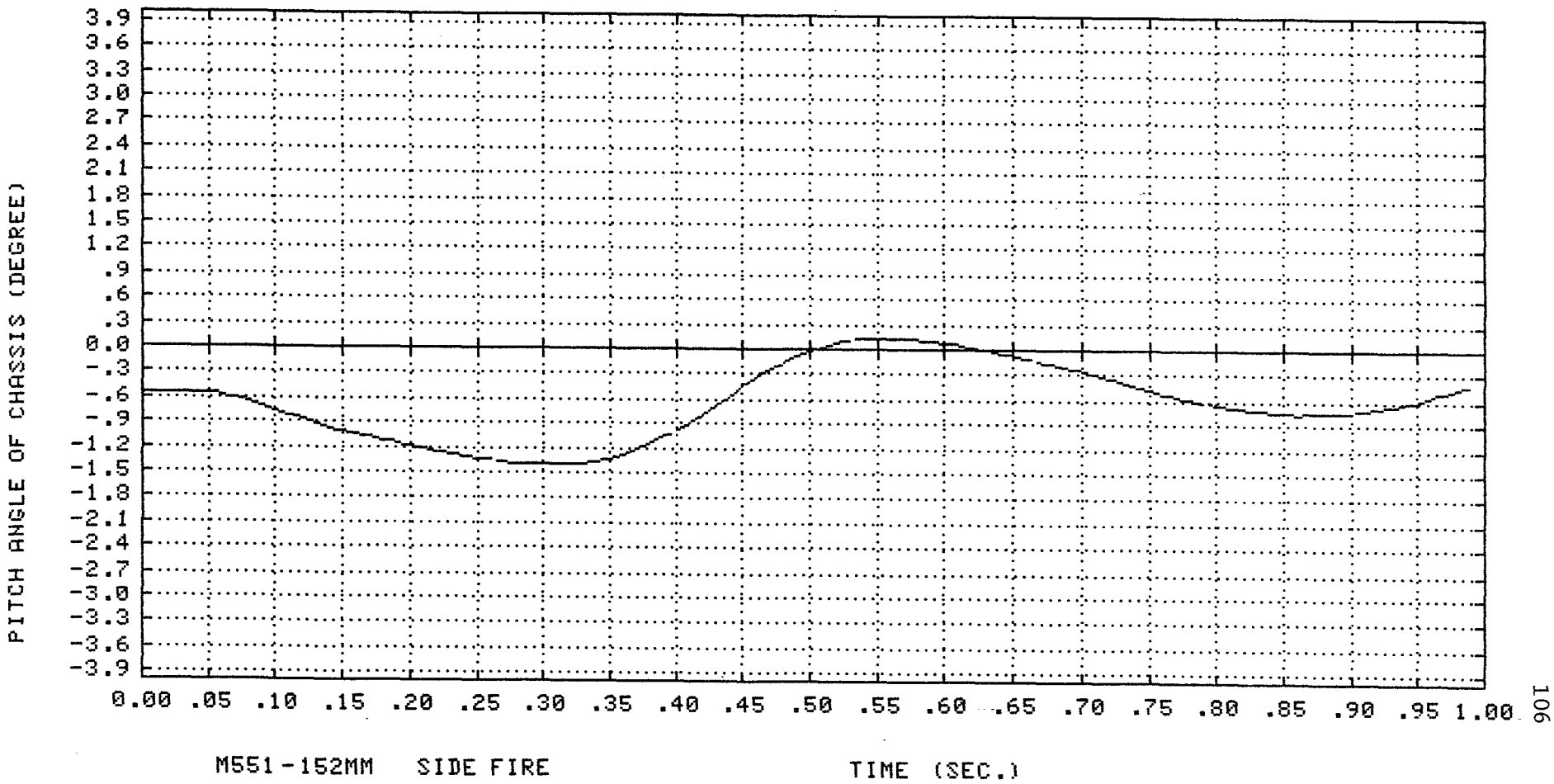

M551-152MM SIDE FIRE

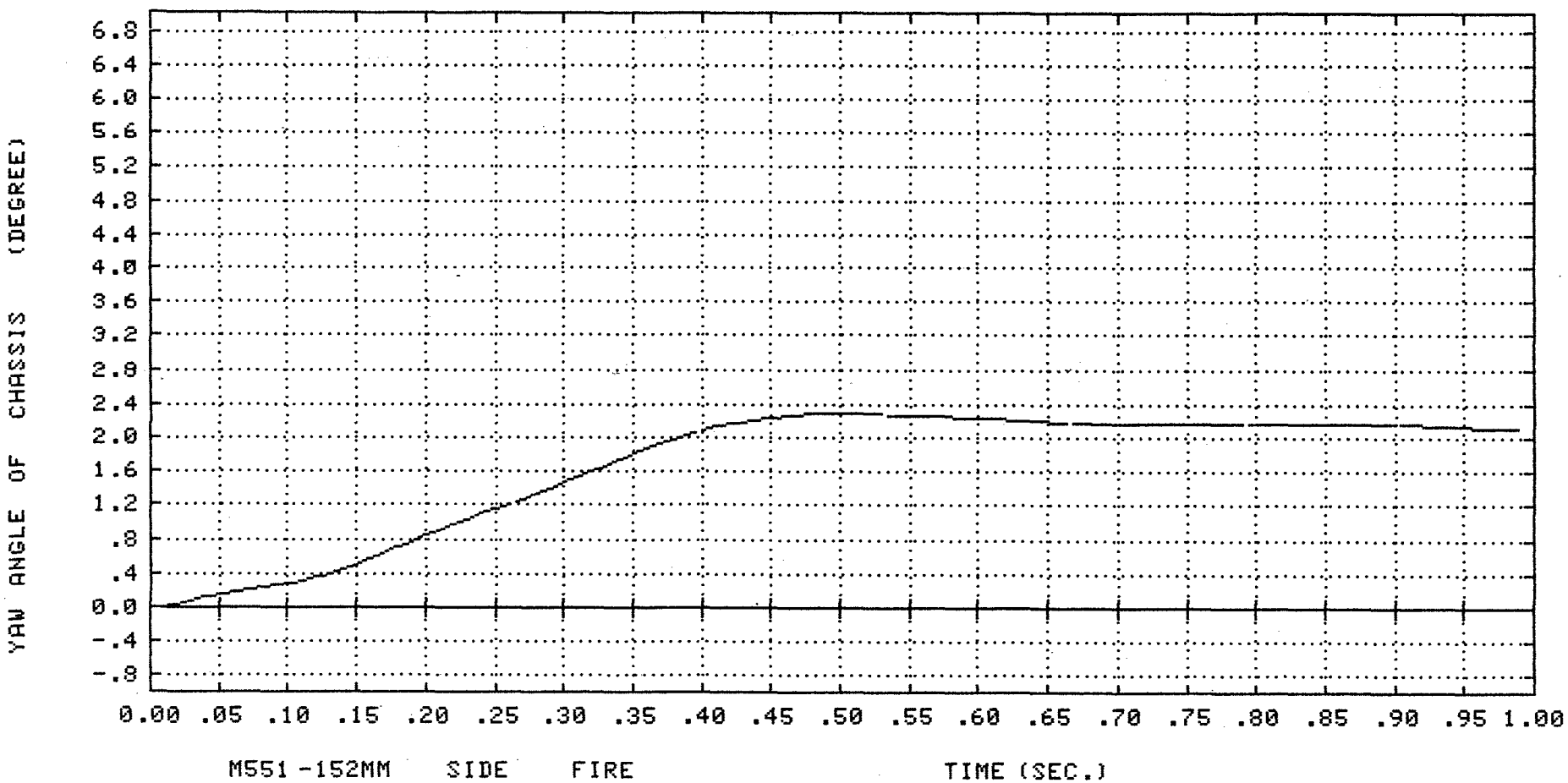
YAW ANGLE OF CHASSIS (DEGREE)
6.8
6.4
6.0
5.6
5.2
4.8
4.4
4.0
3.6
3.2
2.8
2.4
2.0
1.6
1.2
.8
.4
0.0
-.4
-.8
0.00 .05 .10 .15 .20 .25 .30 .35 .40 .45 .50 .55 .60 .65 .70 .75 .80 .85 .90 .95 1.00
M551 -152MM SIDE FIRE
TIME (SEC.)

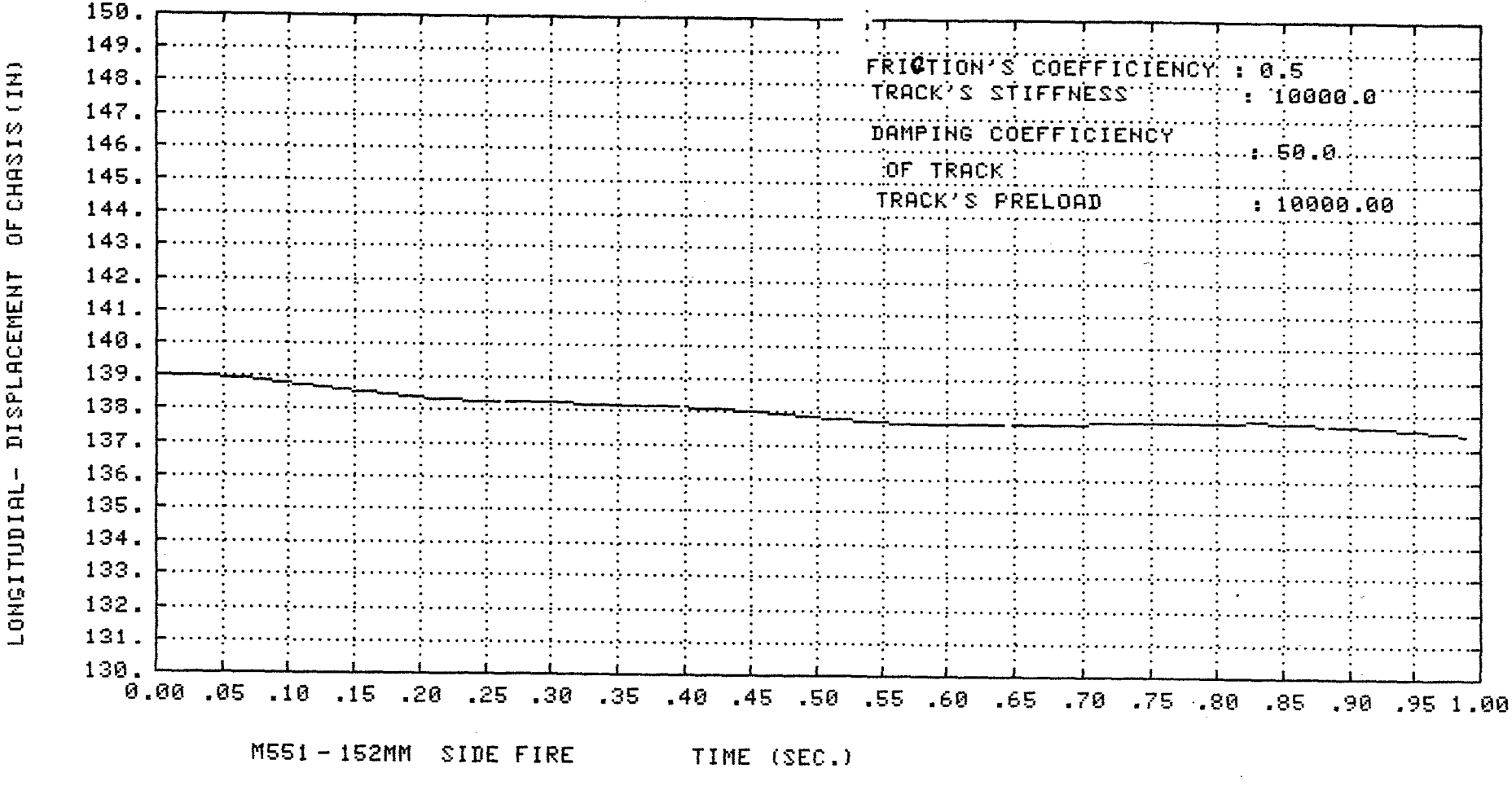
FRICTION'S COEFFICIENCY : 0.5
TRACK'S STIFFNESS : 10000.0
DAMPING COEFFICIENCY
OF TRACK : 50.0
TRACK'S PRELOAD : 10000.00
LONGITUDIAL- DISPLACEMENT OF CHASIS (IN)
150.
149.
148.
147.
146.
145.
144.
143.
142.
141.
140.
139.
138.
137.
136.
135.
134.
133.
132.
131.
130.
0.00 .05 .10 .15 .20 .25 .30 .35 .40 .45 .50 .55 .60 .65 .70 .75 .80 .85 .90 .95 1.00
M551 - 152MM SIDE FIRE
TIME (SEC.)

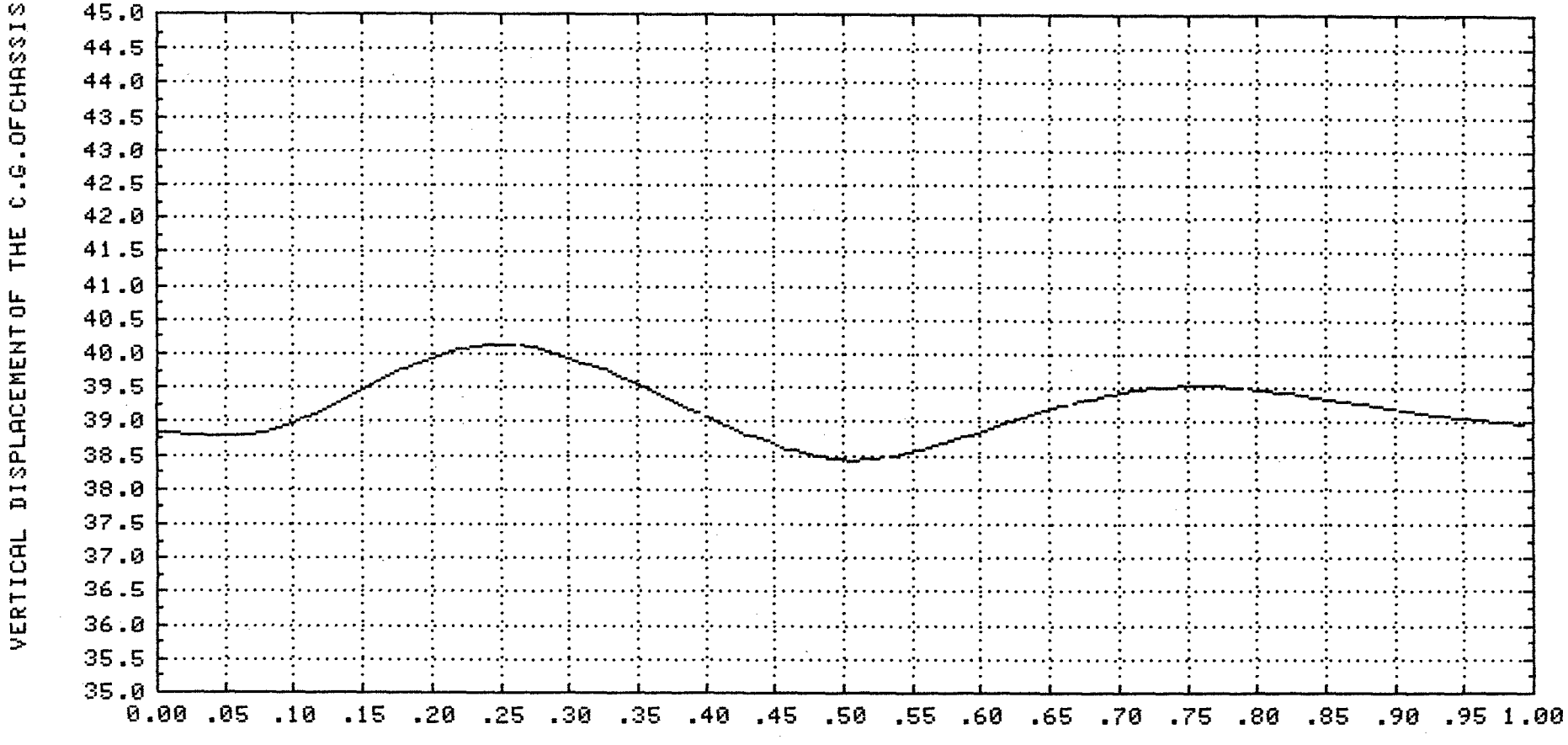
VERTICAL DISPLACEMENT OF THE C.G. OF CHASSIS
45.0
44.5
44.0
43.5
43.0
42.5
42.0
41.5
41.0
40.5
40.0
39.5
39.0
38.5
38.0
37.5
37.0
36.5
36.0
35.5
35.0
0.00 .05 .10 .15 .20 .25 .30 .35 .40 .45 .50 .55 .60 .65 .70 .75 .80 .85 .90 .95 1.00
M551-152MM SIDE FIRE
TIME (SEC.)

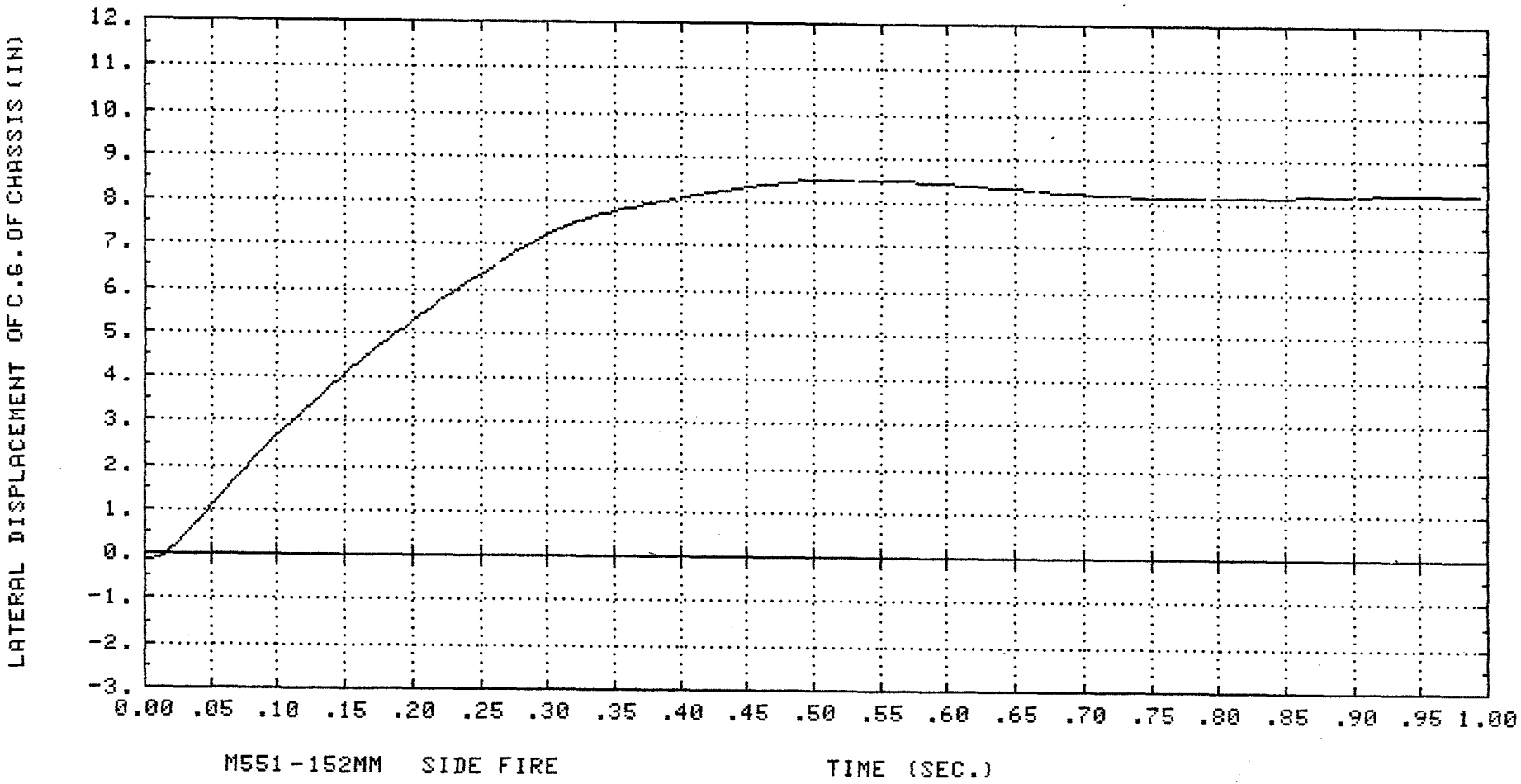
LATERAL DISPLACEMENT OF C.G. OF CHASSIS (IN)
12.
11.
10.
9.
8.
7.
6.
5.
4.
3.
2.
1.
0.
-1.
-2.
-3.
0.00 .05 .10 .15 .20 .25 .30 .35 .40 .45 .50 .55 .60 .65 .70 .75 .80 .85 .90 .95 1.00
M551-152MM SIDE FIRE
TIME (SEC.)

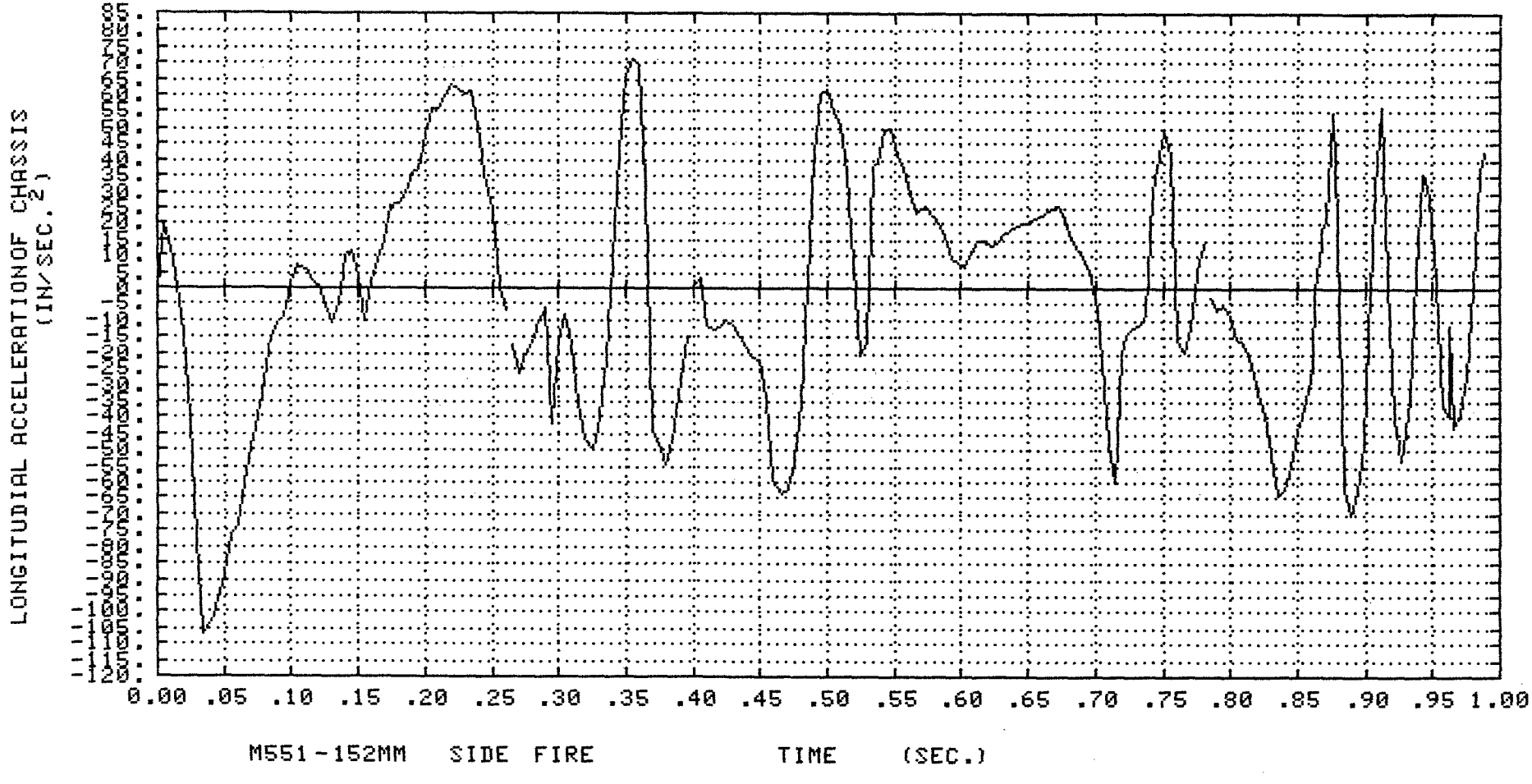
LONGITUDIAL ACCELERATION OF CHASSIS
(IN/SEC.2)
0.00 .05 .10 .15 .20 .25 .30 .35 .40 .45 .50 .55 .60 .65 .70 .75 .80 .85 .90 .95 1.00
M551-152MM SIDE FIRE
TIME (SEC.)

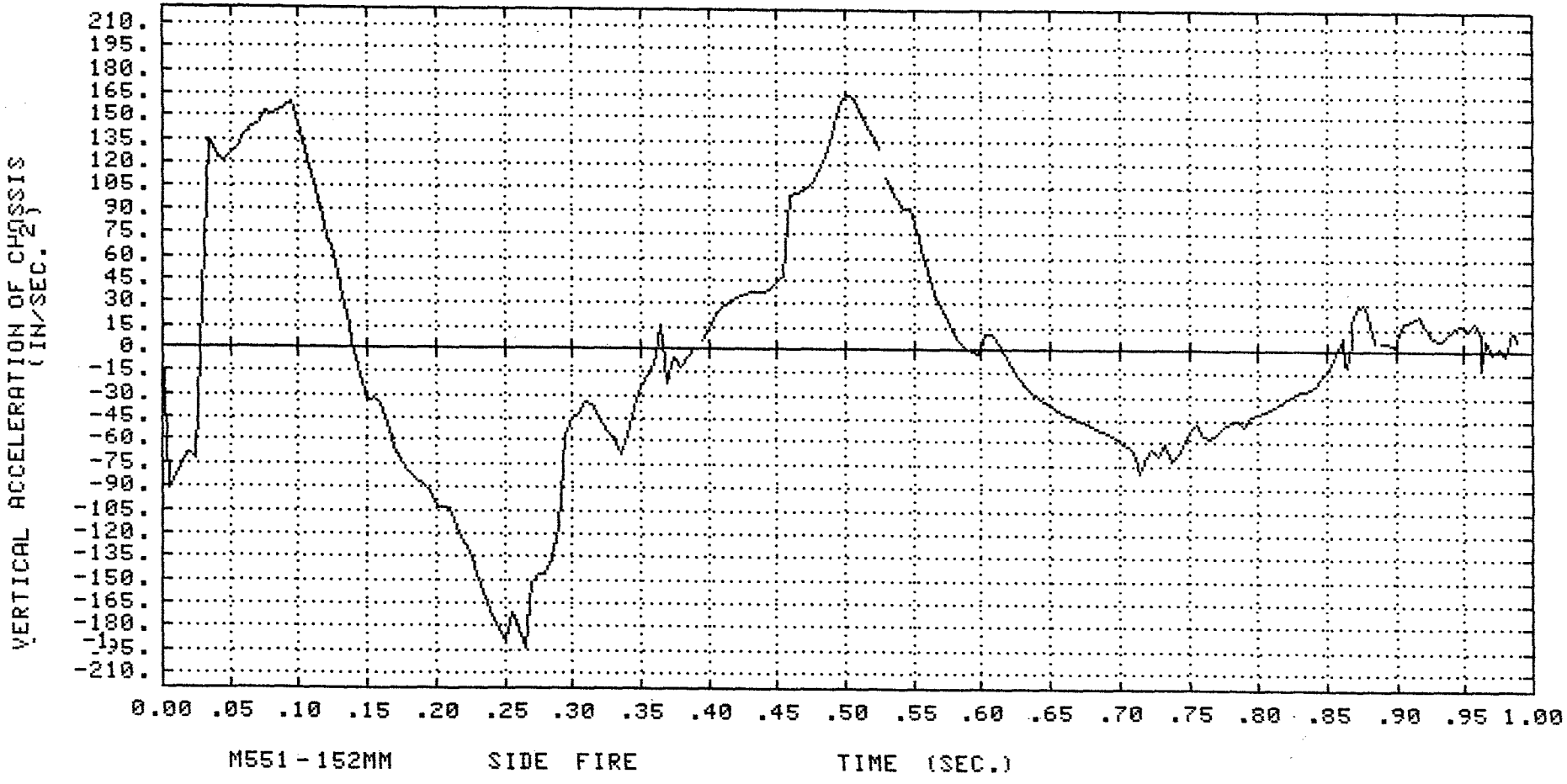
VERTICAL ACCELERATION OF CHASSIS
(IN/SEC.^{2})
210.
195.
180.
165.
150.
135.
120.
105.
90.
75.
60.
45.
30.
15.
0.
-15.
-30.
-45.
-60.
-75.
-90.
-105.
-120.
-135.
-150.
-165.
-180.
-195.
-210.
0.00 .05 .10 .15 .20 .25 .30 .35 .40 .45 .50 .55 .60 .65 .70 .75 .80 .85 .90 .95 1.00
M551-152MM SIDE FIRE
TIME (SEC.)

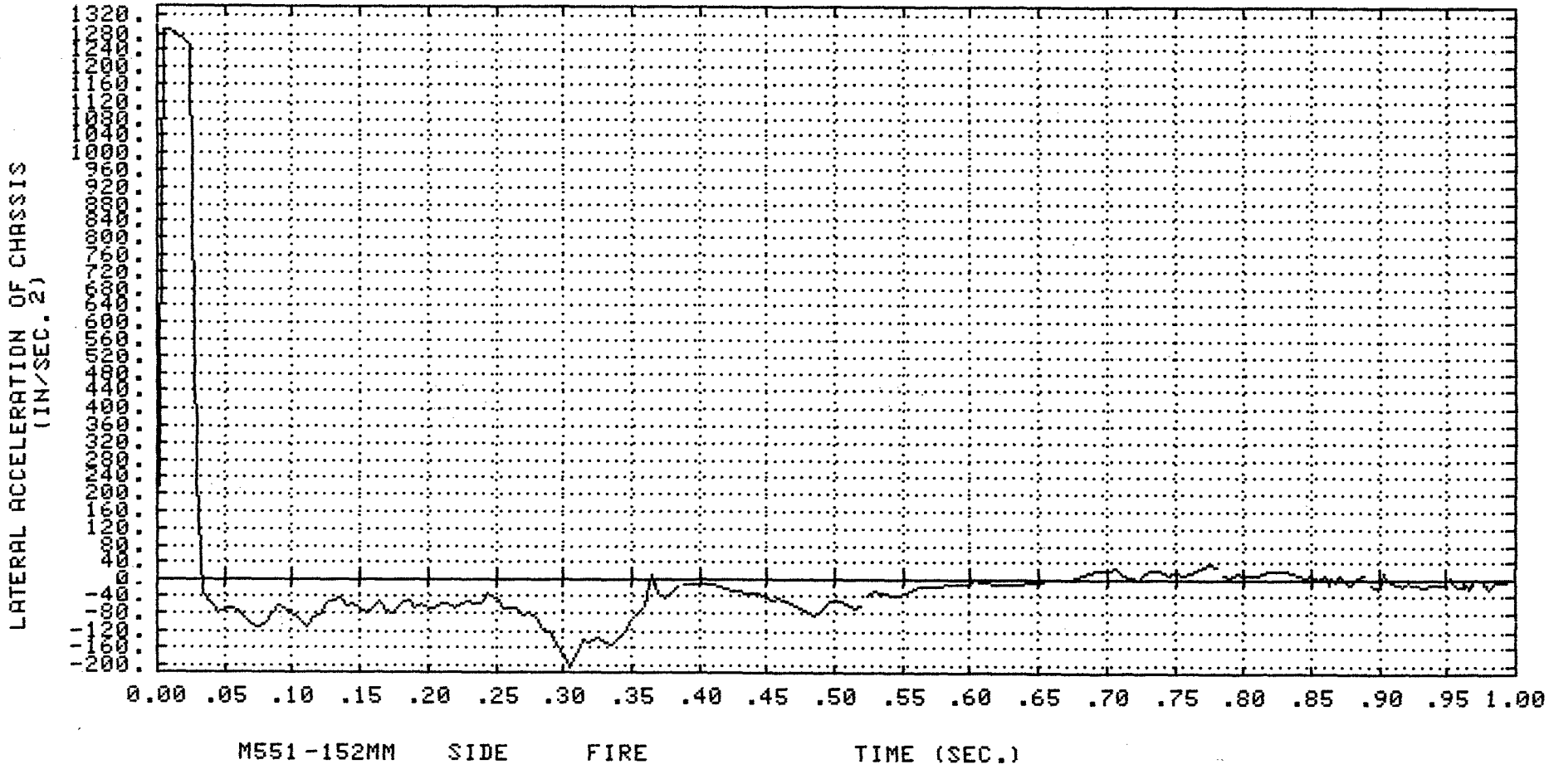
LATERAL ACCELERATION OF CHASSIS
(IN/SEC.^2)
1320.
1280.
1240.
1200.
1160.
1120.
1080.
1040.
1000.
960.
920.
880.
840.
800.
760.
720.
680.
640.
600.
560.
520.
480.
440.
400.
360.
320.
280.
240.
200.
160.
120.
80.
40.
0.
-40.
-80.
-120.
-160.
-200.
0.00 .05 .10 .15 .20 .25 .30 .35 .40 .45 .50 .55 .60 .65 .70 .75 .80 .85 .90 .95 1.00
M551-152MM SIDE FIRE
TIME (SEC.)

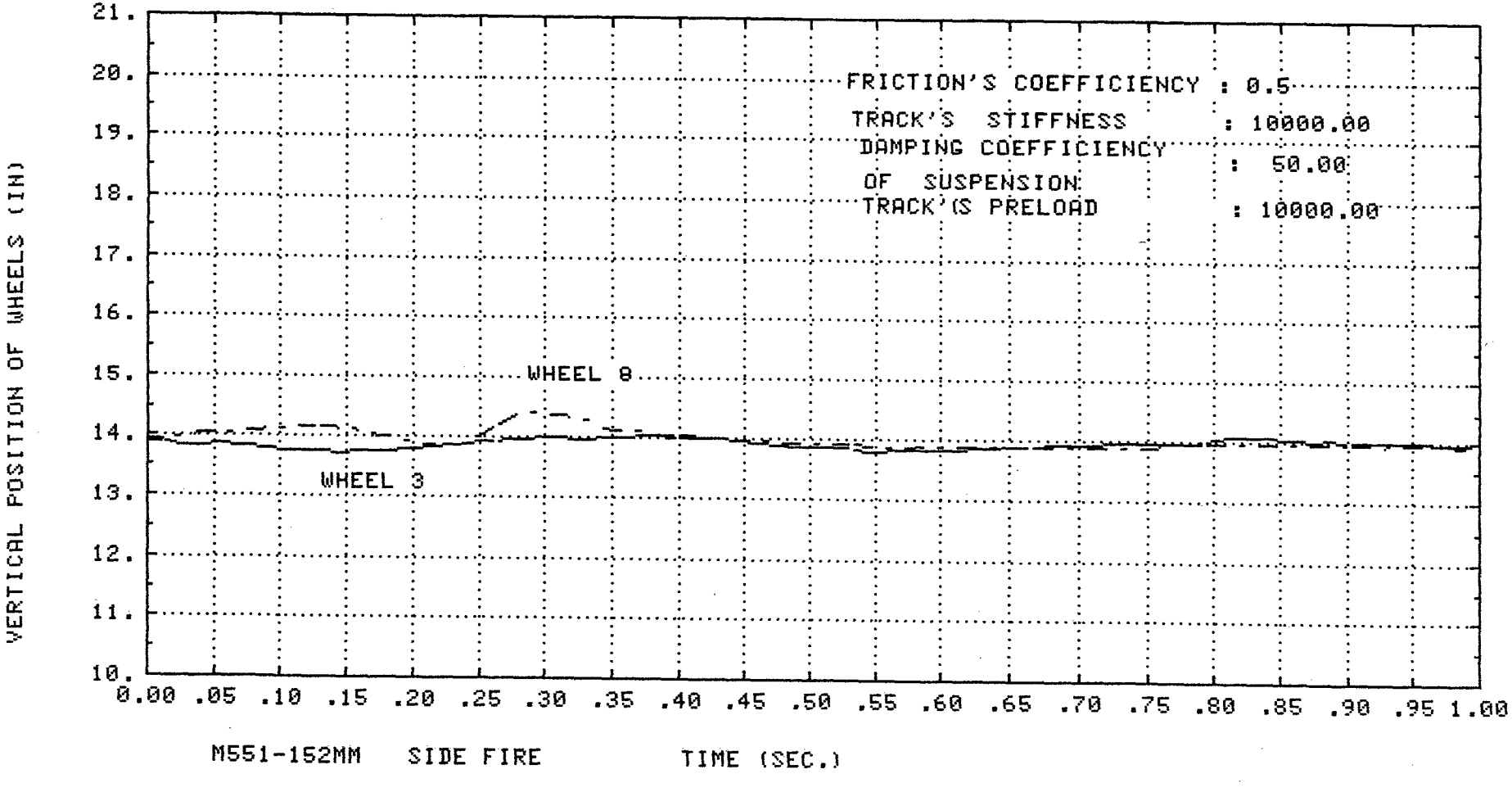
FRICTION'S COEFFICIENCY : 0.5
TRACK'S STIFFNESS : 10000.00
DAMPING COEFFICIENCY : 50.00
OF SUSPENSION
TRACK'S PRELOAD : 10000.00
WHEEL 8
WHEEL 3
VERTICAL POSITION OF WHEELS (IN)
21.
20.
19.
18.
17.
16.
15.
14.
13.
12.
11.
10.
0.00 .05 .10 .15 .20 .25 .30 .35 .40 .45 .50 .55 .60 .65 .70 .75 .80 .85 .90 .95 1.00
M551-152MM SIDE FIRE
TIME (SEC.)

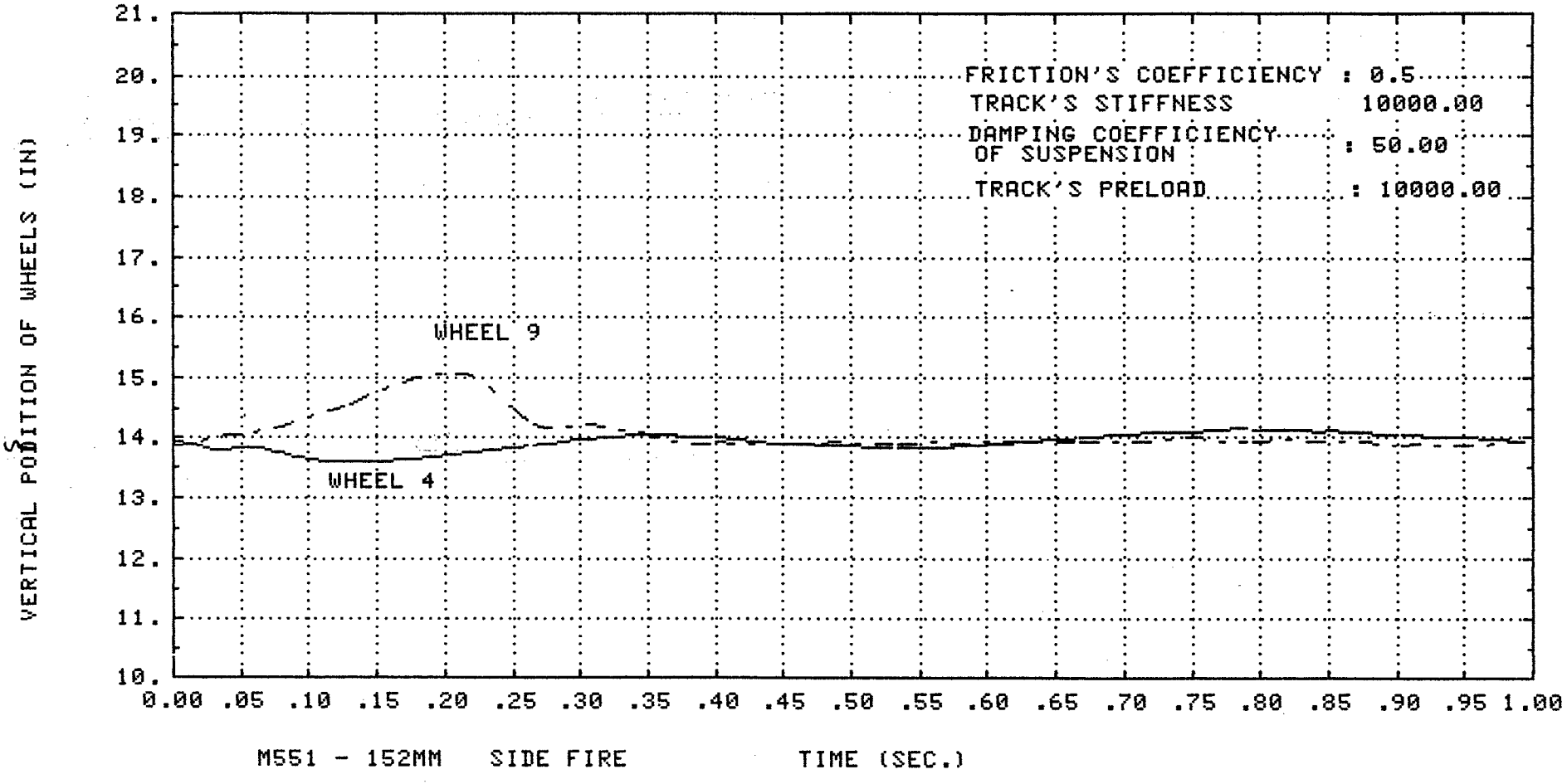
FRICTION'S COEFFICIENCY : 0.5
TRACK'S STIFFNESS 10000.00
DAMPING COEFFICIENCY OF SUSPENSION : 50.00
TRACK'S PRELOAD : 10000.00
WHEEL 9
WHEEL 4
VERTICAL POSITION OF WHEELS (IN)
21.
20.
19.
18.
17.
16.
15.
14.
13.
12.
11.
10.
0.00 .05 .10 .15 .20 .25 .30 .35 .40 .45 .50 .55 .60 .65 .70 .75 .80 .85 .90 .95 1.00
M551 - 152MM SIDE FIRE
TIME (SEC.)

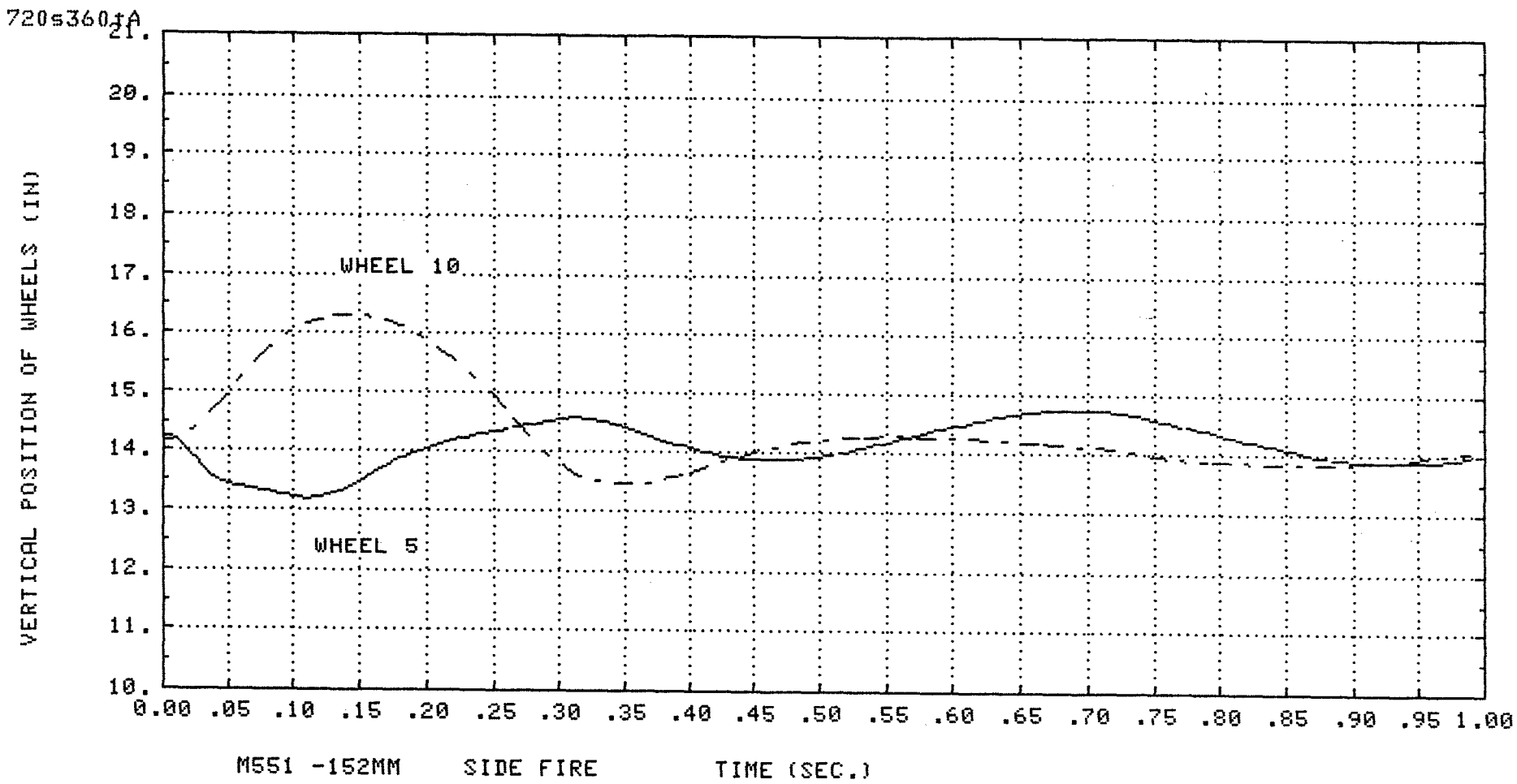
720s360jA
VERTICAL POSITION OF WHEELS (IN)
21.
20.
19.
18.
17.
16.
15.
14.
13.
12.
11.
10.
WHEEL 10
WHEEL 5
0.00 .05 .10 .15 .20 .25 .30 .35 .40 .45 .50 .55 .60 .65 .70 .75 .80 .85 .90 .95 1.00
M551 -152MM SIDE FIRE
TIME (SEC.)

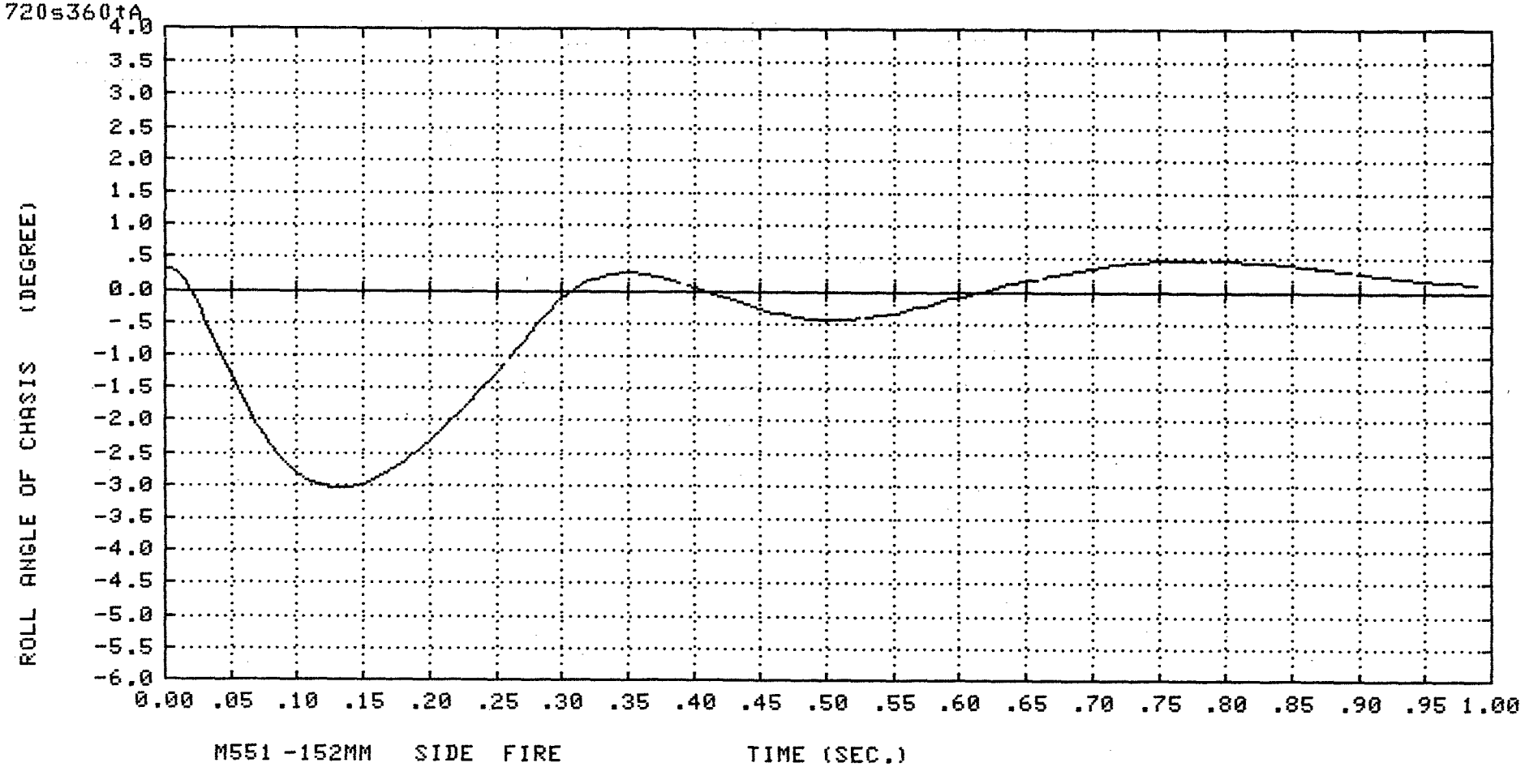
720s360tA
ROLL ANGLE OF CHASIS (DEGREE)
4.0
3.5
3.0
2.5
2.0
1.5
1.0
.5
0.0
-.5
-1.0
-1.5
-2.0
-2.5
-3.0
-3.5
-4.0
-4.5
-5.0
-5.5
-6.0
0.00 .05 .10 .15 .20 .25 .30 .35 .40 .45 .50 .55 .60 .65 .70 .75 .80 .85 .90 .95 1.00
M551 -152MM SIDE FIRE
TIME (SEC.)

Appendix F

User Manual

DADS-3D

Input Data Structure and Format

PART ONE

Data Input to DADS-3D
Revised May 13, 1981

The order in which the following segments appear is arbitrary and need not be followed by the user.

There are three commands which may be inserted in the data. These are LIST, NOLIST, and END. LIST and NOLIST can be used anywhere in the data set (between segments), as often as you wish. Anything after a LIST command is printed in the output until a NOLIST command is encountered (default is NOLIST). The END statement must appear at the end of each data set.

I. Problem Output Label
II. System Information
III. Rigid Body*
IV. Initial Condition*
V. Constraint
VI. Spherical Joint
VII. Universal Joint
VIII. Revolute Joint
IX. Cylindrical Joint
X. Translational Joint
XI. Massless Link
XII. Translational-Spring-Damper-Actuator
XIII. Torsional-Spring-Damper-Actuator
XIV. Pointer
XV. Spline Function
XVI. END Card*

The input segments with a * cannot be eliminated from the input. The elimination of other segments depends on the problem type.

Each segment starts with an identifier card. There are two entries on every identifier card. The first entry contains four letters in columns 1-4, describing the type of the segment, e.g., HEAD, SYST, BODY, etc. The second entry, an integer number in columns 5-8, specifies the number of cards or group of cards to be followed in that segment.

REMARKS

(1) In this manual, all integer variable names begin with one of the four letters: N, J, I, or K.

N: An integer variable beginning with N indicates a "total number of...".

J: An integer variable beginning with J indicates an index; i.e., Jxxxx = 1,2,...,Nxxxx.

I: An integer variable beginning with I indicates a flag in order to enable or disable some actions in the program.

K: An integer variable beginning with K indicates card number.

(2) All integer entries should be right justified.

(3) Where the range of an index is given by J = 1,2,...,N, the cards should be placed consecutively according to J.

(4) Where the range of an index is given by $1 \leq J \leq N$, the cards do not need to be placed in consecutive order.

(5) Statements with a # indicate the nonapplicability of that option in the present version of the program.

(6) X,Y,Z indicates global coordinate system and x,y,z indicates local coordinate system.

I. PROBLEM OUTPUT LABEL

Identifier Card (A4, I4)

Notes	Columns	Variable	Entry
	1 - 4	HEADER	HEAD
	5 - 8	NCARDS	Number of cards for the problem description

Heading Card(s) (20A4)

Notes	Columns	Variable	Entry
	1 - 80	LABEL (20)	Enter the heading information on NCARDS cards. This heading will be printed with the output as label

II. SYSTEM INFORMATION

Identifier Card (A4, I4)

Notes	Columns	Variable	Entry
(1)	1 - 4	HEADER	SYST
(1)	8	NSYST	Number of system cards

System Card(s)

Card 1: (3I4, 8X, 5F10.0)

Notes	Columns	Variable	Entry
	4	K1	Enter 1 if this card is used
	8	IUNIT	Identifies the system of units employed to the problem EQ.0; SI units (Default value) EQ.1; slug-feet units EQ.2; slug-inch units (mixed units, not recommended)
	12	IANGLE	EQ.0; all input angles in radians (Default unit) EQ.1; all input angles in degrees (The program will convert them to radians)
	16	IANAL	Flag that controls the type of analysis EQ.0; static equilibrium and dynamic analysis (default) EQ.1; data check only EQ.2; static equilibrium only EQ.3; dynamic analysis only
	21 - 30	GC	Gravitational constant. Default value is 1.0
	31 - 40	GRC	Ratio of g/gc. Default value: GRC = 9.8066, IF IUNIT.EQ.0 GRC = 32.174 , IF IUNIT.EQ.1
	41 - 50	GLX	Ratio of the projection of the gravitational field vector on the global X-axis to its magnitude gx/g ($-1 \leq$ GLX ≤ 1). Default value is 0.0
	51 - 60	GLY	Ratio of the projection of the gravitational field vector on the global Y-axis to its magnitude gy/g ($-1 \leq$ GLY ≤ 1).
	61 - 70	GLZ	Ratio of the projection of the gravitational field vector on the global Z-axis to its magnitude gz/g ($-1 \leq$ GLZ ≤ 1). Default value is -1.0, and also (GLX)**2+(GLY)**2+(GLZ)**2=1.0 must be satisfied.

Card 2: (I4, 8X, I4, 4X, 2F10.0, 20X, 2F10.0)

Notes	Columns	Variable	Entry
	4	K2	Enter 2 if this card is used
	16	INTRF	EQ.0; forces a solution at the desired reporting intervals designated by COMINT and controlling stepsize H. EQ.1; interpolate the state vector to the desired reporting intervals designated by COMINT EQ.2; interpolate both the state vector and its first time derivative to the desired reporting intervals designated by COMINT
	21 - 30	COMINT	Reporting interval during simulation. Default value is 0.05
	31 - 40	TEND	Final value of the independent variable TIME. Default value is 1.0
	61 - 70	HMAX	Maximum step size allowed. Default value is 0.001
	71 - 80	TSTART	Starting value of the independent variable TIME. Default value is 0.0

Card 3: (4I4, 4X, F10.0)

Notes	Columns	Variable	Entry
	4	K3	Enter 3 if this card is used
	8	ILISTJ #	Flag which controls a symbolic listing of the Jacobian matrix for debugging purposes; EQ.0; no list (Default value) EQ.1; print symbolic listing each time structure of the Jacobian matrix changes and execute the program EQ.2; print symbolic listing for assemble phase only and terminate execution
	12	IRF #	Flag which directs the program to save all data necessary to restart a simulation in the event of termination prior to completion; EQ.0; do not save (Default value) EQ.1; save
	16	ISTART #	Flag that selects the method of starting (or restarting) the integration; EQ.0; all first time derivatives are assumed to be zero (Default value) EQ.-1; all time derivatives are assumed to have been defined GE.1 and LE.5; the program assumes that this is a recovery from earlier run.

21 - 30	EPS	Relative local error tolerance. Default value is 0.001

NOTES

(1) This segment cannot be eliminated. If the default values for the parameters on the 1, 2, and 3 cards are desired, then NSYST should be set to zero and no other cards should follow the identifier for this segment.

III. RIGID BODY

Identifier Card (A4, I4)

Notes	Columns	Variable	Entry
	1 - 4	HEADER	BODY
(1)	5 - 8	NB	Number of rigid bodies (Including the ground)

Rigid Body Card(s)

Card 1: (5I4, 2F10.0)

Notes	Columns	Variable	Entry
(2)	1 - 4	J	Rigid body number; 1,2,...,NB
	8	K1	Enter 1; card 1 of a set of three cards
(3)	9 - 12	JFX #	Integer subscript of a vector of user supplied force-time functions to be entered into the X-equations of motion
(3)	13 - 16	JFY #	Integer subscript of a vector of user supplied force-time functions to be entered into the Y-equations of motion
(3)	17 - 20	JFZ #	Integer subscript of a vector of user supplied force-time functions to be entered into the Z-equations of motion
	21 - 30	M	Mass of the Jth body
	31 - 40	WT	Weight of the Jth body. If blank, WT=GRC*M.

Card 2: (5I4, 6F10.0)

Notes	Columns	Variable	Entry
(2)	1 - 4	J	Rigid body number; 1,2,...,NB
	8	K2	Enter 2; card 2 of a set of three cards
(3)	9 - 12	JTS #	Integer subscript of a vector of user supplied torque-time functions to be entered in the psi-direction
(3)	13 - 16	JTP #	Integer subscript of a vector of user supplied torque-time functions to be entered in the phi-direction
(3)	17 - 20	JTT #	Integer subscript of a vector of user supplied torque-time functions to be entered in the theta-direction
(4)	21 - 30	JINX	Moment of inertia of the Jth body w.r.t. x-axis
(4)	31 - 40	JINY	Moment of inertia of the Jth body w.r.t. y-axis
(4)	41 - 50	JINZ	Moment of inertia of the Jth body w.r.t. z-axis
(4)	51 - 60	JINXY	Product of inertia of the Jth body w.r.t. x- and y-axis
(4)	61 - 70	JINXZ	Product of inertia of the Jth body w.r.t. x- and z-axis

(4)	71 - 80	JINYZ	Product of inertia of the Jth body w.r.t. y- and z-axis

Card 3: (2I4, 12X, 6F10.0)

Notes	Columns	Variable	Entry
(2)	1 - 4	J	Rigid body number; 1,2,...,NB
	8	K3	Enter 3; card 3 of a set of three cards
(3)	21 - 30	FX	Constant force acting on the Jth body center of mass in the X-direction
(3)	31 - 40	FY	Constant force acting on the Jth body center of mass in the Y-direction
(3)	41 - 50	FZ	Constant torque acting on the Jth body center of mass in the Z-direction
(3)	51 - 60	TQS	Constant torque acting on the Jth body center of mass in the psi-direction
(3)	61 - 70	TQP	Constant torque acting on the Jth body center of mass in the phi-direction
(3)	71 - 80	TQT	Constatnt torque acting on the Jth body center of mass in the theta-direction

NOTES

(1) Three cards are required for each rigid body. /Therefore, 3*NB cards should follow the identifier card.

(2) Rigid bodies should be numbered consecutively from 1 to NB.

(2) X-Y-Z is the global (ground) coordinate system and x-y-z is local (body) coordinate system with origin at the center of mass. The units on the mass, moment of inertia, forces and weight should be compatible with the identifier flag, IUNIT, on system information card 1. (Refer to segment II).

(4) JINXY = -INT(xy dm)

JINX = -INT(x**2 dm) and so on.

IV. INITIAL CONDITION

Identifier Card (A4, I4)

Notes	Columns	Variable	Entry
	1 - 4	HEADER	ICON
(1)	5 - 8	NB	Number of initial condition cards (should be equal to NB)

Initial Condition Card(s)

Card 1: (5I4, 6F10.0)

Notes	Columns	Variable	Entry
	1 - 4	J	Rigid body number; 1,2,...,NB
	8	K1	Enter 1; Card 1 of a set of two cards
(2)	12	ICX	EQ.0; flags variables UX and X as initial estimates EQ.1; UX and X are taken as initial conditions
(2)	16	ICY	EQ.0; UY and Y are taken as initial estimates EQ.1; UY and Y are taken as initial conditions
(2)	20	ICZ	EQ.0; UZ and Z are taken as initial estimates EQ.1; UZ and Z are taken as initial conditions
	21 - 30	X	X-coordinate of the body c.g. relative to the global coordinate system
	31 - 40	Y	Y-coordinate of the body c.g. relative to the global coordinate system
	41 - 50	Z	Z-coordinate of the body c.g. relative to the global coordinate system
(3)	51 - 60	PSI	Psi-coordinate of the body c.g. relative to the global coordinate system
(3)	61 - 70	PHI	Phi-coordinate of the body c.g. relative to the global coordinate system.
(3)	71 - 80	THETA	Theta-coordinate of the body c.g. relative to the global coordinate system

Card 2: (5I4, 6F10.0)

Notes	Columns	Variable	Entry
	1 - 4	J	Rigid body number; 1,2,...,NB
	8	K2	Enter 2; card 2 of a set of two cards
(2)	12	ICS	EQ.0; flags variables WS and PSI as initial estimates EQ.1; WS and PSI are taken as initial conditions
(2)	16	ICP	EQ.0; flags variables WP and PHI as initial estimates

			EQ.1: WP and PHI are taken as initial conditions
(2)	20	ICT	EQ.0: flags variables WT and THETA as initial estimates EQ.1: WT and THETA are taken as initial conditions
	21 - 30	UX	Time derivative of X; velocity in X-direction at TSTART
	31 - 40	UY	Time derivative of Y: velocity in Y-direction at TSTART
	41 - 50	UZ	Time derivative of Z; velocity in Z-direction at TSTART
	51 - 60	WS	Time derivative of psi; velocity in psi-direction at TSTART
	61 - 70	WP	Time derivative of phi: velocity in phi-direction at TSTART
	71 - 80	WT	Time derivative of theta; velocity in theta-direction at TSTART

NOTES

(1) Two cards are required for each rigid body. Therefore, 2*NB cards should follow the identifier card.

(2) Initial estimates may be adjusted by the program to satisfy the constraint equations during the initial assembly/static equilibrium step. If given coordinates are not to be changed prior to initialization of the transient analysis step, they should be flagged as initial conditions. Care should be taken to specify initial conditions only on generalized coordinates that are free to change. The general rule to follow is that if any of the existing constraints will determine an exact initial value for a generalized coordinate, then it should not be flagged as an initial condition. Specifying an initial condition on a coordinate causes the program to place a constraint on that degree-of-freedom during the initial assembly process.

(3) Refer to Fig. 8.1.2.1

V. CONSTRAINT

Identifier Card (A4, I4)

Notes	Columns	Variable	Entry
	1 - 4	HEADER	CSTR
	5 - 8	NCR	Number of constraint cards

Constraint Card(s) (4I4, 4X, F10.0)

Notes	Columns	Variable	Entry
(1)	1 - 4	J	Constraint number; $1 \leq J \leq NCR$
(2)	5 - 8	JCB	Body number of the constrained variable
(2)	9 - 12	JCV	Designates the variable to be constrained EQ.1; constrain displacement in X-direction, X(JCB) EQ.2; constrain displacement in Y-direction, Y(JCB) EQ.3; constrain displacement in Z-direction, Z(JCB) EQ.4; constrain displacement in e0-direction, e0(JCB) EQ.5; constrain displacement in e1-direction, e1(JCB) EQ.6; constrain displacement in e2-direction, e2(JCB) EQ.7; constrain displacement in e3-direction, e3(JCB)
	13 - 16	JCF #	EQ.0; JCV is constrained to the constant value VAL GT.0; Integer subscript of a vector of user supplied function of time to which the above variable JCV will be constrained
	21 - 30	VAL	This value is used to constrain variable JCV when JCF .EQ. 0

NOTES

(1) The functions are supplied in the user supplied subroutine(s). The program generates the necessary constraint equations and introduces Lagrange multipliers. Care should be taken to insure that none of the existing constraint equations are violated.

(2) A rigid body may have none, one, or more than one constraint. When a rigid body has no constraints, no cards should be supplied. For rigid bodies with more than one constraint, more than one card is needed. For example, if the Y and e1 on the 4th rigid body are

constrained, on one card JCB=4, JCV=2 and on another card JCB=4, JCV=5 are the proper settings.

In order to constrain a rigid body to ground, the three translational coordinates and just three of the four Euler parameters should be constrained, i.e., constraints x, y, z, e1, e2, and e3.

VI. SPHERICAL JOINT (Type 1 Joint)

Identifier Card (A4, I4)

Notes	Columns	Variable	Entry
	1 - 4	HEADER	SPHR
	5 - 8	NJ1	Number of Spherical Joints

Spherical Joint Card(s) (I4, 4X, 2I4, 4X, 6F10.0)

Notes	Columns	Variable	Entry
	1 - 4	J	Spherical Joint number; 1,2,...,NJ1
	9 - 12	J1BJ1	One of the two body numbers common to this joint (1≤J1BJ1≤NB)
	13 - 16	J1BJ2	The other body number common to this joint (1≤J1BJ2≤NB, J1BJ2/=J1BJ1)
(1)	21 - 30	XJ1	x-coordinate of the joint definition point relative to body J1BJ1
(1)	31 - 40	YJ1	y-coordinate of the joint definition point relative to body J1BJ1
(1)	41 - 50	ZJ1	z-coordinate of the joint definition point relative to body J1BJ1
(1)	51 - 60	XJ2	x-coordinate of the joint definition point relative to body J1BJ2
(1)	61 - 70	YJ2	y-coordinate of the joint definition point relative to body J1BJ2
(1)	71 - 80	ZJ2	z-coordinate of the joint definition point relative to body J1BJ2

NOTES

(1) The same point must be expressed with respect to different coordinate systems. Refer to Fig. 8.5.1.1.

VII. UNIVERSAL JOINT (Type 2 Joint)

Identifier Card (A4, I4)

Notes	Columns	Variable	Entry
	1 - 4	HEADER	UNIV
(1)	5 - 8	NJ2	Number of universal joints

Universal Joint Cards

Card 1: (4I4, 4X, 6F10.0)

Notes	Columns	Variable	Entry
	1 - 4	J	Universal joint number; 1,2,...,NJ2
	8	K1	Enter 1; card 1 of a set of two cards
	9 - 12	J2BJ1	One of the two body numbers common to this joint ($1 \leq J2BJ1 \leq NB$)
	13 - 16	J2BJ2	The other body number common to this joint ($1 \leq J2BJ2 \leq NB$, $J2BJ2 \neq J2BJ1$)
(2)	21 - 30	XJ1	x-coordinate of the joint definition point relative to body J2BJ1
(2)	31 - 40	YJ1	y-coordinate of the joint definition point relative to body J2BJ1
(2)	41 - 50	ZJ1	z-coordinate of the joint definition point relative to body J2BJ1
(2)	51 - 60	XJ2	x-coordinate of the joint definition point relative to body J2BJ2
(2)	61 - 70	YJ2	y-coordinate of the joint definition point relative to body J2BJ2
(2)	71 - 80	ZJ2	z-coordinate of the joint definition point relative to body J2BJ2

Card 2: (2I4, 12X, 6F10.0)

Notes	Columns	Variable	Entry
	1 - 4	J2	Universal joint number; 1,2,...,NJ2
	8	K2	Enter 2; card 2 of a set of two cards
(2)	21 - 30	ALPHJ1	x-coordinate of the joint axis definition point relative to body J2BJ1
(2)	31 - 40	BETAJ1	y-coordinate of the joint axis definition point relative to body J2BJ1
(2)	41 - 50	GAMAJ1	z-coordinate of the joint axis definition point relative to body J2BJ1
(2)	51 - 60	ALPHJ2	x-coordinate of the joint axis definition point relative to body J2BJ2
(2)	61 - 70	BETAJ2	y-coordinate of the joint axis definition point relative to body J2BJ2
(2)	71 - 80	GAMAJ2	z-coordinate of the joint axis definition point relative to body J2BJ2

NOTES

(1) Two cards are required for each universal joint. Therefore, 2*NJ2 cards should follow the identifier card.

(2) Refer to Fig. 8.5.2.1.

VIII. REVOLUTE JOINT (Type 3 Joint)

Identifier Card (A4, I4)

Notes	Columns	Variable	Entry
	1 - 4	HEADER	RVLT
(1)	5 - 8	NJ3	Number of revolute joints

Revolute Joint Cards

Card 1: (4I4, 4X, 6F10.0)

Notes	Columns	Variable	Entry
	1 - 4	J	Universal joint number; 1,2,...,NJ3
	8	K1	Enter 1; card 1 of a set of two cards
	9 - 12	J3BJ1	One of the two body numbers common to this joint (1≤J3BJ1≤NB)
	13 - 16	J3BJ2	The other body number common to this joint (1≤J3BJ2≤NB, J3BJ2/=J3BJ1)
(2)	21 - 30	XJ1	x-coordinate of the joint definition point relative to body J3BJ1
(2)	31 - 40	YJ1	y-coordinate of the joint definition point relative to body J3BJ1
(2)	41 - 50	ZJ1	z-coordinate of the joint definition point relative to body J3BJ1
(2)	51 - 60	XJ2	x-coordinate of the joint definition point relative to body J3BJ2
(2)	61 - 70	YJ2	y-coordinate of the joint definition point relative to body J3BJ2
(2)	71 - 80	ZJ2	z-coordinate of the joint definition point relative to body J3BJ2

Card 2: (2I4, 12X, 6F10.0)

Notes	Columns	Variable	Entry
	1 - 4	J	Revolute joint number; 1,2,...,NJ3
	8	K2	Enter 2; card 2 of a set of two cards
(2)	21 - 30	ALPHJ1	x-coordinate of the joint axis definition point relative to body J3BJ1
(2)	31 - 40	BETAJ1	y-coordinate of the joint axis definition point relative to body J3BJ1
(2)	41 - 50	GAMAJ1	z-coordinate of the joint axis definition point relative to body J3BJ1
(2)	51 - 60	ALPHJ2	x-coordinate of the joint axis definition point relative to body J3BJ2

(2)	61 - 70	BETAJ2	y-coordinate of the joint axis definition point relative to body J3BJ2
(2)	71 - 80	GAMAJ2	z-coordinate of the joint axis definition point relative to body J3BJ2

NOTES

(1) Two cards are required for each revolute joint. Therefore, 2*NJ3 cards should follow the identifier card.

(2) Refer to Fig. 8.5.3.1.

IX. CYLINDRICAL JOINT (Type 4 Joint)

Identifier Card (A4, I4)

Notes	Columns	Variable	Entry
	1 - 4	HEADER	CYLN
(1)	5 - 8	NJ4	Number of cylindrical joints

Cylindrical Joint Cards

Card 1: (4I4, 4X, 6F10.0)

Notes	Columns	Variable	Entry
	1 - 4	J	Cylindrical joint number; 1,2,...,NJ4
	8	K1	Enter 1; card 1 of a set of two cards
	9 - 12	J4BJ1	One of the two body numbers common to this joint ($1 \leq$ J4BJ1 $\leq$ NB)
	13 - 16	J4BJ2	The other body number common to this joint ($1 \leq$ J4BJ2 $\leq$ NB, J4BJ2 /= J4BJ1)
(2)	21 - 30	XJ1	x-coordinate of the joint definition point relative to body J4BJ1
(2)	31 - 40	YJ1	y-coordinate of the joint definition point relative to body J4BJ1
(2)	41 - 50	ZJ1	z-coordinate of the joint definition point relative to body J4BJ1
(2)	51 - 60	XJ2	x-coordinate of the joint definition point relative to body J4BJ2
(2)	61 - 70	YJ2	y-coordinate of the joint definition point relative to body J4BJ2
(2)	71 - 80	ZJ2	z-coordinate of the joint definition point relative to body J4BJ2

Card 2: (2I4, 12X, 6F10.0)

Notes	Columns	Variable	Entry
	1 - 4	J	Cylindrical joint number; 1,2,...,NJ4
	8	K2	Enter 2; card 2 of a set of two cards
(2)	21 - 30	ALPHJ1	x-coordinate of the joint axis definition point relative to body J4BJ1
(2)	31 - 40	BETAJ1	y-coordinate of the joint axis definition point relative to body J4BJ1
(2)	41 - 50	GAMAJ1	z-coordinate of the joint axis definition point relative to body J4BJ1
(2)	51 - 60	ALPHJ2	x-coordinate of the joint axis definition point relative to body J4BJ2

(2)	61 - 70	BETAJ2	y-coordinate of the joint axis definition point relative to body J4BJ2
(2)	71 - 80	GAMAJ2	z-coordinate of the joint axis definition point relative to body J4BJ2

NOTES

(1) Two cards are required for each cylindrical joint. Therefore, 2*NJ4 cards should follow the identifier card.

(2) Refer to Fig. 8.5.4.1.

X. TRANSLATIONAL JOINT (Type 5 Joint)

Identifier Card (A4, I4)

Notes	Columns	Variable	Entry
	1 - 4	HEADER	TRAN
(1)	5 - 8	NJ5	Number of translational joints

Translational Joint Cards

Card 1: (4I4, 4X, 6F10.0)

Notes	Columns	Variable	Entry
	1 - 4	J	Translational joint number; 1,2,...,NJ5
	8	K1	Enter 1; card 1 of a set of three cards
	9 - 12	J5BJ1	One of the two body numbers common to this joint ($1 \leq$ J5BJ1 $\leq$ NB)
	13 - 16	J5BJ2	The other body number common to this joint ($1 \leq$ J5BJ2 $\leq$ NB, J5BJ2/=J5BJ1)
(2)	21 - 30	XJ1	x-coordinate of the joint definition point relative to body J5BJ1
(2)	31 - 40	YJ1	y-coordinate of the joint definition point relative to body J5BJ1
(2)	41 - 50	ZJ1	z-coordinate of the joint definition point relative to body J5BJ1
(2)	51 - 60	XJ2	x-coordinate of the joint definition point relative to body J5BJ2
(2)	61 - 70	YJ2	y-coordinate of the joint definition point relative to body J5BJ2
(2)	71 - 80	ZJ2	z-coordinate of the joint definition point relative to body J5BJ2

Card 2: (2I4, 12X, 6F10.0)

Notes	Columns	Variable	Entry
	1 - 4	J	Translational joint number; 1,2,...,NJ5
	8	K2	Enter 2; card 2 of a set of three cards
(2)	21 - 30	ALPHJ1	x-coordinate of the joint axis definition point relative to body J5BJ1
(2)	31 - 40	BETAJ1	y-coordinate of the joint axis definition point relative to body J5BJ1
(2)	41 - 50	GAMAJ1	z-coordinate of the joint axis definition point relative to body J5BJ1
(2)	51 - 60	ALPHJ2	x-coordinate of the joint axis definition point relative to body J5BJ2

(2)	61 - 70	BETAJ2	y-coordinate of the joint axis definition point relative to body J5BJ2
(2)	71 - 80	GAMAJ2	z-coordinate of the joint axis definition point relative to body J5BJ2

Card 3: (2I4, 12X, 6F10.0)

Notes	Columns	Variable	Entry
	1 - 4	J	Translational joint number; 1,2,...,NJ5
	8	K3	Enter 3; Card 3 of a set of three cards
(2)	21 - 30	SXJ1	x-coordinate of a point relative to body J5BJ1
(2)	31 - 40	SYJ1	y-coordinate of the point relative to body J5BJ1
(2)	41 - 50	SZJ1	z-coordinate of the point relative to body J5BJ1
(2)	51 - 60	SXJ2	x-coordinate of the point relative to body J5BJ2
(2)	61 - 70	SYJ2	y-coordinate of the point relative to body J5BJ2
(2)	71 - 80	SZJ2	z-coordinate of the point relative to body J5BJ2

NOTES

(1) Three cards are required for each translational joint. Therefore, 3*NJ5 cards should follow the identifier card.

(2) Refer to Fig. 8.5.5.1.

XI. MASSLESS LINK (Type 7 Joint)

Identifier Card (A4, I4)

Notes	Columns	Variable	Entry
	1 - 4	HEADER	LINK
(1)	5 - 8	NJ7	Number of massless links

Massless Link Cards

Card 1: (4I4, 4X, 6F10.0)

Notes	Columns	Variable	Entry
	1 - 4	J	Massless link number; 1,2,...,NJ7
	8	K1	Enter 1; card 1 of a set of three cards
	9 - 12	J7BJ1	One of the two body numbers common to this joint ($1 \leq$ J7BJ1 $\leq$ NB)
	13 - 16	J7BJ2	The other body number common to this joint ($1 \leq$ J7BJ2 $\leq$ NB, J7BJ2 /= J7BJ1)
(2)	21 - 30	XJ1	x-coordinate of the joint definition point relative to body J7BJ1
(2)	31 - 40	YJ1	y-coordinate of the joint definition point relative to body J7BJ1
(2)	41 - 50	ZJ1	z-coordinate of the joint definition point relative to body J7BJ1
(2)	51 - 60	XJ2	x-coordinate of the joint definition point relative to body J7BJ2
(2)	61 - 70	YJ2	y-coordinate of the joint definition point relative to body J7BJ2
(2)	71 - 80	ZJ2	z-coordinate of the joint definition point relative to body J7BJ2

Card 2: (4I4, 4X, 6F10.0)

Notes	Columns	Variable	Entry
	1 - 4	J	Massless link number; 1,2,...,NJ7
	8	K2	Enter 2; card 2 of a set of three cards
	9 - 12	LT1	EQ.1; Joint on body J7BJ1 is a spherical joint EQ.2; Joint on body J7BJ1 is a revolute joint
	13 - 16	LT2	EQ.1; Joint on body J7BJ2 is a spherical joint EQ.2; Joint on body J7BJ2 is a revolute joint

(2)	21 - 30	ALPHJ1	x-coordinate of the joint axis definition point relative to body J7BJ1
(2)	31 - 40	BETAJ1	y-coordinate of the joint axis definition point relative to body J7BJ1
(2)	41 - 50	GAMAJ1	z-coordinate of the joint axis definition point relative to body J7BJ1
(2)	51 - 60	ALPHJ2	x-coordinate of the joint axis definition point relative to body J7BJ2
(2)	61 - 70	BETAJ2	y-coordinate of the joint axis definition point relative to body J7BJ2
(2)	71 - 80	GAMAJ2	z-coordinate of the joint axis definition point relative to body J7BJ2

Card 3: (3I4, 8X, 6F10.0)

Notes	Columns	Variable	Entry
	1 - 4	J	Massless link number; 1,2,...,NJ7
	8	K3	Enter 3; Card 3 of a set of three cards
	9 - 12	LTIJ	EQ.0; Angle between two joint axes of J7BJ1 and J7BJ2 is 0 (requires that SXJ2, SYJ2, and SZJ2 be input) EQ.1; Angle between joint axes of J7BJ1 and J7BJ2 is not 0 (input THETIJ)
	21 - 30	LP	Length of link
	31 - 40	THET1	Angle between link and joint axis of J7BJ1
	41 - 50	THET2	Angle between link and joint axis of J7BJ2
	51 - 60	THETIJ	Angle between two joint axes of J7BJ1 and J7BJ2 (when LTIJ=1)
		or SXJ2	x-coordinate of a point on the body J7BJ2 (when LTIJ=0)
	61 - 70	SYJ2	y-coordinate of a point on the body J7BJ2
	71 - 80	SZJ2	z-coordinate of a point on the body J7BJ2

NOTES

(1) Three cards are required for each massless link. Therefore, 3*NJ7 cards should follow the identifier card.

(2) Refer to Fig. 8.5.6.1.

XII. TRANSLATIONAL-SPRING-DAMPER-ACTUATOR

Notes	Columns	Variable	Entry
	1 - 4	HEADER	LSDA
(1)	5 - 8	NLSDA	Number of translational-spring-damper--actuator elements

<u>Linear Spring-Damper-Actuator Card(s)</u>

Card 1: (4I4, 4X, 6F10.0)

Notes	Columns	Variable	Entry
	1 - 4	J	Element number; 1,2,...,NLSDA
	8	K1	Enter 1; card 1 of a set of two cards
	9 - 12	JBSDJ1	One of the two body numbers common to this element (1≤JBSDJ1≤NB)
	13 - 16	JBSDJ2	The other body number common to this element (1≤JBSDJ2≤NB, JBSDJ2/=JBSDJ1)
(2)	21 - 30	XJ1	x-component of the point where the element is attached to body JBSDJ1 relative to the coordinate system of body JBSDJ1
(2)	31 - 40	YJ1	y-component of the point where the element is attached to body JBSDJ1 relative to the coordinate system of body JBSDJ1
(2)	41 - 50	ZJ1	z-component of the point wheree the element is attached to body JBSDJ1 relative to the coordinate system of body JBSDJ1
(2)	51 - 60	XJ2	x-component of the point where the element is attached to body JBSDJ2 relative to the coordinate system of body JBSDJ2
(2)	61 - 70	YJ2	y-component of the point where the element is attached to body JBSDJ2 relative to the coordinate system of body JBSDJ2
(2)	71 - 80	ZJ2	z-component of the point where the element is attached to body JBSDJ2 relative to the coordinate system of body JBSDJ2

Card 2: (5I4, 4F10.0)

Notes	Columns	Variable	Entry
	1 - 4	J	Element number; 1,2,...,NLSDA (same as its corresponding number on card 1)
	8	I2	Enter 2; card 2 of a set of two cards
(3)	9 - 12	JAL #	Integer subscript in a vector of user supplied function of time which

			specifies the actuator length as a function of time
(3)	13 - 16	JAF #	Integer subscript in a vector of user supplied function of time which specifies the actuator force as a function of time
	17 - 20	JKL #	Integer subscript of spring characteristic which is function of deformation. JKL=0 or blank means the spring is linear with spring constant SK.
	21 - 30	SK	Element spring constant
	31 - 40	D	Element damping coefficient
	41 - 50	SDL0	Undeformed element length (SDL0 $\geq$ 0.0)
	51 - 60	AF	Actuator force applied between the two attachment points

NOTES

(1) Two cards are required for each translational-spring-damper-actuator. Therefore, 2*NLSDA cards should follow the identifier card.

(2) Refer to Fig. 9.3.2.

(3) These features allow the actuator length or actuator force to be designated as a constant value or function of time. Both JAF and JAL may not be greater than zero at the same time.

XIII. TORSIONAL-SPRING-DAMPER-ACTUATOR

Identifier Card (A4, I4)

Notes	Columns	Variable	Entry
	1 - 4	HEADER	TSDA
(1)	5 - 8	NTSDA	Number of torsional spring elements

Torsional-Spring-Damper-Actuator Card(s)

Card 1: (4I4, 4X, 6F10.0)

Notes	Columns	Variable	Entry
	1 - 5	J	Element number; 1,2,...,NTSDA
	8	K1	Enter 1; Card 1 of a set of three cards
	9 - 12	JRVLT	The joint number about which this element acts
	12 - 16	JTJ	Type of joint of JRVLT EQ.1; Spherical joint EQ.2; Universal joint EQ.3; Revolute joint
	21 - 30	XJ1	x-coordinate of the spring attachment point relative to the first body
	31 - 40	YJ1	y-coordinate of the spring attachment point relative to the first body
	41 - 50	ZJ1	z-coordinate of the spring attachment point relative to the first body
	51 - 60	XJ2	x-coordinate of the spring attachment point relative to the second body
	61 - 70	YJ2	y-coordinate of the spring attachment point relative to the second body
	71 - 80	ZJ2	z-coordinate of the spring attachment point relative to the second body

Card 2: (4I4, 4X, 4F10.0)

Notes	Columns	Variable	Entry
	1 - 4	J2	Element number; 1,2,...,NTSDA (J1=J2)
	8	K2	Enter 2; Card 2 of a set of three cards
	9 - 12	JAT #	Integer subscript in a vector of user supplied functions of time which specifies the actuator torque as a function of time
	13 - 16	JKT #	Integer subscript of spring characteristic which is function of deformation. EQ.0; The spring is linear with spring constant SKT
	21 - 30	SKT	Element spring constant
	31 - 40	DT	Element damping coefficient

41 - 50	AT	Actuator torque applied between the two rigid bodies about the revolute joint
51 - 60	PHI0	Undeformed angle of the spring

Card 3: (3I4, 8X, 3F10.0)

Notes	Columns	Variable	Entry
	1 - 4	J3	Element number; 1,2,...,NTSDA (J3=J1)
	8	K3	Enter 3; Card 3 of a set of three cards
	9 - 12	JAL #	Integer subscript in a vector of user supplied function of time which specifies the actuator length as a function fo time
	21 - 30	SXJ1	x-coordinate of a point on the joint axis with respect to the first body to specify spring attachment direction by the law of right handed screw from the first body to the second body
	31 - 40	SYJ1	y-coordinate
	41 - 50	SZJ1	z-coordinate

NOTES

(1) 3*NTSDA cards should follow the identifier card.

XIV. POINTER

Identifier Card (A4, I4)

Notes	Columns	Variable	Entry
(1)	1 - 4	HEADER	POIN
	5 - 8	NPTS	Number of pointers

Pointer Card(s) (2I4, 12X, 3F10.0)

Notes	Columns	Variable	Entry
	1 - 4	J	Pointer number; 1,2,...,NPTS
	5 - 8	JB	Rigid body number
	21 - 30	XIJ	x-component of the pointer relative to the coordinate system of body JB
	31 - 40	ETAJ	y-component of the pointer relative to the coordinate system of body JB
	41 - 50	ZTA	z-component of the pointer relative to the coordinate system of body JB

NOTES

(1) This segment enables the user to request for output information at specified location(s) on a rigid body. The position of a pointer should be given with respect to the rigid body coordinate system.

XV. SPLINE FUNCTION

Identifier Card (A4, I4)

Notes	Columns	Variable	Entry
	1 - 4	HEADER	SPLN
	5 - 8	NSPLN	Number of spline functions

NSPLN sets of cards as described below need to be supplied following the identifier card:

a. Spline Function Information Card (4I4, 4X, 6F10.0)

Notes	Columns	Variable	Entry
	1 - 4	JSPLN	Spline function number; 1,2,...,NSPLN
	5 - 8	NPTS	Number of data points in this spline function
(1)	9 - 12	ITYP	EQ.0; NPTS pairs of f(Xi)'s and xi's are provided on b cards
(2)			EQ.1; NPTS f(Xi)'s are provided on b cards; xi is taken constant
	13 - 16	NCALLS	GE.1; The maximum number of arguments that could be assigned to this function
	21 - 30	SLEFT	Slope at the left end of the function
	31 - 40	SRIGHT	Slope at the right end of the function
(2)	41 - 50	X1	Starting value for X. Applicable only when ITYP.EQ.1
(2)	51 - 60	DX	Sample interval for X. Applicable only when ITYP.EQ.1
	61 - 70	XSCAL	Scale factor of SLEFT, SRIGHT, X1, DX, and X. Default value is 1.0 SLEFT = SLEFT/XSCAL SRIGHT = SRIGHT/XSCAL X1 = X1*XSCAL DX = DX*XSCAL X = X*XSCAL
	71 - 80	FXSCAL	Scale factor on SLEFT, SRIGHT, and FX. Default value is 1.0 SLEFT = SLEFT*FXSCAL SRIGHT = SRIGHT*FXSCAL FX = FX*FXSCAL

b. Spline Function Data (when ITYP.EQ.0) (8E10.0)

Notes	Columns	Variable	Entry
(1)	1 - 10	X	xi
	11 - 20	FX	f(xi)
	21 - 30	X	xi+1
	31 - 40	FX	f(xi+1)
	41 - 50	X	xi+2
	51 - 60	FX	f(xi+2)
	61 - 70	X	xi+3
	71 - 80	FX	f(xi+3)

b. Spline Function Data (when ITYP.EQ.1) (8E10.0)

Notes	Columns	Variable	Entry
(2)	1 - 10	FX	f(xi)
	11 - 20	FX	f(xi+1)
	21 - 30	FX	f(xi+2)
	31 - 40	FX	f(xi+3)
	41 - 50	FX	f(xi+4)
	51 - 60	FX	f(xi+5)
	61 - 70	FX	f(xi+6)
	71 - 80	FX	f(xi+7)

NOTES

(1) When ITYP is set to zero on card a, NPTS pairs of data points should be supplied on (NPTS+3)/4 b cards. Pairs of xi and f(xi) should be entered consecutively for i = 1,...,NPTS.

(2) When ITYP is set to one on card a, NPTS data points should be supplied on (NPTS+7)/8 b cards. The data should be taken for constant DX intervals. f(xi)'s should be entered consecutively for i = 1,...,NPTS. It should be noted that x1 is set equal to X1 (card a), x2 = X1 + DX, x3 = X2 + DX and so on.

XVI. END COMMAND

Identifier Card (A4)

Notes	Columns	Variable	Entry
(1)	1 - 3	HEADER	END

NOTES

(1) An END card indicates the end of input data for a given model. Following an END card more sets of data cards for other models may be supplied to the program.

DISTRIBUTION LIST

Please notify USATACOM, DRSTA-ZSA, Warren, Michigan 48090, of corrections and/or changes in address.

Commander (25)
US Army Tk-Autmv Command
R&D Center
Warren, MI 48090

Superintendent (02)
US Military Academy
ATTN: Dept of Engineering
Course Director for
Automotive Engineering

Commander (01)
US Army Logistic Center
Fort Lee, VA 23801

US Army Research Office (02)
P.O. Box 12211
ATTN: Dr. F. Schmiedeshoff
Dr. R. Singleton
Research Triangle Park, NC 27709

HQ, DA (01)
ATTN: DAMA-AR
Dr. Herschner
Washington, D.C. 20310

HQ, DA (01)
Office of Dep Chief of Staff
for Rsch, Dev & Acquisition
ATTN: DAMA-AR
Dr. Charles Church
Washington, D.C. 20310

HQ, DARCOM
5001 Eisenhower Ave.
ATTN: DRCDE
Dr. R.L. Haley
Alexandria, VA 22333

Director (01)
Defense Advanced Research
Projects Agency
1400 Wilson Boulevard
Arlington, VA 22209

Commander (01)
US Army Combined Arms Combat
Developments Activity
ATTN: ATCA-CCC-S
Fort Leavenworth, KA 66027

Commander (01)
US Army Mobility Equipment
Research and Development Command
ATTN: DRDME-RT
Fort Belvoir, VA 22060

Director (02)
US Army Corps of Engineers
Waterways Experiment Station
P.O. Box 631
Vicksburg, MS 39180

Commander (01)
US Army Materials and Mechanics
Research Center
ATTN: Mr. Adachi
Watertown, MA 02172

Director (03)
US Army Corps of Engineers
Waterways Experiment Station
P.O. Box 631
ATTN: Mr. Nuttall
Vicksburg, MS 39180

Director (04)
US Army Cold Regions Research
& Engineering Lab
P.O. Box 282
ATTN: Dr. Freitag, Dr. W. Harrison
Dr. Liston, Library
Hanover, NH 03755

Grumman Aerospace Corp (02)
South Oyster Bay Road
ATTN: Dr. L. Karafiath
Mr. F. Markow
M/S A08/35
Bethpage, NY 11714

Dr. Bruce Liljedahl (01)
Agricultural Engineering Dept
Purdue University
Lafayette, IN 46207

Mr. H.C. Hodges (01)
Nevada Automotive Test Center
Box 234
Carson City, NV 89701

Mr. R.S. Wismer (01)
Deere & Company
Engineering Research
3300 River Drive
Moline, IL 61265

Oregon State University (01)
Library
Corvallis, OR 97331

Southwest Research Inst (01)
8500 Culebra Road
San Antonia, TX 78228

FMC Corporation (01)
Technical Library
P.O. Box 1201
San Jose, CA 95108

Mr. J. Appelblatt (01)
Director of Engineering
Cadillac Gauge Company
P.O. Box 1027
Warren, MI 48090

Chrysler Corporation (02)
Mobility Research Laboratory,
Defense Engineering
Department 6100
P.O. Box 751
Detroit, MI 48231

CALSPAN Corporation (01)
Box 235
Library
4455 Benesse Street
Buffalo, NY 14221

SEM, (01)
Forsvaretsforskningsanstalt
Avd 2
Stockholm 80, Sweden

Mr. Hedwig (02)
RU III/6
Ministry of Defense
5300 Bonn, Germany

Foreign Science & Tech (01)
Center
220 7th Street North East
ATTN: AMXST-GEI
Mr. Tim Nix
Charlottesville, VA 22901

General Research Corp (01)
7655 Old Springhouse Road
Westgate Research Park
ATTN: Mr. A. Viilu
McLean, VA 22101

Commander (01)
US Army Developmant and
Readiness Command
5001 Eisenhower Avenue
ATTN: Dr. R.S. Wiseman
Alexandria, VA 22333

President (02)
Army Armor and Engineer Board
Fort Knox, KY 40121

Commander (01)
US Army Arctic Test Center
APO 409
Seattle, WA 98733

Commander (02)
US Army Test & Evaluation
Command
ATTN: AMSTE-BB and AMSTE-TA
Aberdeen Proving Ground, MD
21005

Commander (01)
US Army Armament Research
and Development Command
ATTN: Mr. Rubin
Dover, NJ 07801

Commander (01)
US Army Yuma Proving Ground
ATTN: STEYP-RPT
Yuma, AZ 85364

Commander (01)
US Army Natic Laboratories
ATTN: Technical Library
Natick, MA 01760

Director (01)
US Army Human Engineering Lab
ATTN: Mr. Eckels
Aberdeen Proving Ground, MD
21005

Director (02)
US Army Ballistic Research Lab
Aberdeen Proving Ground, MD
21005

Director (02)
US Army Materiel Systems
Analysis Agency
ATTN: AMXSY-CM
Aberdeen Proving Ground, MD
21005

Director (02)
Defense Documentation Center
Cameron Station
Alexandria, VA 22314

US Marine Corps (01)
Mobility & Logistics Division
Development and Ed Command
ATTN: Mr. Hickson
Quantico, VA 22134

Keweenaw Field Station (01)
Keweenaw Research Center
Rural Route 1
P.O. Box 94-D
ATTN: Dr. Sung M. Lee
Calumet, MI 49913

Naval Ship Research & (02)
Dev Center
Aviation & Surface Effects Dept
Code 161
Washington, D.C. 20034

Director (01)
National Tillage Machinery Lab
Box 792
Auburn, AL 36830

Director (02)
USDA Forest Service Equipment
Development Center
444 East Bonita Avenue
San Dimes, CA 91773

Engineering Societies (01)
Library
345 East 47th Street
New York, NY 10017

Dr. I.R. Erlich (01)
Dean for Research
Stevens Institute of Technology
Castle Point Station
Hoboken, NJ 07030